MATHEMATICAL MODELLING OF ARABIDOPSIS FLOWERING TIME GENE REGULATORY NETWORK

E HASPOLAT

PhD

2018

MATHEMATICAL MODELLING OF ARABIDOPSIS FLOWERING TIME GENE REGULATORY NETWORK

EMRAH HASPOLAT

A thesis submitted in partial fulfilment of the requirements of the University of Northumbria at Newcastle for the degree of Doctor of Philosophy

Research undertaken in the

Department of Mathematics, Physics and Electrical Engineering

June 2018

Abstract

Experimental studies of the flowering of *Arabidopsis Thaliana* have shown that a large complex gene regulatory network (GRN) is responsible for its regulation. This process has recently been modelled with deterministic differential equations by considering the interactions between gene activators and inhibitors [Valentim et al., 2015, van Mourik et al., 2010]. However, due to the complexity of the models, the properties of the network and the roles of the individual genes cannot be deduced from the numerical solution the published work offers. In this study, deterministic and stochastic dynamic models of Arabidopsis flowering GRN are considered by following the deterministic delayed model introduced in [Valentim et al., 2015]. A stable solution of this model is sought by its linearisation, which contributes to further investigation of the role of the individual genes to the flowering. By decoupling some concentrations, the system has been reduced to emphasise the role played by the transcription factor *Suppressor of Overexpression of Constants1* ($SOC1$) and the important floral meristem identity genes, *Leafy* (LFY) and *Apetala1* ($AP1$). Two-dimensional motifs, based on the dynamics of LFY and $AP1$, are obtained from the reduced network and parameter ranges ensuring flowering are determined. Their stability analysis shows that LFY and $AP1$ are regulating each other for flowering, matching experimental findings (see e.g. [Blázquez et al., 2001, Welch et al., 2004, Yeap et al., 2014]). Moreover, the role of noise is studied by introducing and investigating two types of stochastic elements into the motifs. New sufficient conditions of mean square stability and their domain are obtained analytically for the stochastic models using Lyapunov stability theory. Numerical solutions are obtained by using Euler-Maruyama method and Ito stochastic formula. We demonstrate that the stochastic motifs of Arabidopsis flowering time can capture the essential behaviour of the full system and that stochastic effects can change the behaviour of the stability region through a stability switch. Furthermore, the problem of designing an observer and a controller, in which FT is seen as a control input, is considered in the objective of ensuring flowering conditions are met. This study thus contributes to a better understanding of the role of LFY and $AP1$ in Arabidopsis flowering.

Contents

List of Figures

List of Tables

Acknowledgements

This thesis would not possibly have been finalised without the help and support of many people. I would therefore like to express my thankfulness to those people who have been involved in my PhD journey.

Firstly, I would like to start giving my special thanks and sincerest gratitude to my supervisors, Dr. Benoit Huard, Prof. Maia Angelova and Prof. Krishna Busawon for their patience, encouragement and invaluable continuous support during my studies. Without their support none of this would have been possible. A very special thanks goes to my principal supervisor Dr. Benoit Huard, who supports me from beginning of my studies to the final days of writing the thesis.

I would like to thank all staff members of department of mathematics and PhD students in mathematics and computer science for their friendliness and supports to make so many things easier. I would also like to thank all my friends and their families in the UK for their friendships and support, especially for Burhan Alveroglu and Tayfun Kok.

Importantly, a special thanks goes to my dear family, my fiance, Kubra, and her family for their emotional support and encouragement during the PhD process and my life in general.

Finally, I would like to thank the Republic of Turkey, Ministry of National Education for my sponsorship and Graduate School of Northumbria University for their support in funding my conference attendance.

Emrah HASPOLAT

Declaration

I declare that the work contained in this thesis has not been submitted for any other award and that it is all my own work. I also confirm that this work fully acknowledges opinions, ideas and contributions from the work of others.
Any ethical clearance for the research presented in this thesis has been approved. Approval has been sought and granted by the University Ethics Committee on 7th of April 2014.

I declare that the Word Count of this Thesis is 35857 words.

Name: Emrah Haspolat

Signed:

Date:

Abbreviations

GRN	**G**ene **R**egulatory **N**etwork
ODE	**O**rdinary **D**ifferential **E**quation
DDE	**D**elay **D**ifferential **E**quation
SDE	**S**tochastic **D**ifferential **E**quation
SDDE	**S**tochastic **D**elay **D**ifferential **E**quation
HGO	**H**igh **G**ain **O**bserver
AP1	**A**petala **1**
LFY	**L**ea**f**y
SOC1	**S**uppressor of **O**verexpression of **C**onstant **1**
FD	**FD**
FT	**F**lowering **L**ocus **T**
AGL24	**Ag**amous-**L**ike **24**
SVP	**S**hort **V**egetative **P**hase
FLC	**F**lowering **L**ocus **C**

Chapter 1

Introduction

1.1 Introduction

Genomic and molecular information have been obtained with high throughput genomic and proteomic technologies enabling operating mechanism of diseases, cells, genes, and proteins to be observed. Mathematical and computational biology and the systems biology framework have been developed to analyse genomic and molecular information and understand complex biological systems.

Systems biology aims to study any living system to understand their behaviour at molecular level, effected by the interactions of their internal components. Complex models of regulatory networks that characterise life require quantitative approaches such as differential equations to identify recurrent patterns [Boogerd et al., 2007, Breitling, 2010].

Systems biology is a new expanding area in biological and medical research and one of its purposes is to investigate biological processes and networks from a system perspective. According to Kitano [2002], systems biology is one of the biggest interdisciplinary fields in science because it integrates a crucial relationship between biology, biochemistry, computer science, mathematics, physics and statistics. The origins of systems biology can be traced back, at least, to the 1960's and 1970's when Biochemical Systems Theory [Savageau, 1969a,b] and Metabolic Control Theory [Heinrich and Rapoport,

1974] were introduced, following the work of Higgins [1963]. The main aim was then to formally represent biochemical systems and understand their behaviour around equilibria under the influence of external processes. A historical review can be found in [Haubelt et al., 2002]. Nowadays, systems biology has found applications in many areas such as in the modelling of gene expressions, large scale networks and pathways as well as cellular and protein process.

As mentioned before, the design of mathematical models to describe the dynamics of complex systems and to represent the actual behaviour is the principal focus of systems biology. The development of differential equation models has emerged as a promising area in systems biology. Population dynamics [Bartoszewski et al., 2015, Kepler and Perelson, 1995], chemical reaction networks [Belbas and Kim, 2003, Higham, 2008] and gene regulatory networks (GRNs) analyses [Hecker et al., 2009] are some examples of relevant application areas.

Systems biology provides an approach to study living organism and investigate proteins and genes. The interactions of genes among the proteins, DNA, RNA and other molecules constitute the main components of a gene regulatory network (GRN) [Hecker et al., 2009]. GRNs have a crucial place in life processes such as metabolism and cell differentiation of plant species. Behaviour of regulatory networks can be relatively predicted, thus accelerating the process of biotechnological studies and it also helps to reduce the time and cost of lab experiments. To predict the behaviour of networks, mathematical and computational methods have an important place [Karlebach and Shamir, 2008].

There are different methods for the modelling and simulation of GRNs, and dynamic models that are based on (ordinary and delay) differential equations, are one of the well-known methods utilised for them. These models are used for the simulation of real-time network and the estimation of its response for different environmental conditions [Schlitt and Brazma, 2007].

Stability analysis of dynamic models have a crucial place to understand their behaviour. Most of the dynamic models are constructed by using deterministic differential equations, which are not considering the noise terms. On the other hand, stochastic models

have recently received considerable attention. They are obtained by adding noise terms into the deterministic models to observe more realistic behaviour of the networks. Their stability analysis also allows us to characterise the interplay between noise and equilibrium [Burrage et al., 2000, Carletti, 2007, Klimešová, 2015, Lahrouz et al., 2011, Tang et al., 2015].

Another well-known method used in the literature is control design approach which is a separate process from dynamical modelling [Al Hokayem and Gallestey, 2017, Cosentino and Bates, 2011, Gallestey et al., 2015, Iglesias and Ingalls, 2010, Kalman, 1959, Lantos and Márton, 2010]. This is used to regulate the concentrations of some necessary variables in the regulatory networks. Observer design is an approach to obtain a direct implementation of any control algorithm, which might also be dependent on measured variables.

Over the last twenty years, many methods that depend on genome-wide data have been established to resolve the complexity of gene regulation. *Arabidopsis Thaliana* flowering time is an example of well-known complex GRN. Recently, the dynamics of Arabidopsis flowering time regulation has been analysed mathematically using systems approach along with experimental data to understand the effect of the genes on flowering of *Arabidopsis Thaliana* [Daly et al., 2009, Jaeger et al., 2013, Pullen et al., 2013, Valentim et al., 2015, van Mourik et al., 2010, Wang et al., 2014].

In this study, we focus on a dynamical model of Arabidopsis flowering time GRN, proposed by Valentim et al. [2015]. The main features of this model are that it constitutes the first model making use of delay differential equations along with Hill functions to represent interactions. While we focus on investigating this deterministic dynamic model, we also present new small (simplified and motif) models constituted by decoupling some concentrations in original model and stochastic approaches of the motif model. The validity of simplified model is observed with the control design approach. Therefore, this study also aims to reformulate one of the deterministic simplified model by using two different observers; constant and state-dependent high gain observers.

1.2 Motivation for the modelling of the Arabidopsis flowering time

Observing the main genes, which have effect on behaviour of flowering process, and the time of this process have crucial place for the life cycle of *Arabidopsis Thaliana*. The reactions of input and output concentrations and interactions between each other can be monitored and regulated by defining their regulatory networks. Moreover, these networks of Arabidopsis flowering can be modelled via deterministic and stochastic approaches like other biological networks by using ordinary and delay differential equation models [Shmulevich and Aitchison, 2009] to understand the impact of gene regulations and their interactions between each other. However, there is a limited number of studies of the dynamic modelling of Arabidopsis flowering GRN, and these are aimed at constructing a model by using deterministic ordinary differential equations. This study brings an overview of the most common modelling methods and summarises some existing challenges in GRN modelling. Moreover, it aims to review and extend the modelling of Arabidopsis flowering time GRN, based on the model proposed by Valentim et al. [2015], and reconstruct it from experimental data via computational methods. This model has the feature of being the first and only deterministic delay differential equation model in this network as mentioned before.

System behaviour of the GRNs usually cannot be understood heuristically due to the complexity of interactions in organisms. Stability analysis is used to study the properties of the GRN and thresholds in biological models [Chen and Aihara, 2002, Engelborghs and Roose, 1999, Lahrouz et al., 2011]. It is needed to clarify the features of complex systems and provides specific conditions to ensure appropriate regulation. Moreover, such analysis of the system networks provides a reliability test and more insights into the behaviours of GRN's elements. In the literature, the stability properties of the Arabidopsis flowering system behaviour has not been studied yet. This work, for the first time, analyses the local stability behaviour of an Arabidopsis flowering network. It uses linearisation of the dynamical model around its steady state and introduces simplified versions with three and two differential equations. The motivation for this is to obtain

necessary and sufficient stability range of the modified systems from both the analytical and numerical perspectives.

Stochastic differential equation models have also been developed to analyse the behaviour of the biological systems in order to obtain more realistic solutions [Carletti, 2007, Chen and Chang, 2008, Klimešová, 2015, Qun et al., 2017, Saarinen et al., 2008]. However, no stochastic model of the Arabidopsis flowering has been introduced in the literature yet. Hence, this study represents the first stochastic differential equation model for the GRN of Arabidopsis flowering, which is constructed by incorporating a noise term into the deterministic two differential equations, which is called motif of the dynamical model. Furthermore, the stability behaviour of the stochastic motif models is investigated analytically and numerically by using a Lyapunov function and Ito stochastic formula with the Euler-Maruyama method, respectively, to observe the differences between deterministic and stochastic behaviour of the regulatory network.

Finally, observer and control design methodologies can been applied on the deterministic simplified model to regulate behaviour of the model and estimate non-measured variables from measured ones. Therefore, this study considers an observer design approach, which has been applied by using constant and state-dependent high gain observers. The first one can be simply obtained, being independent of the state variables. However, the second one is more complicated, because it can be obtained from the state variables and performs faster than a normal state observer. Therefore, state-dependent high gain observers are the most commonly used approaches to construct an observer system. The importance of these observers is to estimate the unmeasured variables by using the measured ones, which are the inputs and outputs of the simplified system. Furthermore, the simplified systems can be regulated by a controller (their input) to estimate the variables and to obtain a desired behaviour. To do this, it is necessary to consider the reference value of the measured variable (output) while the non-measured ones are bounded.

1.3 Aims and objectives

The main aim of this study is to investigate the dynamic behaviour of Arabidopsis flowering time gene regulatory network in a more realistic perspective.

The main objectives of this study are:

- Deterministic and stochastic approaches of ordinary and delay differential equation systems that have been inferred from chemical kinetics models (Hill functions) will be used.
- The latest dynamic and quantitative model of Arabidopsis flowering time GRN, proposed by Valentim et al. [2015], will be introduced, and a literature review of the existing studies on that topic with different types of models will be given.
- Steady state and stability analysis of the original dynamic model will be numerically and analytically investigated.
- A simplified model will be analytically constituted by decoupling some concentrations in the original model, and the results will be numerically compared with the original model.
- Motif models of the simplified system will be constructed by considering the behaviour of the original model. They will be analytically calculated to find the range of the parameters for stability of Arabidopsis flowering motifs. Threshold values of concentrations for flowering process in meristem and input parameter values in motifs, which gives the best matching with the original model, will been obtained, and the results will then be discussed numerically.
- Stochastic motifs will be provided with additive and multiplicative white noise.
- Analytical investigation for the local stability of the deterministic and stochastic motifs will be performed to provide explicit conditions for the flowering regulation.

- Observer design of the simplified model will be studied to estimate unmeasured variables in the system by investigating the available experimental measurements of the inputs and outputs of this model.

- A control feedback design will be investigated for the simplified model to modify it by controlling the input variable and to obtain a desired behaviour of the model by targeting a reference output variable.

1.4 Contributions of the thesis

The contributions of this thesis can be listed as follows:

- This thesis contributes the first stability analysis of a dynamical model, constructed for the flowering of *Arabidopsis Thaliana* GRN, in order to represent the importance of steady state and stability of the model for the flowering behaviour.

- This thesis introduces a simplified version of the original dynamical model and its motifs with three and two differential equations, respectively, which is confirmed from numerical solutions that they represent the same behaviour of the original model.

- This thesis analytically investigates the possible range of parameters in motif models for stability of Arabidopsis flowering. Moreover, it analytically and numerically obtains threshold values of concentrations for initiation of flowering process in meristem and necessary input parameter values in motifs for the best matching with the original model.

- This study introduces the first stochastic model for the Arabidopsis flowering, which is formed by using Ito stochastic formula and adding noise terms into the deterministic motif. Analytical and numerical solutions of the stochastic motif have been investigated in probability. The aim is to reveal the effect of noise terms on switching behaviour from non-flowering to flowering.

- This thesis presents observer design approaches to obtain unmeasured variables by using measured ones in the simplified deterministic model. Furthermore, this study produces a way to obtain a desired behaviour by using control design.

Elements of the research introduced in this thesis have also been submitted for publication and presented in conferences as follows:

Journal Papers

- Haspolat, E., Huard, B., Angelova, M. Deterministic and stochastic models of *Arabidopsis Thaliana* flowering. Bulletin of Mathematical Biology - Springer (Submitted).
- Haspolat, E., Huard, B., Krishna, B. Observer design approach for *Arabidopsis Thaliana* flowering model. (in Preparation).

Presentations

- Haspolat, E., Huard, B., Angelova, M. (2016, June 20th) Stability Analysis for a Dynamic Model of Arabidopsis Flowering Gene Regulatory Network.
  EE PGR Conference 2016, Northumbria University, UK.
- Haspolat, E., Huard, B., Angelova, M. (2016, July 14th) Stability Analysis of Network Motifs for Arabidopsis Flowering Gene Regulatory Network.
  ECMTB/SMB 2016, Nottingham, UK.
- Haspolat, E., Huard, B., Angelova, M. (2017, May 24th) Deterministic and Stochastic Stability of Arabidopsis Flowering Model. 2017 SIAM Conference on Dynamical Systems, Utah, USA.
- Haspolat, E., Huard, B., Angelova, M. (2017, June 15th) Deterministic and Stochastic Stability Analyses and Observation Design of Arabidopsis Flowering Model.
  EE PGR Conference 2017, Northumbria University, UK.

Poster

- Haspolat, E. (2014) Gene expression modelling by using ordinary differential equations. PhD Summer School: Methods for Mathematical and Empirical Analysis of Microbial Communities, Isaac Newton Institute for Mathematical Sciences, Cambridge, UK. Date viewed: 29th October.

1.5 Outline of the thesis

The thesis is structured into seven chapters. Following the introductory chapter, a mathematical background of GRNs and their dynamical modelling with both deterministic and stochastic differential equations are given in Chapter 2. Moreover, the stability analysis of these dynamic models and their estimation approaches are introduced, and observer and control design methodologies are reviewed alongside the motivation of the thesis.

Chapter 3 gives an overview of the literature for an *Arabidopsis Thaliana* flowering time GRN and one example network with its deterministic dynamic model constructed with delay differential equations by Valentim et al. [2015]. This chapter also presents steady state and stability solutions of the dynamic model by considering the linearisation of the model around the equilibrium point and produces numerical simulation of the steady state results.

In Chapter 4, simplification approaches for the full deterministic dynamic model, given in Chapter 3, is studied by considering the main concentrations for flowering process. Deterministic motif models are introduced and their analytical and numerical solutions are given.

Stochastic versions of the motif model, constructed with additive and multiplicative white noise, are introduced in Chapter 5, and stochastic stabilities of the models are analytically and numerically studied to analyse the effect of noise terms on stability domain of the motif models.

In Chapter 6, two different closed-loop observers for the simplified model are designed to estimate non-measured variables and their results are compared. This chapter also gives a control design approach for the simplified model and its observer to regulate behaviour of the systems by a controller (input variable) depend on state and output variables.

Finally, all works and their results, studied in this thesis, are summarised in Chapter 7. Moreover, some possible perspectives for future works are provided.

Chapter 2

Background for mathematical modelling of gene regulatory networks

This chapter gives a brief introduction for gene regulatory networks modelling. The study of non-linear dynamical systems for the gene regulatory networks are currently an extensive field of research in biology. The aim of this thesis is to focus the application of mathematical aspects of non-linear systems and control theory to Arabidopsis flowering time gene regulatory networks, which have specific importance to the biological system considered.

2.1 Background of gene regulatory networks

Gene regulatory network is defined by Emmert-Streib et al. [2014] as follows:

Definition 2.1. A gene regulatory network (GRN) is a network which has been inferred from gene expression data.

More extensively, a gene network consists of a set of genes and transcription elements that interact with each other to control a significant cell function. Expression of gene levels is regulated by two sequential processes, namely transcription and translation. The main components are therefore genes, cis-components (areas of non-coding DNA) and transcription elements (e.g., proteins, RNAs and metabolites). The gene expression level during the transcription process is regulated by binding and interactions of these transcription elements to the cis-components in the cis-area of genes. The input signals, interceded by the transcription elements, are collected with the help of the cis-areas. Subsequently, these cis-areas produce particular expression signal for the target gene [Filkov, 2005]. An example of a gene regulation process with its components and interactions of them with each other is shown in following Figure 2.1.

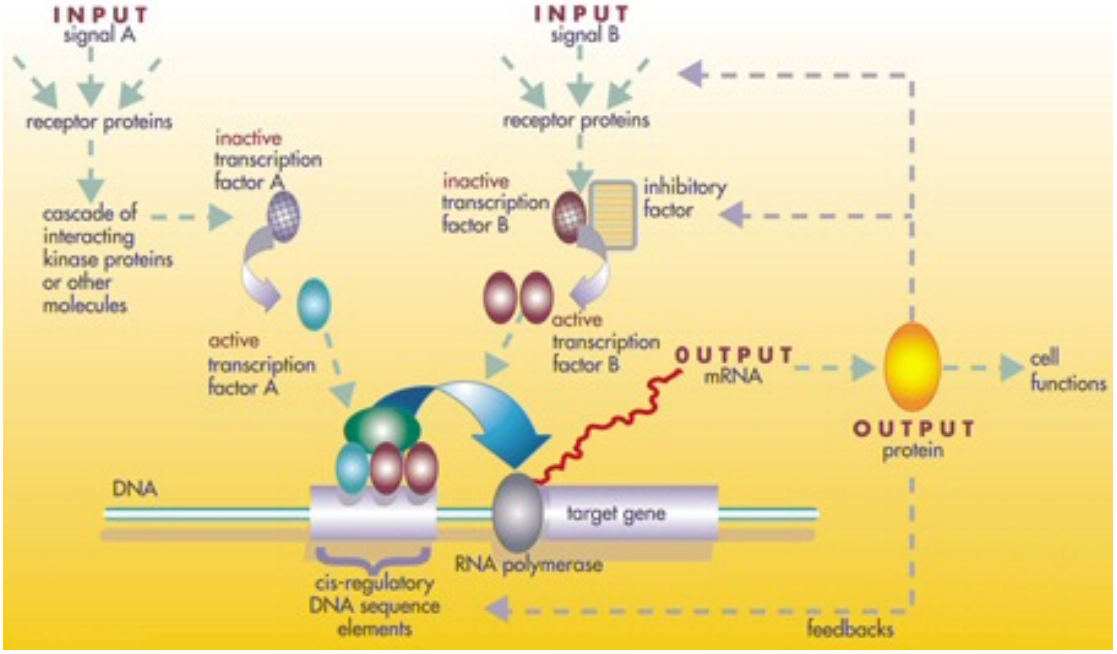

FIGURE 2.1: An example figure of gene regulatory network [Koyuturk, 2007].

There is a variety of gene network modelling levels relying on the degree of concept and accessibility of observational data. They also rely on the analysis aim and objective that might be an assumption testing or complex quantitative network modelling [Emmert-Streib et al., 2014, Filkov, 2005].

Numerous different computational models have been developed for regulatory network analysis. Logical models, which are qualitative approaches to identify the regulatory

networks, are an example of these computational models. An essential comprehension of the various functionalities of a specified network in several states can be achieved with them. Some examples of these models are Boolean networks [Akutsu et al., 1999, Wang et al., 2012] and Bayesian networks [Friedman et al., 2000, Kim et al., 2003].

- **Boolean Networks:** Boolean network models, being one of the widely studied models and the simplest assumption in GRNs, depend on the propositional logic that has an expression level either ON (expressed, active) or OFF (not expressed, inactive) for genes and cells [Chaves et al., 2006, Jönsson, 2005]. They are discrete dynamical networks, and they have been first introduced by Kauffman in 1969 [Hecker et al., 2009, Kaderali and Radde, 2008]. A Boolean network is a directed graph. It can be described as $G = (X, F)$, where $X = (x_1, x_2, ..., x_n)$ is a set of nodes (a vector of Boolean variables), and $F = (f_1, f_2, ..., f_n)$ is a set of Boolean functions. The x_i, $i = \{1, ..., n\}$, symbolise the genes in gene expression networks and the f_i, $f_i : \{0, 1\}^k \longrightarrow \{0, 1\}, k \leq n$, represents the links between them. The values of all nodes identify the state of network at given time t as $x(t) = (x_1(t), x_2(t), ..., x_n(t))$. The corresponding Boolean interactions are being performed to move on to the next step for the state of each gene. The nodes X are updated simultaneously, with the help of Boolean function F and, these updated nodes are deterministic at discrete time-steps, $x(t + 1) = f_i(x_{i1}(t), x_{i2}(t), ..., x_{ik}(t))$.

The description of Boolean networks is uncomplicated and, they are suitable to use for simulation of GRNs [Hecker et al., 2009]. Moreover, a large number of computational methods can be applied to build a Boolean network and this network can be deduced from time course data if there is existing experimental data [Lee and Tzou, 2009]. According to Thieffry and Thomas [1997], a logical Boolean model can be utilised to provide an early examination of a differential model that will help to clarify and create a more advanced version. However, due to Boolean networks being discrete, the dynamics of network cannot be obtained precisely [De Jong, 2002]. Even if they are interesting and efficient in the modelling of regulatory networks because of their simplicity, easy application and fast implementation [Kaderali and Radde, 2008], these models have some problems. They do not include any kinetic constants or continuous

variables [Kim et al., 2007], therefore, noisy data may cause computational instability. Due to the low resolution compared to other models, Boolean models cannot help to solve highly complex problems and have been shown to be incapable of capturing important details of system behaviour.

- **Bayesian Networks:** Bayesian networks belong to the class of graphical probabilistic models, which integrate probability and graph theory. These networks have been first seen in artificial network studies at the end of 1970s [Nielsen et al., 2012, Nielsen, 2003]. They have also started to be used in the study of gene expression data since the end of the 1990s [Friedman et al., 2000]. The aim of Bayesian networks is to construct the GRNs by using gene expression data to ideally describe the measured data. These networks help to realise the transcriptional regulation process by revealing the dependence system among gene expression levels. A Bayesian network is composed of a directed acyclic graph $G(X, E)$, where the nodes $X_1, ..., X_n$ are random variables, symbolise the genes' expression levels and edges point out the interaction between the nodes. Conditional probability distributions $P(x_i|P_a(x_i))$, where $i = 1, \ldots, n$ and $P_a(x_i)$ is the group of parents for each node, help to achieve the random variables. A scoring function is commonly created to benchmark every network, and a heuristic investigation into the solution space selects the best network. One vital feature for this causal network method is the observation for components that are frequently found in high-scoring networks, rather than looking for one single model that clarifies the data [Gebert et al., 2007].

An advantage of Bayesian networks is that they are able to include the prior knowledge and provide tools for approaching missing data. On the other hand, a dynamical form of gene regulation cannot be derived from Bayesian network models. Some applications of this model may have restricted capacity to manage the continuous data. Such information for the most part should be separated into discrete states. The states need to involve interim values that characterise the aggregate scope of values the continuous variable can expect. Even though discretising is an advantageous approach to control

the system size, discrete states may not catch the first dispersion of the variable totally and can prompt lower exactness of variable values [Kragt, 2009].

Continuous models are another example. They were developed to understand and control the behaviour of molecular concentrations in GRNs that depend on time [Cao et al., 2012, Chen et al., 1999, De Hoon et al., 2002, de Hoon et al., 2002, De Jong, 2002]. Some other modelling methods that are used to predict GRNs are: state-space model [Wu et al., 2004], artificial neural networks [Lee and Yang, 2008], dynamics bayesian networks [Li et al., 2007] and stochastic models [Chen et al., 2005, Shmulevich and Aitchison, 2009].

The flowering time regulation pathway of *Arabidopsis Thaliana* has been widely examined in the literature and shown to involve a large complex network. A qualitative approach helps to identify which genes direct one another in flowering time regulation. In addition to this method, a quantitative approach provides an understanding of the numerical amounts of gene products involved in the interactions. Therefore, a quantitative and dynamic modelling of *Arabidopsis Thaliana* flowering time GRN, based on a system of differential equations with numerous parameters, is required. In recent years, a few studies have been introduced with that aim [Jaeger et al., 2013, Valentim et al., 2015, Wang et al., 2014].

In this work, we consider quantitative models, in the form of deterministic and stochastic differential equations, and study their behaviour using stability analysis and control design methods.

2.2 Quantitative modelling of gene regulatory networks

Quantitative mathematical models have an essential place in GRNs to characterise the functions in complex network systems. The dynamics of GRNs can be quantitatively modelled by differential equations to capture the behaviour of gene expression. Ordinary and delay differential equations (ODEs, DDEs) in deterministic or stochastic form, are frequently used modelling approaches in GRN. The equations can be either linear

or non-linear. Linear equations are generally easier to treat, but the non-linear forms very often provide a better description of the GRN and allow to study more complex phenomena.

The formalisation of gene expression dynamics into a general deterministic differential equations system can be written as

$$\frac{dx_i}{dt} = f_i(x_1(t), x_2(t), ..., x_m(t)), \quad (i = 1, 2, ..., n), \quad n \in \mathbb{N}, \tag{2.1}$$

where $x_i = (x_1, x_2, ..., x_n)$ is the vector components of the system representing concentration variables, more precisely, x_i defines the expression level of gene i at time t as a continuous function. The functions $f_i = (f_1, f_2, ..., f_n)$ measure the mutual impact of its arguments or regulators on the x_i. Moreover, each f_i function comprises the biochemical effects of interactions and degradations. The input argument set $(x_1, x_2, ..., x_m)$, $m \geq n$, in the f_i function, which generates an output rate of each gene, represents a subset of x_i functions [Filkov, 2005]. The definition of f and the value of parameters fitted using parameters evaluated signals x at time t is the meaning of GRNs inference [Hecker et al., 2009, Ristevski, 2013].

To build an identification model of GRNs, differential equations rely on where the concentration of genes, proteins, mRNA and different molecules are frequently utilised as essential variables. These variables consist of non-negative real numbers, and they are expected to change persistently in time. In the following subsections, deterministic ordinary and delay differential equations and their general stochastic counterparts will be introduced.

2.2.1 Deterministic differential equations

2.2.1.1 Ordinary differential equations

Ordinary Differential Equations (ODEs) are a good model to identify GRNs as they describe changes of the concentration of any metabolites over time and are widely used in the modelling of biological systems [Masoudi-Nejad et al., 2015]. They describe a

deterministic or stochastic quantitative variation of a system in an interval of time with details [Kaderali and Radde, 2008]. One of the main differences of differential equation models in GRNs from other models is that they use continuous variables instead of discrete variables and thus, they are appropriate modelling methods in dynamic systems of GRNs.

Many examples of applications of ODEs for the study of complex GRNs can be seen. For instance, Sakamoto and Iba [2001] utilised the observed gene expression time-series data to show the definition of an arbitrary GRN by using an evolutionary method (EM). This network model was based on an ODE system. A similar approach was employed by Iba [2008]. Unlike the previous study, Iba extended the method to the derivation of systems of differential equation with transcendental functions. Similarly, Ando et al. [2002] used a hybrid evolutionary modelling method to form of a system of differential equations from observed time-series data. They also used a hybrid EM method of genetic programming (GP) and least mean squares (LMS) methods to describe a brief regulation form among variables. The target networks in this study are selected from the chemical reaction model, metabolic network (E-cell simulation model) and S-system gene network models. In [de Hoon et al., 2002] and [De Hoon et al., 2002], authors applied a linear system of differential equations to identify a method for inferring sparseness' degree of the GRNs from time-series gene expression data. They used Akaike's Information Criterion to predict the number of non-zero coefficients of their system from the data.

Discrete-time gene expression models have a limited place for the application of general biological data sets. Therefore, a continuous-time ODEs model was developed to identify the process description of gene expression models [Zak et al., 2003]. This ODEs model was used in three simulated systems application. These are linear gene expression models, auto-regulatory gene expression model and microarray data from a non-linear transcriptional network, respectively. The methodology was commonly appropriate for recognizing gene expression progress models, fit for precisely distinguishing parameters for little quantities of data samples in the existence of simple test noise [Zak et al., 2003]. Tabus et al. [2004] also used gene expression time-series data to constituting GRNs. Their aim was to determine gene-gene collaborations and to infer

the gene regulatory network system by testing gene expression data. They introduced an algorithm to derive the GRN systems by working with the exact solutions of the differential equations while the current derivation of the network structure of genetic algorithms depended on the change of differential equation systems into an approximate discretized framework. Gebert et al. [2007] investigated many data around a state of cell that are produced by microarray chips to portray the regulation systems inside a cell. They introduced a model depending on time-series that is composed of linear differential equations for illustration of the interaction between genes and the building of the elemental regulatory network. Their model was catching the most pertinent regulating cooperation and presented a methodology based on the discrete least squares approximation to compute model parameters from time-series data [Gebert et al., 2007].

In addition of these examples, ODE models have been seen in GRNs to constitute from linear types of simple models to non-linear systems of complex models such as linear, piecewise linear, pseudo-linear or continuous non-linear [De Jong, 2002, Kaderali and Radde, 2008].

In the equation (2.1), the function f can be either linear or non-linear. These linear and non-linear differential equations have an important place in the approaches of GRNs inference. One of the first example for the modelling of GRNs through the linear ODEs can be seen in [Chen et al., 1999] which presents a simple linear function formalisation as

$$f(x(t)) = Kx(t),$$

where K is a constant $n \times n$ matrix, f is a linear function of x and t is time. The advantage of linear ODEs models is that they have analytical solutions. However, the concentrations in the linear models are not always being non-negative and bounded in GRNs. Additionally, they cannot capture the non-linear phenomena (oscillations and multistationary) that are the most important points of an appropriate biological network. Therefore, linear models are generally not the best solutions for the regulatory networks [Kaderali and Radde, 2008].

The non-linear ordinary differential equation models describe the non-negative concentrations of gene products such as protein, mRNA and other molecules by continuous, time dependent variables. The values of variables are also non-negative. Equation system (2.1) can be a formal description of the non-linear ODEs for the GRNs, where f_i is the non-linear function which performs as an interaction of the regulatory system.

Non-linear ODEs are more accurate models for the dynamic systems of GRNs, though they are not as easy to solve as linear equations. Therefore, many recent papers are established based on non-linear differential equations [Floares and Birlutiu, 2012, Wu et al., 2014, Zhang et al., 2013].

2.2.1.2 Delay differential equations

Delay differential equations (DDEs) have been utilised in many biological applications in the numerical formulation of real life phenomena such as modelling of genetic regulation [Ling et al., 2012] and population dynamics [Bocharov and Rihan, 2000]. In contrast to ODEs, the evolution of system at a determined time instant depends of the condition of the system at prior times in DDEs. This requires to transform equations (2.1) into a delay differential system by incorporating delays occurring in the translation, transcription and other synthesis processes or in the protein transports. Recasting system (2.1) into DDEs helps explain the effect of delays caused by the aforementioned mechanisms [De Jong and Geiselmann, 2005]. An example of non-linear DDE system with related history functions $H(t)$ in a given time interval is formalized as:

$$\begin{aligned} \frac{dx_i}{dt} &= f_i(t, x(t), x(t-\tau_1), x(t-\tau_2), ..., x(t-\tau_m)),\ t \geq t_{in}, \\ x(t) &= H(t),\ m \leq t \leq t_{in}, \end{aligned} \tag{2.2}$$

where $x(t) \in R^n$, $x(t-\tau_i)$ are the delayed terms, $m = min_{1\leq i\leq m}\{min_{t\geq t_{in}}(t-\tau_i)\}$, and the delays $\{\tau_i\}_{i=1}^m$ are unknown, non-negative and constant [Mehrkanoon et al., 2014].

In this study, the first and only system of delay differential equations for the Arabidopsis flowering GRN in the literature, introduced by Valentim et al. [2015], will be studied, and will be used to constitute new reduced models.

2.2.2 Stochastic approach for differential equations

Deterministic approaches only consider the dynamics of internal changes in systems. However, there are also non-modelled external effects in real life systems which cannot be included in deterministic models. Therefore, stochastic approaches are becoming more important to understand and analyse the behaviour of real life systems in a more realistic perspective.

A stochastic differential equation (SDE) consists in a deterministic differential equation into which noise terms are incorporated. SDEs are used to model systems coming from many fields such as finance, physics, control and biology where random phenomena can be important. The main aim of SDE models is to observe changes of behaviour that can occur in the presence of random noise, also called Wiener processes or Brownian motion, to obtain more realistic solutions.

Before we define a Wiener process, which is the most important stochastic process in continuous systems, it is necessary to introduce the following definitions [Socha, 2007].

Definition 2.2 (**Stochastic Processes:**). Let $I \subset \mathbb{R}$. A family $W = \{W(t)\}_{t\in I}$ of $\mathbb{R}$-valued random variables $W(t)$, $t \in I$, defined on Ω is called a **stochastic process**. The process W is said to be a stochastic process in discrete time if I is discrete (e.g. $I = \{1, 2, \cdots\}$) and in continuous time if I is an interval (e.g. $I = [0, \infty]$).

Throughout this section, unless otherwise specified, $W = \{W(t)\}_{t\geq 0}$ is a stochastic process.

Definition 2.3. A stochastic process $\{W(t)\}_{t\geq 0}$ is said to have *independent increments* if for any $0 \leq t_0 < t_1 < ... < t_n < \infty$, random variables $W(t_0)$, $W(t_1) - W(t_0)$, $W(t_2) - W(t_1)$,...,$W(t_n) - W(t_{n-1})$ are independent.

Definition 2.4. A stochastic process $\{W(t)\}_{t\geq 0}$ with independent increments is said to have stationary independent increments if its increments $W(t_1)-W(t_0)$, $W(t_2)-W(t_1)$,...,$W(t_n)-W(t_{n-1})$ depend only on differences $t_1 - t_0$, $t_2 - t_1$,...,$t_n - t_{n-1}$ respectively.

The stochastic process with stationary independent increments have very important place in stochastic analysis, and they are called as Wiener process (or Brownian motion), defined as follow.

Definition 2.5 (Wiener process)**.** A stochastic process $\{W(t)\}_{t\geq 0}$ is called a Wiener process (or Brownian motion), if the following conditions satisfy:

1. $W(0) = 0$, (with probability 1).
2. $\{W(t)\}_{t\geq 0}$ has independent increments such as the increment $W(t) - W(s)$ is independent with the increment $W(u) - W(v)$ for $0 \leq v < u < s < t \leq T$.
3. The increment $W(t) - W(s)$ is normally distributed with mean zero $\mathcal{N}_m(0, 1)$ and variance $\Delta_t = t - s$ as $W(s + \Delta_t) - W(s) \sim \mathcal{N}_m(0, \Delta_t)$ for $0 \leq s < t \leq T$.

   In other words, the increments follow a Gaussian distribution,

$$\mathbb{E}[W(t) - W(s)] = 0, \tag{2.3}$$

$$\mathbb{E}\big[(W(t) - W(s))^2\big] = \sigma^2|t - s|, \tag{2.4}$$

   where σ^2 is positive constant.

Most of the realisations of $\{W(t)\}_{t\geq 0}$ are continuous. In the case when $\sigma^2 = 1$, $\{W(t)\}_{t\geq 0}$ is called a standard Wiener motion.

Definition 2.6. A stochastic process $W(t) = (W_1(t), W_2(t), ..., W_d(t))$, $t \geq 0$ is called a d-dimensional Wiener process if for each $i = 1, 2, ..., d$, the process $W_i(t)$, $t \geq 0$, is a Wiener process and all processes $W_i(t)$ are mutually independent.

Definition 2.7. A generalised derivative of a Wiener process $W(t)$ for $t \geq 0$, which can be demonstrated as $\dfrac{dW(t)}{dt} = \eta(t)$, is called a Gaussian white noise, and it is particularly used in the form $dW(t) = \eta(t)dt$.

Using these definitions, an SDE model for random variable X in terms of Wiener process can be introduced with continuous functions F and G as

$$dX(t) = F(t, X(t))dt + G(t, X(t))dW(t). \tag{2.5}$$

or equivalently as a stochastic integral equation as follows

$$X(t) = X(0) + \int_0^t F(s, X(s))ds + \int_0^t G(s, X(s))dW(s). \tag{2.6}$$

An important result regarding equation (2.5) is Ito's formula. Now, we can introduce Ito stochastic differential equations.

2.2.2.1 Itô stochastic differential equations

A system of Itô stochastic differential equations on the interval [0, T] has the form

$$X(t) = X(0) + \int_0^t F(s, X(s))ds + \sum_{j=1}^{m} \int_0^t G_j(s, X(s))dW_j(s), \quad s \geq 0, \tag{2.7}$$

where $W(t) = [W_1(t), W_2(t), ..., W_m(t)]^T$ is an m-dimensional vector of independent standard Wiener processes on the probability space, $F : [0, T] \times R^n \to R^n$ and $G : [0, T] \times R^n \to R^{n \times m}$ are measurable functions. The process $X(t) = [X_1(t), X_2(t), ..., X_m(t)]^T$ is the solution of the stochastic differential equation

$$dX_i(t) = F_i(t, X(t))dt + G_i(t, X(t))dW_i(t),$$

for $0 \leq t \leq T$ and $i = 1, 2, ..., n$.

2.3 Hill functions

Hill functions represent a more extensive form of Michaelis-Menten function and provide a good approach to represent non-linear biochemical reactions. As such, they are commonly used in enzyme kinetics modeling [Chen et al., 2017, Cosentino and Bates, 2011, Murray, 2002].

A reaction rate equation for the enzyme kinetics can be represented as

$$E + nS \underset{k_2}{\overset{k_1}{\rightleftharpoons}} ES_n \xrightarrow{k_3} P + E. \tag{2.8}$$

where k_i, $\{i = 1, 2, 3\}$, are constant reaction rates, and n presents inhibition ($n < 1$) and activation ($n \geq 1$) of the process. Equation (2.8) represents that an enzyme E reacts with n substrates nS to form a complex ES_n which is transformed into the enzyme and product form P.

Let us define $K_m = \dfrac{k_2 + k_3}{k_1}$ as an equilibrium constant and $V_{max} = k_2 E$ as a maximum reaction velocity. By using for n substrate molecules with n equilibrium constants, the production rate can be formulated as a Hill equation

$$\frac{dP}{dt} = \frac{V_{max} S^n}{K_m^n + S^n}. \tag{2.9}$$

Non-linear Hill-type functions are extensively used in higher-level models of gene regulatory networks. An example of a simple activation–inhibition network with two genes is shown in Figure 2.2. *Gene*1 and *Gene*2 that are transported by the DNA, P_1 and P_2 represent the proteins for the inhibitor and activator of *Gene*2 and *Gene*1, respectively.

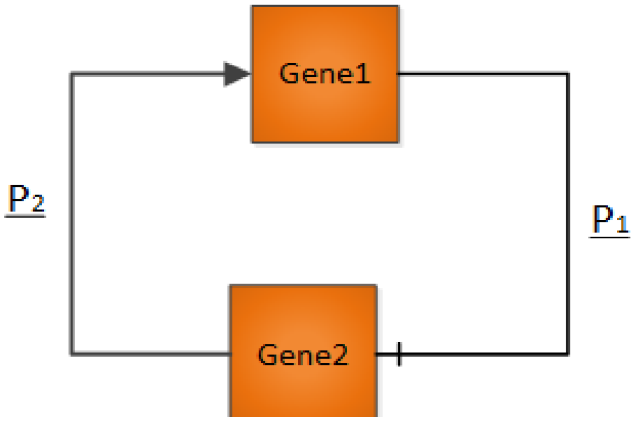

FIGURE 2.2: An example of simplified network model with two genes and their proteins P_1 and P_2 is described.

A simple non-linear ODE model of the dynamics of transcription and translation network can be represented by two differential equations

$$\frac{dx_1}{dt} = \beta_1 h(x_2, k_2, m_2) - d_1 x_1, \tag{2.10}$$

$$\frac{dx_2}{dt} = \beta_2 h(x_1, k_1, m_1) - d_2 x_2, \tag{2.11}$$

where

$$h^-(x_i, k_i, m_i) = \frac{k_i^{m_i}}{k_i^{m_i} + x_i^{m_i}},$$
$$h^+(x_i, k_i, m_i) = \frac{x_i^{m_i}}{k_i^{m_i} + x_i^{m_i}}.$$

In these equations, $h^-(x_i, k_i, m_i)$ represents the Hill function for the inhibition case and $h^+(x_i, k_i, m_i)$ represents the Hill function for the activation case (see Fig. 2.3). All parameters in these equations are positive and defined as below:

- x_1 and x_2 represent the concentration of translated proteins,
- k_1 and k_2 are the expression thresholds,
- m_1 and m_2 are the Hill coefficients representing the cooperativity degree of the interactions,
- β_1 and β_2 are the parameters for the maximum rate of protein synthesis and,
- d_1 and d_2 are the parameters of constant degradation rates.

The first terms in the right-hand side of equations (2.10) and (2.11), $\beta_1 h(x_2, k_2, m_2)$ and $\beta_2 h(x_1, k_1, m_1)$, account for inhibition and activation effects, respectively. The degradation of proteins is generally not regulated, which means they depend only on their own concentrations. Therefore, the degradation terms of the equations in (2.10) and (2.11) are taken as $d_1 x_1$ and $d_2 x_2$, respectively.

In the following chapters, non-linear Hill functions, which are commonly utilised as an activity switch for modelling of step-regulated reactions [Chen et al., 2017], are considered in the form :

$$f(x) = \frac{\beta x^n}{k^n + x^n}, \tag{2.12}$$

where β and k are the Hill coefficients with the same meaning as in equations (2.10) and (2.11). The coefficient k determines the turning point of the functions, which can be seen in Figures 2.3 and 2.4 for $k = 1$ and $k = 2$, respectively. Therefore, it is also

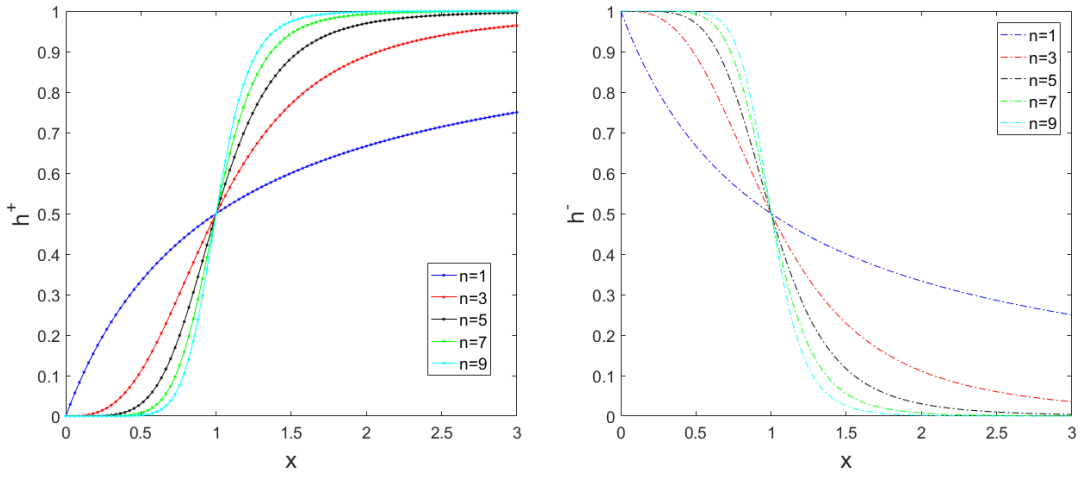

FIGURE 2.3: Hill function representation for inhibition and activation for $k = 1$.

called half maximal output. The value of β determines the maximum output of the Hill function which is set as $\beta = 1$ in Figure 2.3 and $\beta = 10$ in Figure 2.4.

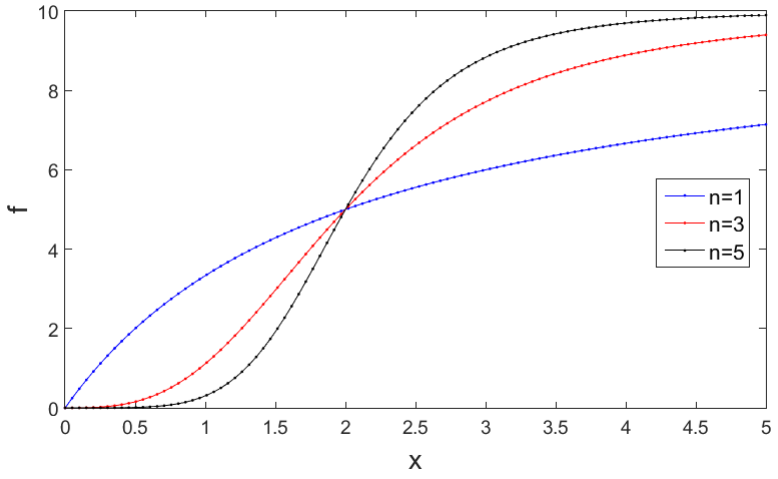

FIGURE 2.4: A plot of Hill function f for $k = 2$ and $\beta = 10$ within range $0 \leq x \leq 5$.

2.4 Stability analysis of dynamic models

Stability analysis of non-linear differential equations systems with numerical simulations is an important approach to understand their behaviour. Stability analysis is generally difficult for large systems of non-linear differential equations. Linearisation around steady states is a general approach to investigate local stability of a non-linear system

by studying a linear system. In this section, stability of a sample dynamic model for a small network will be discussed. Hence, equilibrium points and nullclines, which are important concepts for the stability analysis of a differential equations system, will be introduced.

A system of differential equations with two independent variables x_1 and x_2 can be defined as

$$\begin{aligned} \dot{x}_1(t) &= f(x_1(t), x_2(t), k) \\ \dot{x}_2(t) &= g(x_1(t), x_2(t), k) \end{aligned} \tag{2.13}$$

where k represents external input constants and $\dot{x}_i$ the time derivative of x_i, $\{i = 1, 2\}$. The functions f and g are non-linear and continuous.

The phase plane in (x_1, x_2) coordinates can supply a deeper understanding and global way of looking at the system. It can be constructed for every k by considering each value of time and point of the coordinates and associating a unique vector $(f(x_1, x_2, k), g(x_1, x_2, k))$. Nullclines are zero solutions of the equation $(f, g) = 0$ while x_1-nullcline and x_2-nullcline are defined as the zero solutions of $f(x_1, x_2, k)$ and $g(x_1, x_2, k)$, respectively. The steady states of the system can be obtained from the intersections of these nullclines.

To analyse the local stability of a system of differential equations, at least one steady state point must be present. This fixed point represents a stationary solution for the system dynamics.

Definition 2.8. A point $\bar{x}$ is called a steady state or equilibrium point of $\dot{x} = f(x)$ if $x(t_n) = \bar{x}$ for some t_n implies $x(t_m) = \bar{x}$ for $t_m \geq t_n$. For an autonomous system the set of equilibrium points is equal to the set of real solutions of the equation $f(x) = 0$.

From definition 2.8, steady state $\bar{x}_i$ points are determined by considering the derivative of the variables are equal to zero which means $f(\bar{x}_1, \bar{x}_2, k) = g(\bar{x}_1, \bar{x}_2, k) = 0$. These equilibrium points in non-linear dynamical systems are important to specify the potential starting conditions in phase space that will reach biological significance. At that point one can consider the dynamical system properties close to the equilibria.

Definition 2.9. (Local Stability): Assume that there exists a region nearby an equilibrium point, and a positive constant, ε, corresponding to the distance between boundary of the region and the equilibrium point. If any initial conditions in this region will continue to stay between the equilibrium and boundary of the region as time increases, in other words, the trajectory of system is guaranteed not to move away by more than the distance between boundary of the region and the equilibrium point, then this equilibrium point is said to be locally stable. More formally, an equilibrium point $\bar{x}$ is locally stable if for all $\varepsilon > 0$, there exists a $\delta > 0$ such that

$$\|x(0) - \bar{x}\| < \delta \Rightarrow \|x(t) - \bar{x}\| < \varepsilon \text{ for all } t > 0.$$

Definition 2.10. (Asymptotically Stability): [Cosentino and Bates, 2011] A stable equilibrium point $\bar{x}$ is said to be asymptotically stable if it is stable and the trajectory tends asymptotically to that point,

$$\|x(0) - \bar{x}\| < \delta \Rightarrow \lim_{t\to\infty} \|x(t) - \bar{x}\| = 0.$$

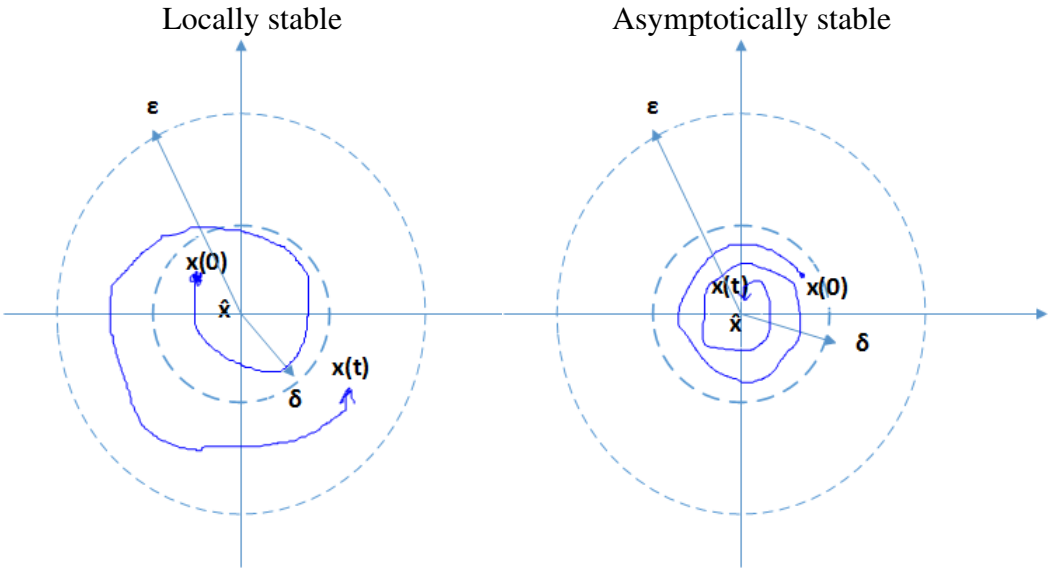

FIGURE 2.5: Local and asymptotic stability of an equilibrium point.

Definition 2.11. (Exponentially Stability): A stable equilibrium point $\bar{x}$ is said to be exponentially stable if there exist two strictly positive numbers λ and α such that

$$\|x(t) - \bar{x}\| \leq \lambda \|x(0) - \bar{x}\| e^{-\alpha t}.$$

If a system has only one stable equilibrium point, and there is no limitation of the initial conditions being in a region, ε, which means for any initial conditions whether they are in or out of the region, ε, will move into and stay in that region as time increase, then the equilibrium point is said to be **globally stable**. Formally, an equilibrium point is globally stable if it is the only fixed point of the system and the trajectories of the solution will move within a region, ε, around that fixed point for any initial condition, $x(0)$, as time increases,

$$x(0) \in \mathbb{R} \Longrightarrow \|x(t) - \bar{x}\| < \varepsilon, \text{ for } t > 0.$$

The local stability of the linearised systems at the fixed points can be analysed by evaluating the matrix of partial derivatives of the system, called Jacobian matrix, given in the following form for the 2×2 system (2.13)

$$J_{(\bar{x}_1,\bar{x}_2)} = \begin{bmatrix} \dfrac{\partial f}{\partial x_1} & \dfrac{\partial f}{\partial x_2} \\ \\ \dfrac{\partial g}{\partial x_1} & \dfrac{\partial g}{\partial x_2} \end{bmatrix}_{|x=\bar{x}}. \tag{2.14}$$

The corresponding linearised system is obtained as:

$$\dot{X} = J_{(\bar{x}_1,\bar{x}_2)}X, \quad X = [x_1, x_2]^T. \tag{2.15}$$

The eigenvalues λ_i, $\{i = 1, 2\}$, which are obtained as the solution of the equation

$$det(J - \lambda I) = 0 \tag{2.16}$$

give information about the behaviour of the system around the equilibrium.

A steady state point in a linearised system is stable if all eigenvalues have negative real parts and it is unstable if there is at least one has positive real part. It is unstable if both eigenvalues have positive real part and a saddle point occurs when they have different

sign. The different behaviours of system trajectories around a steady state point are represented in Figure 2.6.

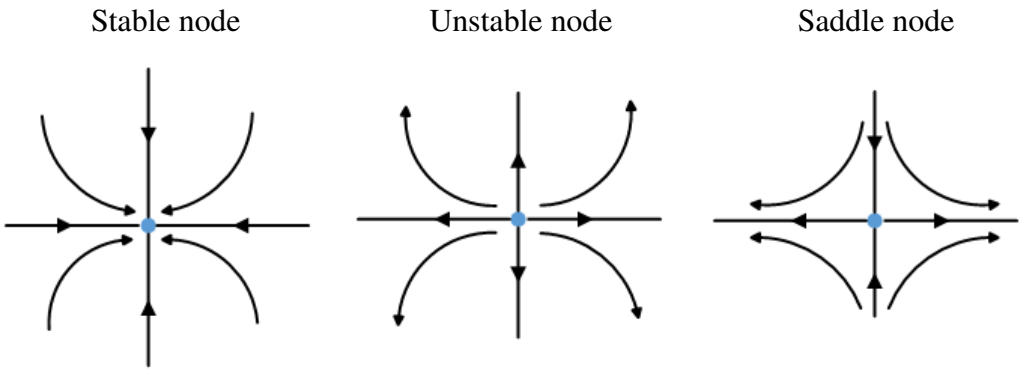

FIGURE 2.6: Phase trajectories around a steady state point.

Stability conditions can generally be formulated by using Routh–Hurwitz stability criterion. Equation (2.16) for an n-dimensional system gives the following n-degree characteristic polynomial,

$$\lambda^n + a_1\lambda^{n-1} + \cdots + a_{n-1} + a_n = 0. \tag{2.17}$$

The Routh-Hurwitz stability criterion provides necessary and sufficient conditions ensuring all roots are either negative or have negative real part. These conditions are obtained by requiring that the following Hurwitz matrices have positive determinant.

$$H_1 = \begin{pmatrix} a_1 \end{pmatrix}, \quad H_2 = \begin{pmatrix} a_1 & 1 \\ a_3 & a_2 \end{pmatrix}, \quad H_3 = \begin{pmatrix} a_1 & 1 & 0 \\ a_3 & a_2 & a_1 \\ a_5 & a_4 & a_3 \end{pmatrix}, \quad \cdots \text{ and,}$$

$$H_n = \begin{pmatrix} a_1 & 1 & 0 & 0 & \cdots & 0 \\ a_3 & a_2 & a_1 & 1 & \cdots & 0 \\ a_5 & a_4 & a_3 & a_2 & \cdots & 0 \\ \vdots & \vdots & \vdots & \vdots & \cdots & \vdots \\ 0 & 0 & 0 & 0 & \cdots & a_n \end{pmatrix}, \quad \text{where } a_j = 0 \text{ if } j > n.$$

The details of the Routh-Hurwitz stability criterion can be found, for instance, in Gantmacher et al. [1960] and Saeed [2008].

Non-linear systems can be understood by describing the linearised system behaviour in regions close to the equilibrium points. However, linearisation can only provide the local behaviour of the non-linear system in the neighbourhood of the steady state point. Analytical description of the stability region is generally difficult task but numerical solutions can be obtained, and approximation to the stability region is possible by using level curves of suitable Lyapunov functions [Al Hokayem and Gallestey, 2017].

2.4.1 Lyapunov and LaSalle stability theories

In this part, we introduce the direct approach to stability, developed by the Russian mathematician Aleksandr Mikhailovich Lyapunov in 1892 [Lyapunov, 1992]. We also present developed versions called LaSalle's or Barbashin-Krasovskii method for invariant and positively invariant sets of non-autonomous systems.

2.4.1.1 Lyapunov's direct method

Lyapunov's second stability theorem, which is known as Lyapunov's direct method, can be stated locally and globally as follows (see e.g. [Cosentino and Bates, 2011, Gallestey et al., 2015, Iglesias and Ingalls, 2010, Lantos and Márton, 2010]).

Theorem 2.12. *Let $\bar{x} \equiv 0$ be an equilibrium point for a continuously differentiable system $\dot{x} = f(x)$ where $x \in \mathcal{D} \subset \mathbb{R}^n$, and $\mathcal{D}$ is defined as a neighborhood of $\bar{x}$. Suppose that there exists a candidate (positive definite) Lyapunov function $V(x) : \mathcal{D} \to \mathbb{R}$ which is continuously differentiable such that*

- $V(0) = 0$, *and*
- $V(x) > 0$, $\forall x \in \mathcal{D}\backslash\{0\}$, *and*
- $\dot{V}(x) = \sum_{j=1}^{n} \frac{\partial V}{\partial x_j}\dot{x}_j = \sum_{j=1}^{n} \frac{\partial V}{\partial x_j} f_j(x) \leq 0$, *(negative semidefinite),*
  then, the equilibrium point $\bar{x} = 0$ is locally stable. If $\dot{V}(x)$ is strictly less than zero,
- $\dot{V}(x) < 0$, *(negative definite),*
  then, the equilibrium point $\bar{x} = 0$ is locally asymptotically stable.

Theorem 2.12 shows that a fixed point $\bar{x}$ is locally stable for all x in the region $\mathcal{D}$ if and only if the derivative of positive definite Lyapunov function, $\dot{V}(x)$, is less than or equal to zero. It is locally asymptotically stable if and only if $\dot{V}(x)$ is strictly less than zero. If the conditions above are satisfied for all $x \in \mathbb{R}$, which means x is not bounded in the defined region $\mathcal{D}$, then $\bar{x}$ is said to be globally asymptotically stable as defined in following theorem.

Theorem 2.13. *Let $\bar{x} \equiv 0$ be an equilibrium point for $\dot{x} = f(x)$. Suppose that there exists a candidate (positive definite) Lyapunov function $V(x) : \mathbb{R}^n \to \mathbb{R}$ which is continuously differentiable such that*

- $V(0) = 0$, *and*
- $V(x) > 0$, $\forall x \neq 0$, *and*
- $V(x) \to \infty$ *as* $\|x\| \to \infty$, *(radially unbounded)*
- $\dot{V}(x) = \sum_{j=1}^{n} \dfrac{\partial V}{\partial x_j} \dot{x}_j = \sum_{j=1}^{n} \dfrac{\partial V}{\partial x_j} f_j(x) \leq 0$,
  then the equilibrium point $\bar{x} = 0$ is globally asymptotically stable.

Additionally, Lyapunov's second method was extended by LaSalle and Barbashin-Krasovskii for locating limit sets of nonautonomous systems which can be seen with the name LaSalle theorem [LaSalle, 1960, 1968] and Barbashin - Krasovskii theorem [Barbashin and Krasovskii, 1961].

2.4.1.2 Barbashin - Krasovski - LaSalle invariance principle

The main difference between Barbashin - Krasovski - LaSalle invariance principle and Lyapunov's theorem is that the candidate function $V(x)$ is not required to be a positive definite function in Barbashin - Krasovski - LaSalle invariance principle. Before defining the Barbashin - Krasovski - LaSalle invariance method, we should give the definition of invariant and positively invariant sets by following [Aström and Murray, 2010, Gallestey et al., 2015, Haddad and Chellaboina, 2011, Khalil, 2002, Lantos and Márton, 2010].

Definition 2.14. A domain $D \subset \mathbb{R}^n$ is said to be an invariant set of a system $\dot{x}(t) = f(x(t))$ if for all initial values of x chosen in D, all trajectories $x(t)$ remain in D. It is positively invariant if all future trajectories remain in D.

Theorem 2.15 (LaSalle invariance principle [Lantos and Márton, 2010])**.** *Suppose that $\bar{x} = 0$ is an equilibrium point of continuously differentiable system $\dot{x} = f(x)$ where $x \in \mathcal{D} \subset \mathbb{R}^n$, and $\mathcal{D}$ is defined as a neighborhood of $\bar{x}$. Suppose that there exists a function $V(x) : \mathcal{D} \to \mathbb{R}$ which is continuously differentiable such that $\dot{V}(x) \leq 0$ in a positively invariant compact set $M \subset D$. Let E be the set of all points in compact set M where $\dot{V}(x) = 0$. Let S be the largest invariant set in E. Then every solution starting in M approaches S as $t \to \infty$.*

The special case of the LaSalle's invariance principle is Barbashin - Krasovskii theorem, can be defined as follow.

Theorem 2.16 (Barbashin - Krasovskii theorem [Khalil, 2002])**.** *Suppose that $\bar{x} = 0$ is an equilibrium point of continuously differentiable system $\dot{x} = f(x)$ such that $f(0) = 0$. Suppose there exists a continuously differentiable positive definite function $V(x) : \mathcal{D} \to \mathbb{R}$, which is on a domain D containing the origin such that*

- $V(x) > 0$, $\forall x \in \mathcal{D} \backslash \{0\}$,
- $\dot{V}(x) = \sum_{j=1}^{n} \frac{\partial V}{\partial x_j} \dot{x}_j = \sum_{j=1}^{n} \frac{\partial V}{\partial x_j} f_j(x) \leq 0$ *on D, and*
- $S = \{x \in D | \dot{V}(x) = 0\}$.

If the only solution that can remain inside S is the trivial solution $x(t) \equiv 0$, then the origin is asymptotically stable.

If V is radially unbounded such that

- $V(x) \to \infty$ *as* $\|x\| \to \infty$, *and*
- $\dot{V}(x) < 0$,

then the origin is globally asymptotically stable.

2.5 Observer and control design

The dynamic behaviour of gene regulatory networks has been analysed by using the mathematical tools given in previous subsections. The same mathematical tools, along with elements of linear algebra, can be employed to synthesise controllers and observers for these systems, which is the main objective of the observer and control design chapter. Before this, we give a preliminary presentation of the observer design approaches from basic to complex gain observers, the theory of state and output feedback controller design and their observer-based approximations for continuous systems of differential equations.

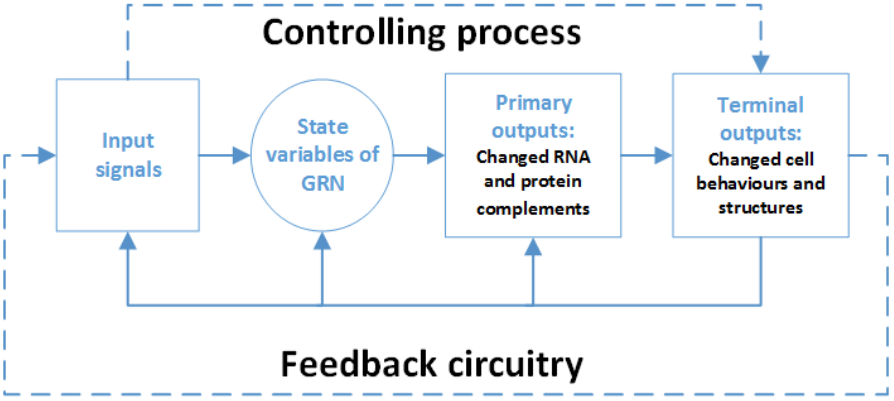

FIGURE 2.7: An example figure for the control process of a gene regulatory network.

2.5.1 Observer design

In this section, a brief background for the observer design and the methods for linear and non-linear differential equations are introduced.

Over the last decades, observer design methodology has been used in many fields, especially in engineering and finance, as well as in biology more recently. Designing an observer for a linear system is relatively simple due to the fact that observability in the linear case is independent of the inputs. However, the task of devising one for non-linear systems proves to be more complex since non-linear observability depends on the inputs; thus giving rise to singular inputs. Therefore, many studies have been presented to develop either general or simpler approaches, depending on the structure of

the nonlinearity as well as on the observability properties of the systems. One particular class of non-linear systems for which observer design is well-established is the class of uniformly observable systems [Gauthier et al., 1992, Gauthier and Kupka, 1994]. This class of systems does not possess any singular inputs; that is, they are observable for all inputs. As a matter of fact, the systems with which we are dealing with in this study are uniformly observable. Many different approaches for observer design of non-linear systems have been proposed in the literature. One such method, the separation approach consists in dividing the system into a linear part and non-linear perturbations, which satisfy a boundedness condition.

An observer is basically a software sensor and corresponds to the initial condition problem, presented in Figure 2.8.

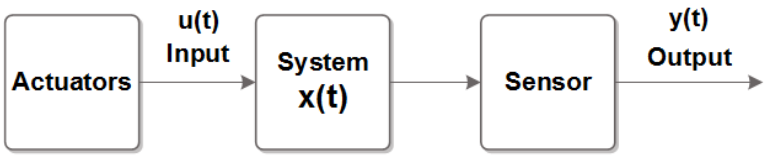

FIGURE 2.8: Principle of a software sensor.

The main purpose of observer in control theory is to provide an online estimation of unmeasured state variables from measurements of the inputs and outputs of a given dynamical system in following non-linear form

$$\begin{aligned} \dot{x}(t) &= f(x(t), u(t)), \\ y(t) &= h(x(t), u(t)). \end{aligned} \tag{2.18}$$

Here, $x(t) \in R^n$, $u(t) \in R^m$ and $y(t) \in R^p$ represent the vector of states, inputs (actuators) and outputs of the dynamical system, respectively, represented as

$$x = \begin{pmatrix} x_1 \\ \vdots \\ x_n \end{pmatrix} \in R^n, \quad u = \begin{pmatrix} u_1 \\ \vdots \\ u_m \end{pmatrix} \in R^m \quad \text{and} \quad y = \begin{pmatrix} y_1 \\ \vdots \\ y_p \end{pmatrix} \in R^p.$$

The linear form of a dynamical system can be written as

$$\begin{aligned} \dot{x}(t) &= Ax(t) + Bu(t) \\ y(t) &= Cx(t), \end{aligned} \tag{2.19}$$

where A, B and C are $n \times n$, $n \times m$ and $p \times n$ constant matrices, respectively.

Note that p should be less than n to enable the observation of a system. Otherwise, there is no need for an observer design as all variables are being measured. Therefore, it is assumed that $p < n$, and this gives that $n - p$ state variables not being measured in the system while p state variables are measured. It is also necessary that the dynamical system should be observable to design its observer. Observability is defined in the following way.

Definition 2.17. (Observability): A system is said to be observable on a time interval $t \in [0, T]$ if for any initial state x_0 and input (control) u, the current state can be obtained in this time interval $[0, T]$ by using only the output signals $y(x_0, u, t)$, which correspond to each initial state. In particular, a (linear or non-linear) system is locally observable on a time interval $[0, T]$ if and only if the Jacobian matrix (for linear or non-linear) of the following map has full rank for a fixed d.

$$\Theta : x \rightarrow \begin{pmatrix} y = h(x, u) \\ \dot{y} = L_f h(x, u) \\ \vdots \\ y^d = L_f^d h(x, u) \end{pmatrix},$$

which means map Θ is locally invertible at the initial state, x_0. Here, $L_f h(x, u)$ represents the Lie derivative of $h(x, u)$ with respect to x along the vector field f, which can be generally formulated as

$$L_f^d h(x) := \frac{\partial L_f^{d-1} h(x)}{\partial x} f(x),$$

where

$$L_f^0 h(x) := h(x).$$

Hence, the Jacobian matrix of the map Θ,

$$\Omega(x) = \frac{d\Theta(x)}{dx},$$

which is also called observability matrix, is required to have full rank at x_0,

$$rank\left(\left.\frac{d\Theta(x)}{dx}\right|_{x=x_0}\right) = n.$$

For linear and non-linear systems, this condition can be expressed as;

For linear systems (2.19)

$$rank\begin{pmatrix} C \\ CA \\ \vdots \\ CA^{n-1} \end{pmatrix} = n$$

For non-linear systems (2.18)

$$rank\begin{pmatrix} \nabla h(x,u) \\ \nabla L_f h(x,u) \\ \vdots \\ \nabla L_f^{n-1} h(x,u) \\ \vdots \end{pmatrix} = n.$$

The observability property does not depend on inputs in linear systems and it is sufficient to consider the sequence $\{C, CA, \cdots, CA^{n-1}\}$, which truncates as a consequence of the Cayley-Hamilton theorem, where the fixed number in the map Θ then can be obtained as $d = n - 1$, due to A^n being expressed in terms of lower powers, $A^n = f(A^{n-1}, A^{n-2}, \cdots, A^0)$. However, for non-linear systems, the sequence $\{\nabla L_f^{n-1} h(x,u)\}$ may not truncate, depending on the nonlinearity structure, and the fixed number d in map Θ cannot be derived like in linear systems since no such theorem exists for non-linear systems.

Figure 2.9 shows a state estimation process by using input, state and output variables of a system and as a result of their state variables in an observer.

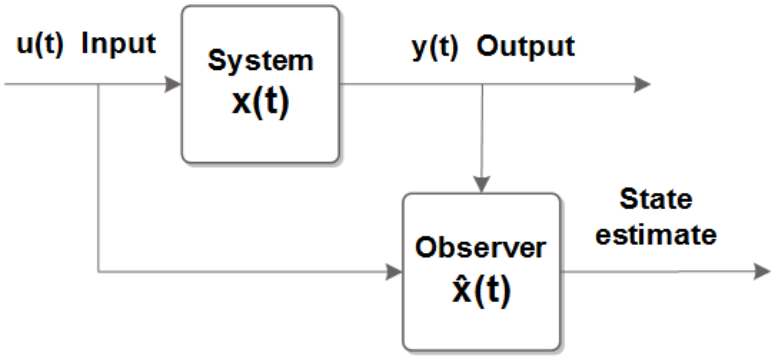

FIGURE 2.9: An example network for a state observer model. Here, u, x and y represent the input, state and output variables of the system, respectively, and $\hat{x}$ represents the state variables of the observer.

For linear systems as given in the form (2.19), the state observer can be written as

$$\begin{aligned} \dot{\hat{x}}(t) &= A\hat{x}(t) + Bu(t) + K(y(t) - \hat{y}(t)) \\ \hat{y}(t) &= C\hat{x}(t), \end{aligned} \tag{2.20}$$

where K is a constant matrix, called the observer gain matrix, chosen such that the dynamics of the absolute observer error $\varepsilon(t) = x(t) - \hat{x}(t)$ converges exponentially and asymptotically to 0,

$$\lim_{t\to\infty} \|\varepsilon(t)\| = \lim_{t\to\infty} \|x(t) - \hat{x}(t)\| = 0.$$

This gives the following error dynamics

$$\begin{aligned} \dot{\varepsilon}(t) &= A(x(t) - \hat{x}(t)) - K(Cx(t) - C\hat{x}(t)) \\ &= (A - KC)\varepsilon, \end{aligned} \tag{2.21}$$

which is required to be stable.

This kind of observer is quite simple because it only involves constant matrices and does not depend on the input and output vectors. The idea here is to choose the gain matrix K such that the eigenvalues of the matrix $(A - KC)$ lie in the left-half complex plane and therefore it will be stable while the error signal goes to zero. This kind of observer ways designed in the early 1960 's [Luenberger, 1964] and is known as a linear Luenberger

observer. The stability of the observer error can be established by using the Lyapunov stability approach as follows.

Let $V(\varepsilon(t)) = \varepsilon^T(t)P\varepsilon(t)$ be chosen as an appropriate candidate Lyapunov function, where P is a symmetric positive definite (SPD) matrix.

Then, the derivative of the Lyapunov function is obtained as

$$\begin{aligned}\dot{V}(\varepsilon(t)) &= \dot{\varepsilon}^T(t)P\varepsilon(t) + \varepsilon^T(t)P\dot{\varepsilon}(t) \\ &= \varepsilon^T(t)(A - KC)^T P\varepsilon(t) + \varepsilon^T(t)P(A - KC)\varepsilon(t) \\ &= \varepsilon^T(t)\Big[(A - KC)^T P + P(A - KC)\Big]\varepsilon(t). \end{aligned} \tag{2.22}$$

Since $(A - KC)$ is assumed to be stable, there exists a SPD matrix Q such that

$$(A - KC)^T P + P(A - KC) = -Q. \tag{2.23}$$

This gives,

$$\dot{V}(\varepsilon(t)) = -\varepsilon^T(t)Q\varepsilon(t) < 0, \tag{2.24}$$

which proves that the chosen Lyapunov function demonstrates the stability of ε.

A state observer of the non-linear system (2.18) can be written as follows:

$$\begin{aligned}\dot{\hat{x}}(t) &= f(\hat{x}(t), u(t)) + K_{(\hat{x},u,y)}(y(t) - \hat{y}(t)) \\ \hat{y}(t) &= h(\hat{x}(t), u(t)), \end{aligned} \tag{2.25}$$

where the observer gain matrix K is a non-linear function and depends on $\hat{x}$, u, y. The function $f : R^n \to R$ is non-linear and it is assumed to be continuously differentiable with respect to x. Moreover, this function is assumed to be globally Lipschitz continuous with respect to x, uniformly in u. Hence, we assume that there exists $\lambda_u > 0$, dependent on u, such that

$$\|f(x, u) - f(\hat{x}, u)\| \leq \lambda_u \|x - \hat{x}\|, \ \forall\ x, \hat{x} \in R^n, u \in R^m.$$

The dynamics of the observer errors can be obtained as

$$\dot{\varepsilon(t)} = f(x(t), u(t)) - f(\hat{x}(t), u(t)) - K_{(\hat{x},u,y)}(y(t) - \hat{y}(t)), \tag{2.26}$$

where the gain matrix must be chosen such that the observer and error dynamics are asymptotically stable. These kinds of systems are more complex and not easy to solve. Many different methodologies to design an observer in both linear and non-linear systems have been devised, such as Kalman Filter [Kalman, 1959] and Luenberger [Luenberger, 1964] style, separation principle [Shiriaev et al., 2008], classical high gain observer [Gauthier et al., 1992], control and non-control affine systems and canonical forms [Gauthier and Kupka, 1994]. The observer design for special classes of non-linear systems has been considered in [Busawon et al., 1998a, Busawon and De Leon-Morales, 1999, Gauthier and Kupka, 2001].

There are different kinds of gain matrices which have been introduced for non-linear systems in the literature. Some of them can be presented as follows.

- A gain matrix for a high gain extended Luenberger observer, introduced by [Gauthier et al., 1992, Gauthier and Kupka, 1994], is defined as

  $$K_{(\hat{x},u,y)} = S_\theta^{-1} C^T = \Delta_\theta^{-1} K.$$

  Here, $\Delta_\theta = diag\left[\frac{1}{\theta}, \frac{1}{\theta^2}, \cdots, \frac{1}{\theta^n}\right]$ is a diagonal matrix and K can be chosen as a column vector $K = col(C_n^1, C_n^2, \cdots, C_n^n)$ where $C_n^p = \frac{n!}{(n-p)!p!}$, while S_θ is the solution of the algebraic equation

  $$-\theta S_\theta - A^T S_\theta - S_\theta A + C^T C = 0,$$

  for θ large enough, $\theta \geq 1$.

  The explicit solution of the algebraic equation is

  $$S_\theta(i, j) = \frac{(-1)^{i+j} C_{i+j-2}^{j-1}}{\theta^{i+j-1}}, \quad i, j = \{1, 2, \cdots, n\},$$

  where S_θ is a symmetric positive definite matrix for every $\theta > 0$. Here, C and the Brunovsky form A matrices are defined as

$$C = \begin{bmatrix} 1 & 0 & \cdots & 0 \end{bmatrix} \in \mathbb{R}^n \quad \text{and} \quad A = \begin{bmatrix} 0 & 1 & & 0 \\ \vdots & \ddots & \ddots & \\ \vdots & & \ddots & 1 \\ 0 & \cdots & \cdots & 0 \end{bmatrix} \in \mathbb{R}^{n\times n}.$$

In fact, it is not necessary that the gain matrix $\Delta_\theta^{-1}K$ be equal to $S_\theta^{-1}C^T$. The main aim of the observation problem consists in finding the gain matrix where $(A-KC)$ is stable so that the observer error $\varepsilon(t) = x(t) - \hat{x}(t)$ converges exponentially and asymptotically towards zero.

- Another gain matrix for a high gain observer, used in [Bououden, 2016, Busawon et al., 1998b], is given as

$$K_{(\hat{x},u,y)} = \Omega^{-1}(\hat{x},u)\Delta_\theta^{-1}K,$$

where $\Omega(\hat{x},u)$ defines the observability matrix $\left(\frac{d\Theta}{dx}\right)_{x=\hat{x}}$.

- For an extension of the gain matrix above, an improvement gain matrix for the high gain observer design is introduced in [Busawon and Leon-Morales, 2000] as

$$K_{(\hat{x},u,y)} = \Omega_1^{-1}(\hat{x},u)[L(\hat{x},u) + \Delta_\theta^{-1}K].$$

For this kind of high gain observer and previous one, the observation problem consists in finding gain matrices $\Omega_1^{-1}(\hat{x},u)[L(\hat{x},u)+\Delta_\theta^{-1}K]$ and $\Omega^{-1}(\hat{x},u)\Delta_\theta^{-1}K$ such that for both of them $(A-KC)$ is stable, and the observer error $\varepsilon(t) = x(t) - \hat{x}(t)$ converges exponentially and asymptotically towards zero. The column vector L and lower triangular matrix Ω_1 can be obtained by applying the following steps [Busawon and De Leon-Morales, 1999, Busawon and Leon-Morales, 2000] :

In the first step, a square matrix $B(\xi,u)$ is obtained by using the lower diagonal (observability) matrix Ω, the Jacobian matrices of f at the point $\xi \in R^n$ with respect to x, and Brunovsky form A as follows

$$B(\xi,u) = \Omega(\xi,u)F(\xi,u)\Omega^{-1}(\xi,u) - A = \begin{bmatrix} 0 & 0 & \cdots & 0 \\ \vdots & \vdots & \vdots & \vdots \\ 0 & 0 & \cdots & 0 \\ b_1(\xi,u) & b_2(\xi,u) & \cdots & b_n(\xi,u) \end{bmatrix}.$$

A column vector $L(\xi, u)$ can be constructed by considering the last row of matrix $B(\xi, u)$ (while the other rows are zero) as

$$L(\xi, u) = col[b_n(\xi, u), \cdots, b_2(\xi, u), b_1(\xi, u)] = \begin{bmatrix} b_n(\xi, u) \\ \vdots \\ b_2(\xi, u) \\ b_1(\xi, u) \end{bmatrix},$$

and this gives a setting matrix $\bar{A}(\xi, u)$

$$\bar{A}(\xi, u) = A + L(\xi, u)C = \begin{bmatrix} b_n(\xi, u) & 1 & & 0 \\ \vdots & & \ddots & \\ b_2(\xi, u) & 0 & & 1 \\ b_1(\xi, u) & 0 & \cdots & 0 \end{bmatrix},$$

which is used to construct a lower triangular matrix $W(\xi, u)$

$$W(\xi, u) = \begin{bmatrix} H(\xi, u) \\ H(\xi, u)\bar{A}(\xi, u) \\ \vdots \\ H(\xi, u)\bar{A}^{n-1}(\xi, u) \end{bmatrix},$$

where $H(\xi, u)$ is the Jacobian matrices of h at the point $\xi \in R^n$ with respect to x. This gives another nonsingular lower triangular matrix

$$\Omega_1(\xi, u) = W^{-1}(\xi, u)\Omega(\xi, u),$$

which has diagonal

$$diag[\Omega_1(\xi, u)] = \left[1, \frac{\partial f^1}{\partial x_2}(\xi, u), \cdots, \prod_{i=1}^{n-1} \frac{\partial f^i}{\partial x_{i+1}}(\xi, u)\right].$$

This kind of gain matrices bring extremely complex observer systems and their simulations are not simple in most of the non-linear systems with Matlab Simulink.

In order to prove the asymptotic stability of errors one again uses a Lyapunov stability approach by choosing a proper Lyapunov function for each observer gain. All details of the matrices above and stability of the systems can be found in [Busawon and De Leon-Morales, 1999, Busawon and Leon-Morales, 2000].

2.5.2 Control design theory

Control theory aims to propose a general methodology for designing control laws in order to modify the behaviour of dynamical systems according to some desired specifications. In practical terms, the aim of control theory is to build a control panel for operating a given dynamical system by a controller with a reformative behaviour. The roles of a controller are given below step by step.

- Monitor the process of a dynamical system by measuring some outputs.
- Comparing this actual behaviour with the desired one.
- Computing reformative operations from output to input of the system based on its dynamical model.
- Applying the controller to obtain a desired solution.

An essential requirement of the control design is that the dynamical system must be controllable, and in contradistinction to observability, controllability depends on the inputs as given following definition.

Definition 2.18. (Controllability): A linear system as given in the form (2.19), is controllable on a time interval $[0, T]$ if and only if the controllability matrix, $M = \left[B\ AB\ \ldots\ A^{n-1}B\right]$ has full rank, i.e.

$$\operatorname{rank}\left[\begin{array}{cccc} B & AB & \cdots & A^{n-1}B \end{array}\right] = n.$$

In biology, the behaviour of a dynamical system with internal variables, which depends on the external (environmental) conditions, changes over time. In control systems, the process starts with a reaction triggered by external inputs which then gives back output signals to their environment. Interactions between (two or more) equations with each other in a dynamical system indicates a feedback process, such as the one presented in Figure 2.10.

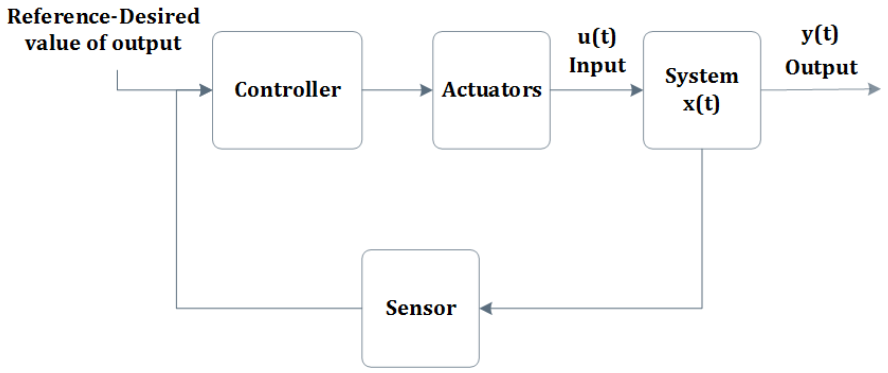

FIGURE 2.10: A representative feedback loop

In following Subsection 2.5.2.1, we introduce two different feedback process of a system: state and output feedback, and we also introduce a feedback approach based on the observer system.

2.5.2.1 State and output feedback control

The local behaviour of a system can be formed by using the state feedback of the system. Controllability helps to understand the necessary feedback approach to be used to design a system dynamics. It is necessary to remember that the dynamics of the closed loop system must be stable (bounded) and must have additional desired behaviour.

Firstly, the construction of state feedback control is introduced by considering the state variables of a system. Then, a second output feedback control is presented, this one based only on the output variable of a system.

Consider again the linear equation which now includes a state feedback

$$\dot{x}(t) = Ax(t) + Bu(t). \tag{2.27}$$

In this case, by defining a control law as,

$$u(t) = -Kx(t), \tag{2.28}$$

which can be replaced in equation (2.27), we find the following closed-loop system

$$\begin{aligned} \dot{x}(t) &= Ax(t) + B(-Kx(t)) \\ &= (A - BK)x(t). \end{aligned} \tag{2.29}$$

The stability of this equation depends on the chosen controller gain K, which has an effect on the eigenvalues of the matrix $(A - BK)$. The above closed-loop system is represented in Figure 2.11.

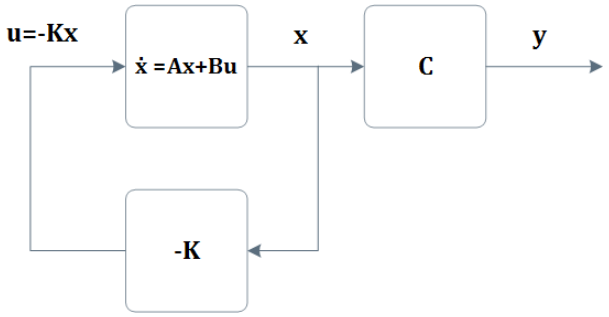

FIGURE 2.11: State feedback controller for the linear systems

By considering the non-linear systems as given in (2.18) before,

$$\dot{x}(t) = f(x(t), u(t)), \tag{2.30}$$

the state feedback can be designed by replacing the input with a control law function $u(x(t)) = \tilde{u}(x(t))$, which gives a closed loop system as follows:

$$\dot{x}(t) = f(x(t), \tilde{u}(x(t))). \tag{2.31}$$

The following Figure 2.12 represents the network of the process for non-linear state feedback control.

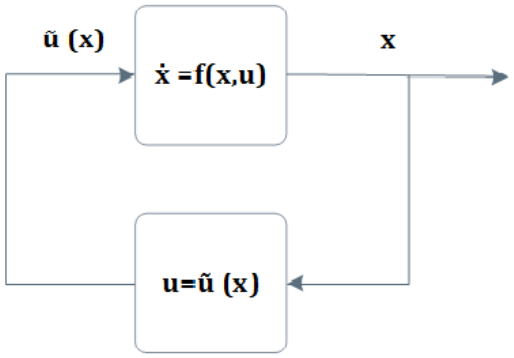

FIGURE 2.12: State feedback controller for non-linear systems

Remarks 1. The above state feedback controllers cannot be applied in practice if the state variables x are not measured. For this reasons, sometimes output feedback controllers are preferred. However, output feedback controllers have only a limited region of stability.

Output feedback controller design is obtained by making use only of the output $y(t)$ of a system, and not from any other state of the system.

The linear and non-linear output feedbacks can then be obtained by replacing the input in a system as $u(t) = -Ky(t)$ and $u = \tilde{u}(y(t))$, respectively. This leads to the diagrams presented in Figure 2.13.

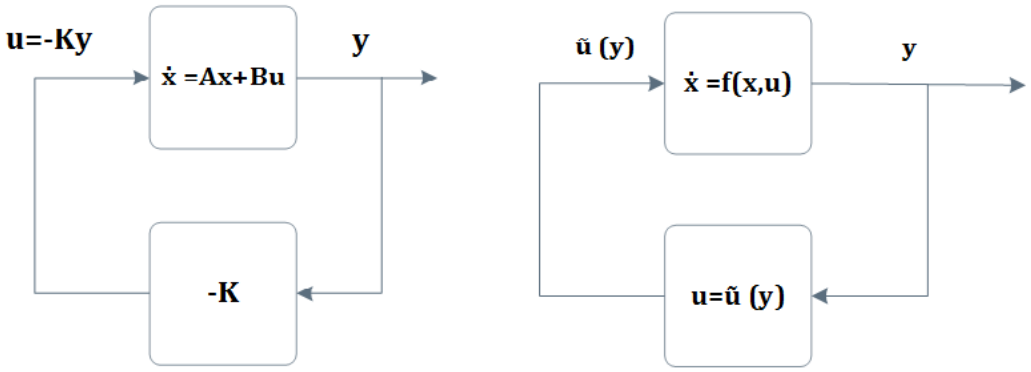

FIGURE 2.13: Output feedback controller for linear (on the left) and non-linear (on the right) systems.

2.5.2.2 Observer-based state and output feedback control

Once the observer is designed, the system can be controlled using an observer-based control as illustrated in Figure 2.14 and 2.15, respectively. Note that in observer-based state feedback control design, the controller depends on the estimated state variables $\hat{x}$; not on the unmeasured state variables x and in observer-based output feedback control design, it depends on the estimated output variables $\hat{y}$.

The advantage of the observer-based feedback is that the system can be made stable over the entire state space region, by choosing the gain appropriately. Also, the observer should be made to operate faster than the controller since the observer needs to estimate the state before it changes significantly.

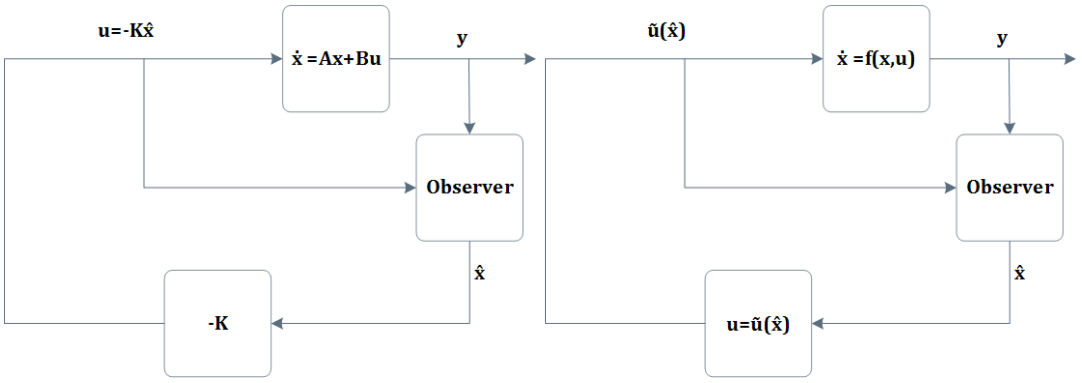

FIGURE 2.14: Observer-based state feedback control design for linear (on the left) and non-linear (on the right) systems.

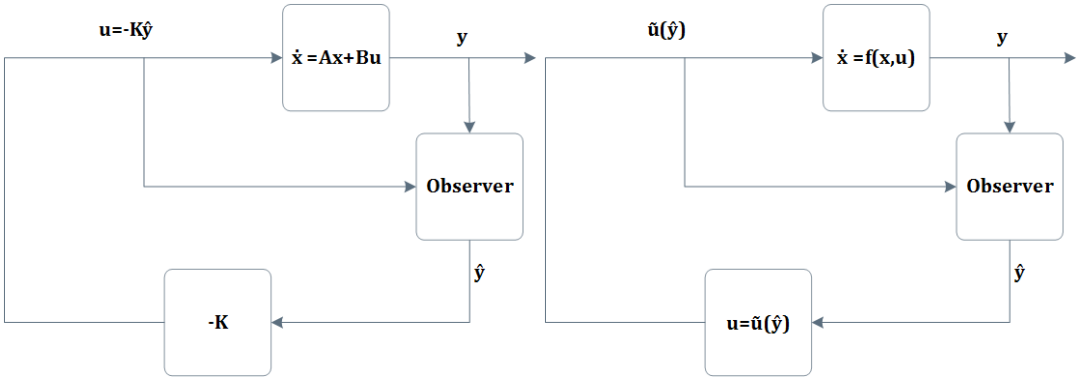

FIGURE 2.15: Observer-based output feedback control design for linear (on the left) and non-linear (on the right) systems.

2.6 Conclusion

The flowering time regulation pathway of *Arabidopsis Thaliana* involves a large complex network. Quantitative models are important to provide an understanding of the numerical amounts of gene products involved in the interactions and they can capture important details of complex system behaviour. Continuous variables and dynamical form of gene regulation can be derived and managed from these models. Therefore, the background of quantitative and dynamic modelling of GRNs were briefly introduced in this chapter.

Dynamics of internal changes in real life systems can be analysed with deterministic approaches. Moreover, stochastic models are also required to understand the systems in a more realistic perspective by incorporating random fluctuations due to external changes. The features of both deterministic and stochastic differential systems, which were constructed using Hill functions, were given in this chapter. Furthermore, Hill functions and their importance within activation–inhibition networks were introduced.

In addition to this, relevant techniques such as Lyapunov and Lasalle stability principles, which are used to characterise the dynamical system behaviour, were given for both deterministic and stochastic systems.

Finally, the necessary background for the observer and control design has been discussed. The class of uniformly observable systems for well-established observer design methods was briefly presented. In turn, the basic theory for state and output feedback control of dynamical systems was also described.

Chapter 3

Mathematical models of the Arabidopsis flowering gene regulatory networks

3.1 Introduction

Arabidopsis Thaliana is a small, annual flowering plant in the Brassicaceae (mustard) family which is a favourite model organism for plant biology research due mainly to its small size, simple genome and rapid life cycle. The life cycle of this plant can be observed to last around six to eight weeks. The transition from vegetative to reproductive development, which is an initiation of flower growth (see Figures 3.1 and 3.2), is crucial for the life cycle of any angiosperm plant like *Arabidopsis Thaliana* [Krizek and Fletcher, 2005, Ó'Maoiléidigh et al., 2014, Wang et al., 2014]. This is because flowering on time is a key factor to achieve reproductivity of these plants. Physiological and environmental conditions of the plant regulate the timing of mutation for the optimal reproductive achievement and their reactions are integrated into a complex GRN which monitors and regulates this transition [Kardailsky et al., 1999, Levy and Dean, 1998, Wellmer and Riechmann, 2010].

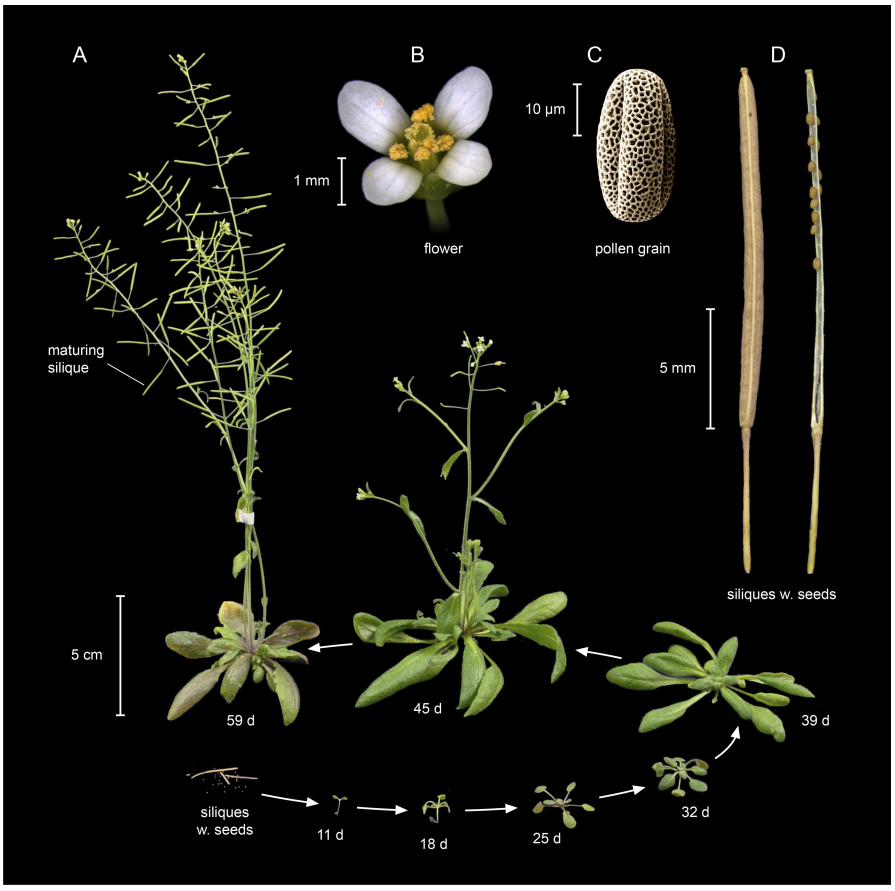

FIGURE 3.1: Figure taken from [Krämer, 2015], showing the process of *Arabidopsis Thaliana* life cycle. From seed (initial step) to vegetative growth takes 39 days. The flowering process occurs from vegetative (39 days) to end of reproductive growth (59 days), which starts after 45 days.

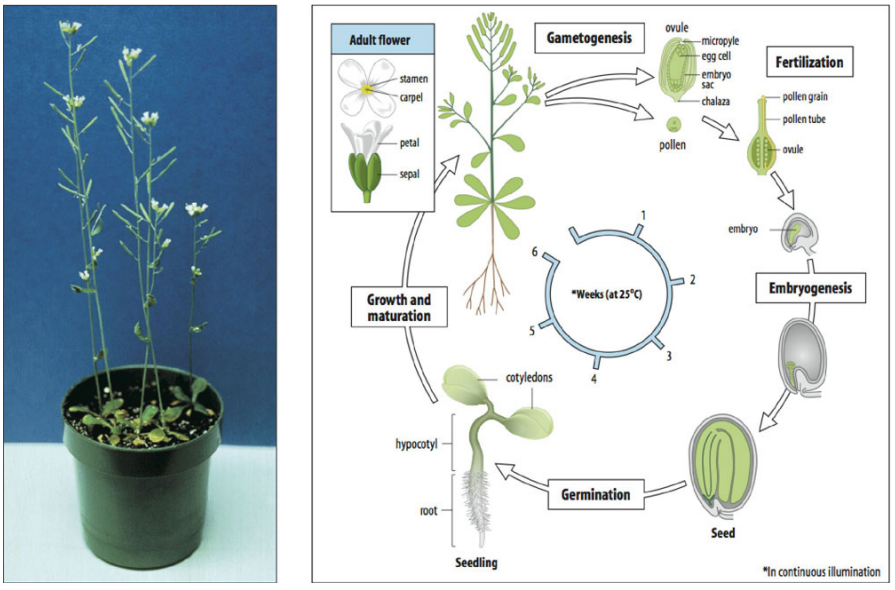

FIGURE 3.2: Figure taken from [Staveley, 2016], showing the life cycle of *Arabidopsis Thaliana* under the condition of 25°C.

Genes and their regulatory interactions are significant factors in biological systems at the molecular level since the understanding of their impact on each other's regulation and the level of these impacts on one another is crucial to comprehend the response of gene disturbances on flowering time. Therefore, in this work, a deterministic delay differential equation model, introduced by Valentim et al. [2015], is studied to explain the interactions of the concentrations in Arabidopsis flowering GRN and devise more targeted subsystems.

This chapter is organized as follows. In Section 3.2, a dynamic model of Arabidopsis flowering is presented. The steady state of the full system is investigated analytically and numerically in Section 3.3. A theorem for the local stability of the full system is formulated, and the corresponding analysis is given in Section 3.4. Finally, our concluding remarks are given in Section 3.5.

3.2 The dynamical model

Numerous genes appear to be acting as flowering time regulators of *Arabidopsis Thaliana* [Ryan et al., 2015] and different pathways have been constructed to reveal the flowering process of this plant [Amasino, 2010, Greenup et al., 2009, Kardailsky et al., 1999, Yant et al., 2009] as seen in Figure 3.3.

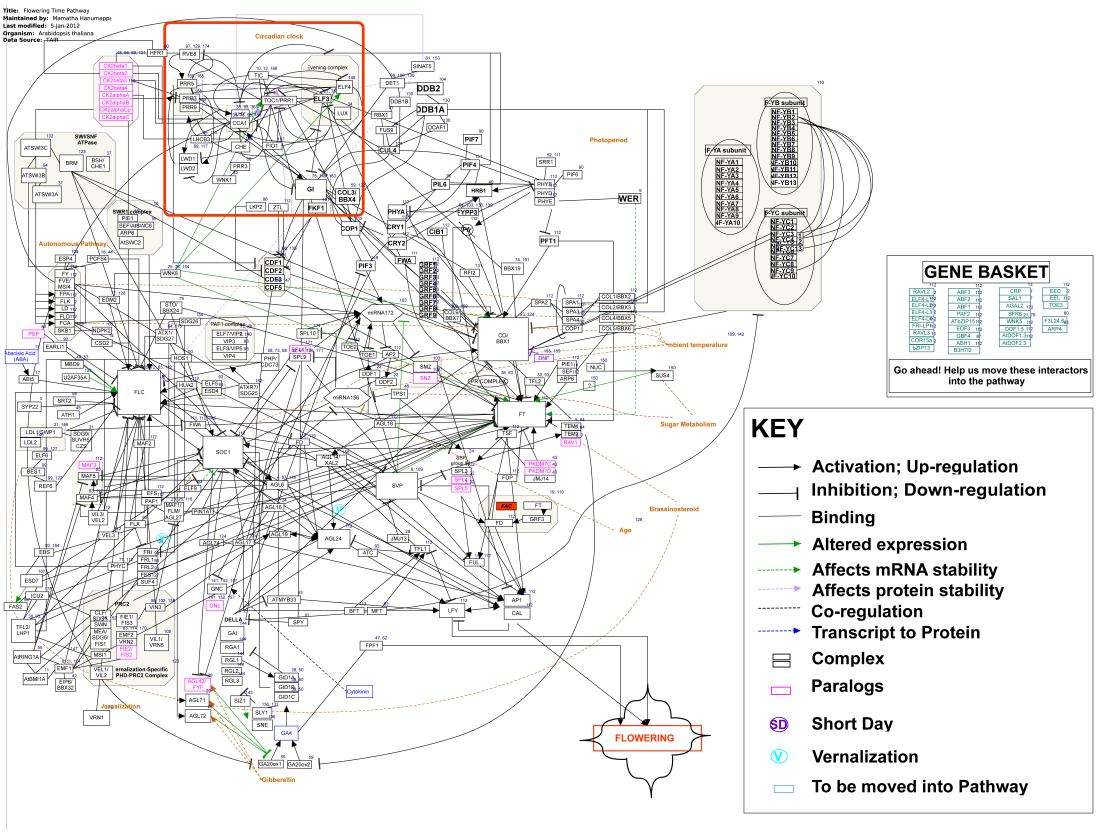

FIGURE 3.3: Flowering time pathway of the *Arabidopsis Thaliana*, taken from [Hanumappa et al.].

This complex network of many interacting genes can be dynamically modelled using systems with a large number of equations [Jaeger et al., 2013, Valentim et al., 2015, van Mourik et al., 2010, Wang et al., 2014]. In this chapter, we consider the deterministic dynamic model of delay-differential equations describing the flowering of the Arabidopsis species proposed by Valentim et al. [2015]. This model involves core set of gene-regulator interactions while protein-protein interactions are not explicitly included. The model is based on a feedback loop, constructed with eight genes, where six of them are internal: $Apetala1$ ($AP1$), $Leafy$ (LFY), $Suppressor\ of\ Overexpression\ of\ Constants1$ ($SOC1$), $Agamous-Like24$ ($AGL24$), $Flowering\ Locus\ T$ (FT) and FD. The other two genes are considered as external inputs: $Short\ Vegetative\ Phase$ (SVP) and $Flowering\ Locus\ C$ (FLC). The model is represented schematically in Figure 3.4.

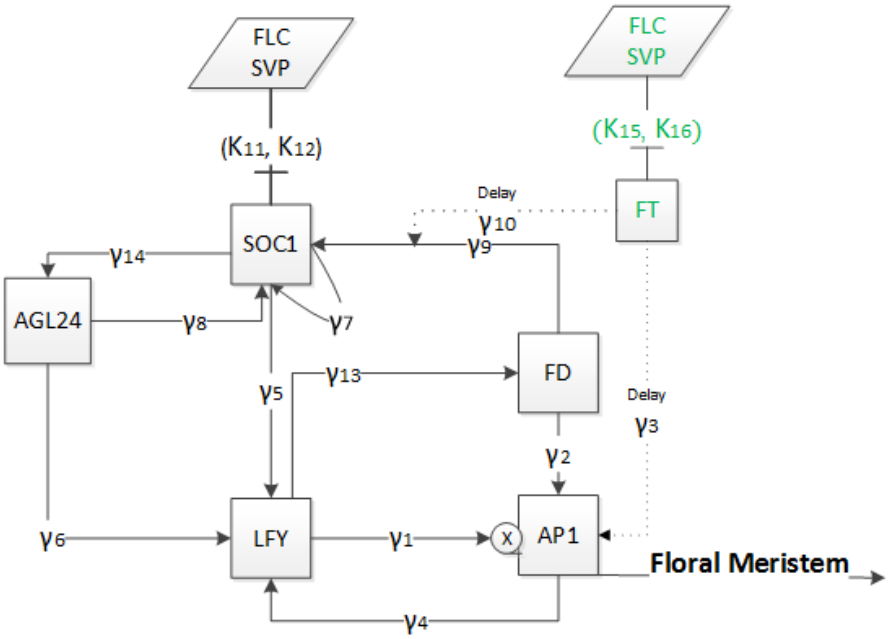

FIGURE 3.4: Flowchart of the model. Green and black labels represent expression in leaf and meristem tissues, respectively. Direction arrows represent activation with γ (Hill) functions where squares describe the dynamic variables, blocked ones inhibition with κ functions and parallelograms describe the input variables. Dashed arrows show the delayed transport and action of FT onto $AP1$ and $SOC1$. Junction symbol next to $AP1$ shows the multiple interactions from LFY to $AP1$.

The deterministic model proposed in [Valentim et al., 2015] for the network in Figure 3.4 is given by a system of six differential equations with one delay. It is formulated as follows:

$$\begin{aligned}
\dot{x}_1 &= \beta_1\gamma_1^n(x_2) + \beta_2\gamma_2(x_4) + \beta_3\gamma_3(x_6(t-\tau)) - d_1x_1,\\
\dot{x}_2 &= \beta_4\gamma_4(x_1) + \beta_5\gamma_5(x_3) + \beta_6\gamma_6(x_5) - d_2x_2,\\
\dot{x}_3 &= \left[\beta_7\gamma_7(x_3) + \beta_8\gamma_8(x_5) + \beta_9\gamma_9(x_4)\gamma_{10}(x_6(t-\tau))\right]\kappa_{11}(x_7)\kappa_{12}(x_8) - d_3x_3,\\
\dot{x}_4 &= \beta_{10}\gamma_{13}(x_2) - d_4x_4,\\
\dot{x}_5 &= \beta_{11}\gamma_{14}(x_3) - d_5x_5,\\
\dot{x}_6 &= \beta_{12}\kappa_{15}(x_9)\kappa_{16}(x_{10}) - d_6x_6,
\end{aligned} \tag{3.1}$$

where the functions are defined as

$$\gamma_j^n(x_i) = \frac{x_i^n}{x_i^n + K_j^n}, \quad \gamma_j(x_i) = \gamma_j^1(x_i), \quad \kappa_j(x_i) = \frac{K_j}{x_i + K_j}, \quad i = 1,\ldots,10, \quad j = 1,\ldots,16.$$

Here the variables x_i are concentrations of gene expressions, which depend on time t and represent the genes as follows:

$$AP1 \to x_1,\ LFY \to x_2,\ SOC1 \to x_3,\ FD \to x_4,\ AGL24 \to x_5,\ FT \to x_6,$$
$$SVP_m \to x_7,\ FLC_m \to x_8,\ SVP_l \to x_9 \text{ and } FLC_l \to x_{10},$$

and their initial values are averagely estimated using polynomial data fitting method by [Valentim et al., 2015] as $0.00056nM$, $0.68nM$, $33.3nM$, $0.431nM$, $27.69nM$, $0.00056nM$, $3.507nM$, $0.423nM$, $156.947nM$ and $1.047nM$, respectively.

The transcription of FT is controlled by SVP and FLC in the leaves as shown in Figure 3.4. After FT is created in the leaves, it transfers to the meristem to interact with FD. They activate the $SOC1$ expression together and $AP1$ individually [Valentim et al., 2015, Wang et al., 2014]. $SOC1$ is activated by FT/FD, $AGL24$ and itself. Moreover, the expression of $SOC1$ is repressed by SVP and FLC in the meristem. LFY is assumed to move through a positive feedback loop with the dimerization of $AGL24$ and $SOC1$. LFY is also a positive regulator of FD and $AP1$. The progression to flowering is determined by a direct positive input interaction among LFY and $AP1$. When the $AP1$ expression is started, the transcription variable $AP1$ arranges the floral transition by identifying the status of floral meristem and regulating the gene expressions comprised in flower progress [Kaufmann et al., 2010, Valentim et al., 2015]. Following Valentim et al. [2015], protein and RNA levels are assumed to be linearly correlated with each other. SVP_l and FLC_l represent the gene expression of SVP and FLC in the leaves and SVP_m and FLC_m in the meristem. These four components, SVP_l, FLC_l, SVP_m and FLC_m, are independent input variables for the system which are linearly interpolated from the experimental data.

The delayed time $\tau = t - \Delta$ appears in the equations for x_1 and x_3. The reason for this is that FT occurs in the leaves and then moves to the meristem with some time delay Δ, which is assumed to take less than 24 hours [Valentim et al., 2015]. The Hill functions γ_j and κ_j represent activation and inhibition kinetics, respectively. The coefficient n of the Hill function γ_1 represents the cooperativity in the regulation of $AP1$ by LFY and is assumed to be a positive integer. The meaning of the other coefficients is provided in

Table 3.1. Their values, estimated from experimental data using polynomial data fitting in [Valentim et al., 2015], are given in Table 3.2.

Parameters	**Description**	**Range**
β_i, $(i = 1, 2, ..., 12)$	The maximum transcription rate	[0.001, 200] nM$*$min^{-1}
$\mathbf{K_i}$, $(i = 1, 2, ..., 16)$	The abundance at half maximum transcription rate	[0.001, 2000] nM
$\mathbf{d_i}$, $(i = 1, 2, ..., 6)$	The gene products degradation rate	[0.001, 1] min^{-1}
Δ	Delay	[0, 1] days

TABLE 3.1: Description and range for the parameters in the dynamic model.

Parameters	**Estimated Values**	**Parameters**	**Estimated Values**	**Parameters**	**Estimated Values**
β_1	99.8 nM$*$min^{-1}	$\mathbf{K_1}$	9.82 nM	$\mathbf{K_{13}}$	7.9 nM
β_2	5 nM$*$min^{-1}	$\mathbf{K_2}$	700 nM	$\mathbf{K_{14}}$	125 nM
β_3	10 nM$*$min^{-1}	$\mathbf{K_3}$	10.1 nM	$\mathbf{K_{15}}$	0.63 nM
β_4	22 nM$*$min^{-1}	$\mathbf{K_4}$	346 nM	$\mathbf{K_{16}}$	985 nM
β_5	2.4 nM$*$min^{-1}	$\mathbf{K_5}$	842 nM	$\mathbf{d_1}$	0.86 min^{-1}
β_6	0.79 nM$*$min^{-1}	$\mathbf{K_6}$	1011 nM	$\mathbf{d_2}$	0.017 min^{-1}
β_7	64 nM$*$min^{-1}	$\mathbf{K_7}$	695 nM	$\mathbf{d_3}$	0.11 min^{-1}
β_8	0.52 nM$*$min^{-1}	$\mathbf{K_8}$	1182 nM	$\mathbf{d_4}$	0.0075 min^{-1}
β_9	189 nM$*$min^{-1}	$\mathbf{K_9}$	2.4 nM	$\mathbf{d_5}$	0.001 min^{-1}
β_{10}	8.5 nM$*$min^{-1}	$\mathbf{K_{10}}$	4.8 nM	$\mathbf{d_6}$	0.1 min^{-1}
β_{11}	100 nM$*$min^{-1}	$\mathbf{K_{11}}$	909 nM	Δ	0.5 day
β_{12}	51 nM$*$min^{-1}	$\mathbf{K_{12}}$	501 nM		

TABLE 3.2: Model parameters, estimated from experimental gene expression data using a polynomial regression fitting [Valentim et al., 2015].

The behaviour of system (3.1) is simulated in Figure 3.5 using the parameters in Table 3.2 and the experimental data used in [Valentim et al., 2015]. The initial conditions

are taken from experimental data. The sharp rise in $AP1$ from 13 to 17 days after germination can be interpreted as a predictor of flowering [Valentim et al., 2015].

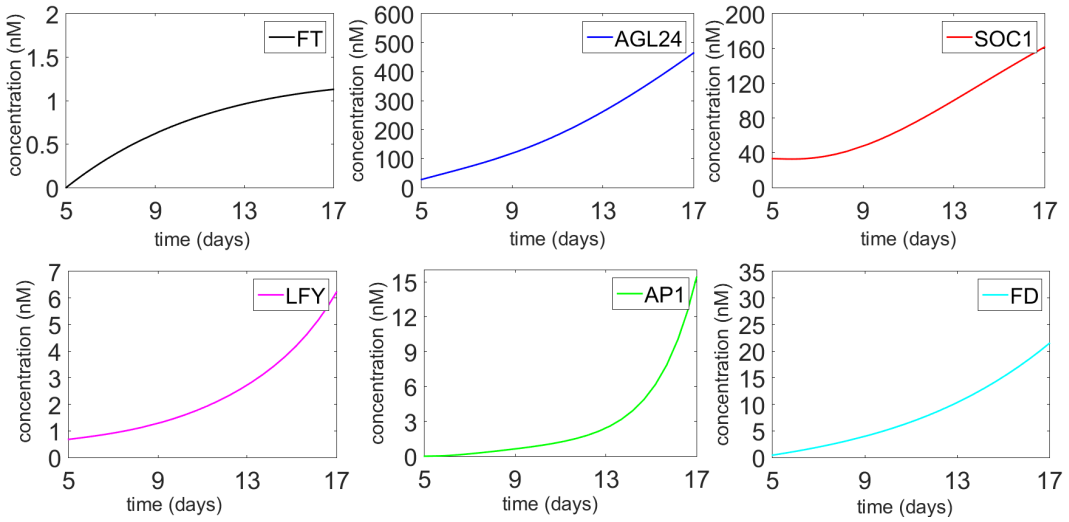

FIGURE 3.5: Numerical simulation of the system (3.1) after germination. The initial values for FT, $AGL24$, $SOC1$, LFY, $AP1$ and FD are taken from [Valentim et al., 2015] as $0.00056nM$, $27.69nM$, $33.3nM$, $0.68nM$, $0.00056nM$ and $0.431nM$, respectively.

As it is known from laboratory experiments (see [Krämer, 2015, Staveley, 2016]), *Arabidopsis Thaliana* is an annual plant and its flowering is limited to approximately two to four weeks after germination. In this context, a non-trivial stable steady state can be seen as an attracting point for the flowering process. Hence, in the next section, we turn to the analysis of the steady state of the flowering model to determine its behaviour, give conditions on its initiation and investigate the terminal stages of the flowering process.

3.3 Steady state and stability analysis of the deterministic model

The steady states of the system represent the equilibrium points about which the dynamics can be studied using linear stability analysis. It helps to describe the behaviour of a delayed system solution by considering the trajectories in a phase space of all dependent variables. The state is locally asymptotically stable when all sufficiently close

trajectories converge to the steady state as $t \to \infty$, and unstable if they deviate from the fixed point (see e.g. [Lakshmanan and Senthilkumar, 2011]). As mentioned previously, we interpret a stable steady state as an attractor for the flowering process. Therefore, if the Arabidopsis flowering is successful, then there exists at least one strictly positive stable steady state.

Hence, for DDEs of the form (3.1), which can be presented as

$$\frac{dx_i}{dt} = f_i(x_1, x_2, ..., x_5, x_6, x_6(\tau)), \quad i = 1, 2, .., 6, \tag{3.2}$$

the equilibrium points $\bar{X} = (\bar{x}_1, \bar{x}_2, \ldots, \bar{x}_5, \bar{x}_6)$ can be found by considering the equations

$$f_i(\bar{x}_1, \bar{x}_2, ..., \bar{x}_5, \bar{x}_6, \bar{x}_6) = 0, \quad i = 1, 2, .., 6,$$

where f_i represent the functional form of the right-hand side of the system. Since at the equilibrium, variables do not change with respect to time, $x_6(\tau)$ is also set as $\bar{x}_6(\tau) = \bar{x}_6$ in this system.

In our further considerations, we assume that the independent input variables $x_7, ..., x_{10}$ in system (3.1) are constant and equal to their initial values as given in Table 3.3, to derive the steady states.

Input variables	**Described in the model**	**Initial values**
SVP – meristem	$SVP_m \to x_7$	3.507 nM
FLC – meristem	$FLC_m \to x_8$	0.423 nM
SVP – leaves	$SVP_l \to x_9$	156.947 nM
FLC – leaves	$FLC_l \to x_{10}$	1.047 nM

TABLE 3.3: Input variables with the initial values

This results into the following set of equations

$$\bar{x}_1 = \frac{\beta_1\gamma_1^n(\bar{x}_2) + \beta_2\gamma_2(\bar{x}_4) + \beta_3\gamma_3(\bar{x}_6)}{d_1}, \tag{3.3a}$$

$$\bar{x}_2 = \frac{\beta_4\gamma_4(\bar{x}_1) + \beta_5\gamma_5(\bar{x}_3) + \beta_6\gamma_6(\bar{x}_5)}{d_2}, \tag{3.3b}$$

$$\bar{x}_3 = \frac{[\beta_7\gamma_7(\bar{x}_3) + \beta_8\gamma_8(\bar{x}_5) + \beta_9\gamma_9(\bar{x}_4)\gamma_{10}(\bar{x}_6)] \times \kappa_{11}(x_7)\kappa_{12}(x_8)}{d_3}, \tag{3.3c}$$

$$\bar{x}_4 = \frac{\beta_{10}\gamma_{13}(\bar{x}_2)}{d_4}, \tag{3.3d}$$

$$\bar{x}_5 = \frac{\beta_{11}\gamma_{14}(\bar{x}_3)}{d_5}, \tag{3.3e}$$

$$\bar{x}_6 = \frac{\beta_{12}\kappa_{15}(x_9)\kappa_{16}(x_{10})}{d_6} = u, \tag{3.3f}$$

where u is a constant.

3.3.1 Derivation of steady state and numerical simulation

As system (3.1) is underdetermined, the contribution of the input variables is considered constant and we take into account its effect on the equilibrium for the value $n = 3$, which is the value obtained by Valentim et al. [2015] by fitting experimental data. To find all equilibrium points using the assumption above, we follow the steps:

- From (3.3a), by substituting $\bar{x}_4$ and $\bar{x}_6$ from (3.3d) and (3.3f), respectively, we find;

$$\begin{aligned}\bar{x}_1 &= \frac{\beta_1\bar{x}_2^3}{d_1K_1^3 + d_1\bar{x}_2^3} + \frac{\beta_2\beta_{10}\bar{x}_2}{d_1d_4K_2K_{13} + (d_1d_4K_2 + d_1\beta_{10})\bar{x}_2} + \frac{\beta_3 u}{d_1(K_3 + u)} \\ &= \frac{\beta_1\bar{x}_2^3}{z_1 + d_1\bar{x}_2^3} + \frac{z_2\bar{x}_2}{z_3 + z_4\bar{x}_2} + U_1 \end{aligned} \tag{3.4}$$

  where all U_1, z_1, z_2, z_3 and z_4 are constants defined by

  $z_1 = d_1K_1^3$, $z_2 = \beta_2\beta_{10}$, $z_3 = d_1d_4K_2K_{13}$, $z_4 = (d_1d_4K_2 + d_1\beta_{10})$ and $U_1 = \dfrac{\beta_3 u}{d_1(K_3 + u)}$.

Equation (3.4) can be rearranged

$$\bar{x}_1 = \frac{p_1\bar{x}_2^4 + p_2\bar{x}_2^3 + p_3\bar{x}_2 + p_7U_1}{p_4\bar{x}_2^4 + p_5\bar{x}_2^3 + p_6\bar{x}_2 + p_7}, \tag{3.5}$$

where the constants are defined by,

$$p_1 = (d_4K_2 + \beta_{10})(\beta_1 + d_1U_1) + \beta_2\beta_{10}, \quad p_2 = d_4K_2K_{13}(\beta_1 + d_1U_1),$$
$$p_3 = K_1^3(\beta_2\beta_{10} + d_1U_1(d_4K_2 + \beta_{10})), \quad p_4 = d_1(d_4K_2 + \beta_{10}), \quad p_5 = d_1d_4K_2K_{13},$$
$$p_6 = d_1K_1^3(d_4K_2 + \beta_{10}), \quad p_7 = d_1d_4K_1^3K_2K_{13} \quad \text{and} \quad U_1 = \frac{\beta_3 u}{d_1(K_3 + u)}.$$

Equation (3.5) establishes the link between $\bar{x}_1$ and $\bar{x}_2$.

- From (3.3b), by substituting $\bar{x}_1$ from (3.5) and $\bar{x}_5$ from (3.3e), we find;

$$\begin{aligned}\bar{x}_2 &= \frac{\beta_4\bar{x}_1}{d_2(\bar{x}_1 + K_4)} + \frac{\beta_5\bar{x}_3}{d_2(\bar{x}_3 + K_5)} + \frac{\beta_6\bar{x}_5}{d_2(\bar{x}_5 + K_6)} \\ &= \frac{\beta_4p_1\bar{x}_2^4 + \beta_4p_2\bar{x}_2^3 + \beta_4p_3\bar{x}_2 + \beta_4p_7U_1}{d_2(K_4p_4 + p_1)\bar{x}_2^4 + d_2(K_4p_5 + p_2)\bar{x}_2^3 + d_2(K_4p_6 + p_3)\bar{x}_2 + d_2p_7(K_4 + U_1)} \\ &\quad + \frac{(\beta_6\beta_{11} + d_5\beta_5K_6 + \beta_5\beta_{11})\bar{x}_3^2 + (\beta_6\beta_{11}K_5 + d_5\beta_5K_6K_{14})\bar{x}_3}{d_2(d_5K_6 + \beta_{11})\bar{x}_3^2 + d_2(d_5K_5K_6 + \beta_{11}K_5 + d_5K_6K_{14})\bar{x}_3 + d_2d_5K_5K_6K_{14}}.\end{aligned} \tag{3.6}$$

Equation (3.6) can be rewritten as

$$\frac{s_{10}\bar{x}_2^5 + (s_{11} - s_6)\bar{x}_2^4 - s_7\bar{x}_2^3 + s_{12}\bar{x}_2^2 + (s_{13} - s_8)\bar{x}_2 - s_9}{(s_{10}\bar{x}_2^4 + s_{11}\bar{x}_2^3 + s_{12}\bar{x}_2 + s_{13})} = \frac{s_1\bar{x}_3^2 + s_2\bar{x}_3}{(s_3\bar{x}_3^2 + s_4\bar{x}_3 + s_5)}, \tag{3.7}$$

where the constants s_i are given by

$$s_1 = \beta_6\beta_{11} + d_5\beta_5K_6 + \beta_5\beta_{11}, \quad s_2 = \beta_6\beta_{11}K_5 + d_5\beta_5K_6K_{14}, \quad s_3 = d_2(d_5K_6 + \beta_{11}),$$
$$s_4 = d_2(d_5K_5K_6 + \beta_{11}K_5 + d_5K_6K_{14}), \quad s_5 = d_2d_5K_5K_6K_{14}, \quad s_6 = \beta_4p_1, \quad s_7 = \beta_4p_2,$$
$$s_8 = \beta_4p_3, \quad s_9 = \beta_4U_1p_7, \quad s_{10} = d_2(K_4p_4 + p_1), \quad s_{11} = d_2(K_4p_5 + p_2),$$
$$s_{12} = d_2(K_4p_6 + p_3) \quad \text{and} \quad s_{13} = d_2p_7(K_4 + U_1).$$

- From (3.3c), by substituting $\bar{x}_4$, $\bar{x}_5$ and $\bar{x}_6$ from (3.3d), (3.3e) and (3.3f), respectively, we obtain;

$$\bar{x}_3 = \frac{m_1\bar{x}_3}{d_3\bar{x}_3 + m_2} + \frac{m_3\bar{x}_3}{m_4\bar{x}_3 + m_5} + \frac{m_6\bar{x}_2}{m_7\bar{x}_2 + m_8} \tag{3.8}$$

where the constants are represented by

$$m_1 = \beta_7\kappa_{11}(x_7)\kappa_{12}(x_8), \quad m_2 = d_3K_7, \quad m_3 = \beta_8\beta_{11}\kappa_{11}(x_7)\kappa_{12}(x_8),$$
$$m_4 = d_3(d_5K_8 + \beta_{11}), \quad m_5 = d_3d_5K_8K_{14}, \quad m_6 = u_1\beta_9\beta_{10}\kappa_{11}(x_7)\kappa_{12}(x_8),$$
$$m_7 = d_3(d_4K_9 + \beta_{10})(K_{10} + u_1), \quad m_8 = d_3d_4K_9K_{13}(K_{10} + u_1).$$

By moving occurrences of $\bar{x}_3$ to the left hand side, we find

$$\frac{n_1\bar{x}_3^3 + n_2\bar{x}_3^2 + n_3\bar{x}_3}{n_1\bar{x}_3^2 + n_4\bar{x}_3 + n_5} = \frac{m_6\bar{x}_2}{m_7\bar{x}_2 + m_8}, \tag{3.9}$$

where the constants are

$$n_1 = d_3m_4, \quad n_2 = d_3m_5 + m_2m_4 - d_3m_3 - m_1m_4, \quad n_3 = m_2m_5 - m_1m_5 - m_2m_3,$$
$$n_4 = d_3m_5 + m_2m_4, \quad n_5 = m_2m_5.$$

Eliminating $\bar{x}_2$ from (3.7) and (3.9), we obtain a generic 17^{th} degree polynomial equation for $\bar{x}_3$ which we do not reproduce here. Our analysis of the equilibrium shows that $\bar{x}_6$ is obtained directly from the input concentrations while $\bar{x}_1$, $\bar{x}_2$, $\bar{x}_3$, $\bar{x}_4$ and $\bar{x}_5$ are non-linearly linked with each other.

Since the concentrations are positive, we are only interested in positive roots of this polynomial. Using values for the independent input variables (Table 3.3) and estimated parameters (Table 3.2), it can be seen numerically that there exists a unique positive steady state, given in Table 3.4.

$\bar{x}_1$	$\bar{x}_2$	$\bar{x}_3$	$\bar{x}_4$	$\bar{x}_5$	$\bar{x}_6$
121.567	452.395	827.835	1113.882	86881.258	2.037

TABLE 3.4: Unique positive steady state for concentrations (in nM), obtained by using the parameters in Table 3.2 and initial values in Table 3.3.

Numerical simulation of system (3.1), with Matlab R2015b, showing convergence to the steady state, is presented in Figure 3.6. The time for which $AP1$ sees a sharp rise is in agreement with the time at which the most dramatic part of flowering takes place, and the time for which $AP1$ reaches its steady state is in agreement with the ending of flowering process, which has been observed between two to four weeks in lab experiments [Krämer, 2015, Sanda et al., 1997, Staveley, 2016, Valentim et al., 2015]. Moreover, $AGL24$ and FD may have a less crucial role in the initiation of flowering of Arabidopsis, as the latter has already happened before these two variables reach the steady state. Our simulations show that the main features of the system behaviour would not change for different values of the input variables, apart from a slight variation in the numerical values of the steady state concentrations.

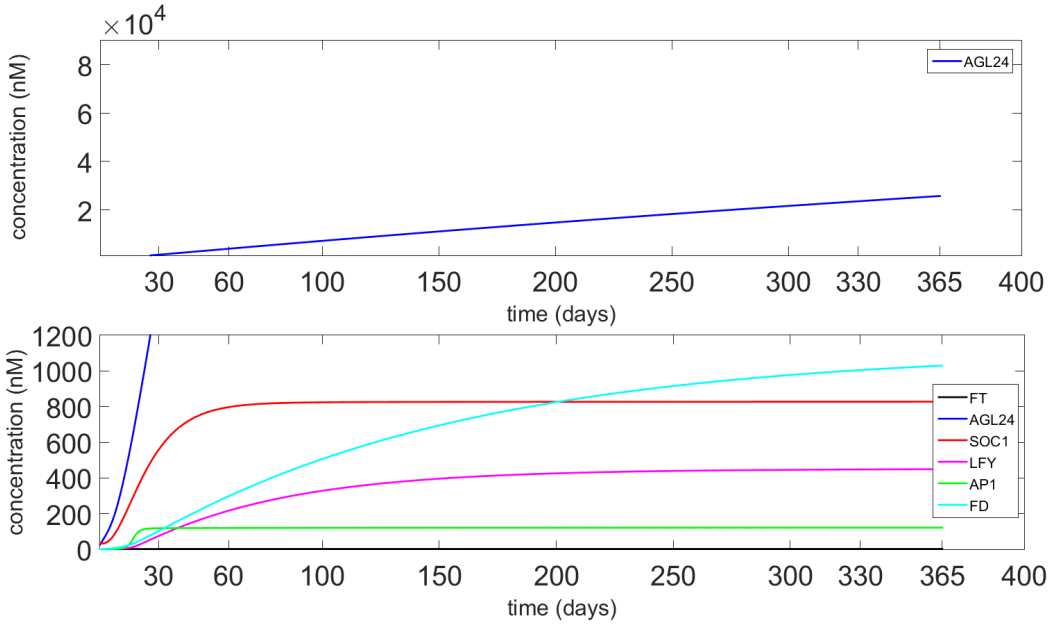

FIGURE 3.6: Numerical solution of the system (3.1) showing the asymptotic stability of the steady state. The initial values are as in Figure 3.5.

3.4 Linear stability analysis of the dynamical model

Linearisation of the non-linear system (1) is helpful to analyse the local stability of this dynamic model around a steady state point $\bar{x} = (\bar{x}_1, \bar{x}_2, \bar{x}_3, \bar{x}_4, \bar{x}_5, \bar{x}_6)$. Stability analysis is used to establish threshold conditions on the model parameters for the flowering of

the plant. Therefore, in this Section, the linear stability of the model is analysed in detail, and explicit conditions for local stability are formulated using the Routh-Hurwitz criterion.

To linearise the system with time delay, the following equation is introduced

$$\dot{X} = J_0 X + J_\tau X_\tau, \tag{3.10}$$

to describe the behaviour in a neighbourhood of the steady state point, where $X = (x_1, x_2, x_3, x_4, x_5, x_6)$, $X_\tau = (x_1(t-\tau), x_2(t-\tau), x_3(t-\tau), x_4(t-\tau), x_5(t-\tau), x_6(t-\tau))$. In this equation, J_0 and J_τ are Jacobians of the system with respect to non-delayed and delayed variables,

$$J_0 = \left(\frac{\partial f_i}{\partial x_j}\right)\Big|_{X=X_\tau=\bar{x}} \quad \text{and} \quad J_\tau = \left(\frac{\partial f_i}{\partial x_j(t-\tau)}\right)\Big|_{X=X_\tau=\bar{x}},$$

respectively. The matrix form of the linearised system (3.10) is given as

$$\begin{bmatrix} \dot{x_1} \\ \dot{x_2} \\ \dot{x_3} \\ \dot{x_4} \\ \dot{x_5} \\ \dot{x_6} \end{bmatrix} = \underbrace{\begin{bmatrix} -d_1 & A & 0 & B & 0 & 0 \\ C & -d_2 & D & 0 & E & 0 \\ 0 & 0 & F-d_3 & G & H & 0 \\ 0 & K & 0 & -d_4 & 0 & 0 \\ 0 & 0 & L & 0 & -d_5 & 0 \\ 0 & 0 & 0 & 0 & 0 & -d_6 \end{bmatrix}}_{\mathbf{J_0}} \begin{bmatrix} x_1 \\ x_2 \\ x_3 \\ x_4 \\ x_5 \\ x_6 \end{bmatrix} + \underbrace{\begin{bmatrix} 0 & 0 & 0 & 0 & 0 & M \\ 0 & 0 & 0 & 0 & 0 & 0 \\ 0 & 0 & 0 & 0 & 0 & N \\ 0 & 0 & 0 & 0 & 0 & 0 \\ 0 & 0 & 0 & 0 & 0 & 0 \\ 0 & 0 & 0 & 0 & 0 & 0 \end{bmatrix}}_{\mathbf{J_\tau}} \begin{bmatrix} x_1(\tau) \\ x_2(\tau) \\ x_3(\tau) \\ x_4(\tau) \\ x_5(\tau) \\ x_6(\tau) \end{bmatrix}, \tag{3.11}$$

where the following notation is used,

$A = \beta_1 \gamma_1^{3\prime}(\bar{x}_2)$, $B = \beta_2 \gamma_2{}'(\bar{x}_4)$, $C = \beta_4 \gamma_4{}'(\bar{x}_1)$, $D = \beta_5 \gamma_5{}'(\bar{x}_3)$, $E = \beta_6 \gamma_6{}'(\bar{x}_5)$,
$F = \beta_7 \gamma_7{}'(\bar{x}_3)\kappa_{11}(x_7)\kappa_{12}(x_8)$, $G = \beta_9 \gamma_9{}'(\bar{x}_4)\gamma_{10}(\bar{x}_6)\kappa_{11}(x_7)\kappa_{12}(x_8)$,
$H = \beta_8 \gamma_8{}'(\bar{x}_5)\kappa_{11}(x_7)\kappa_{12}(x_8)$, $K = \beta_{10} \gamma_{13}{}'(\bar{x}_2)$, $L = \beta_{11} \gamma_{14}{}'(\bar{x}_3)$, $M = \beta_3 \gamma_3{}'(\bar{x}_6)$, and
$N = \gamma_{10}{}'(\bar{x}_6)\gamma_9(\bar{x}_4)\kappa_{11}(x_7)\kappa_{12}(x_8)$.

Here, $\gamma_j{}'(\bar{x}_i)$, for $j = 1, ..., 16$ and $i = 1, ..., 6$ denote derivatives of γ_j with respect to x_i at the steady state points. The determinant below is introduced to obtain the characteristic

equation,

$$det(J_0+e^{-\lambda\tau}J_\tau-\lambda I) = \begin{vmatrix} -d_1-\lambda & A & 0 & B & 0 & Me^{-\lambda\tau} \\ C & -d_2-\lambda & D & 0 & E & 0 \\ 0 & 0 & F-d_3-\lambda & G & H & Ne^{-\lambda\tau} \\ 0 & K & 0 & -d_4-\lambda & 0 & 0 \\ 0 & 0 & L & 0 & -d_5-\lambda & 0 \\ 0 & 0 & 0 & 0 & 0 & -d_6-\lambda \end{vmatrix} = 0, \tag{3.12}$$

where I is an identity matrix. This gives the following characteristic equation,

$$P_1(\lambda) = (d_6+\lambda)P_2(\lambda), \tag{3.13}$$

where

$$\begin{aligned} P_2(\lambda) &= \Big[(d_3+\lambda-F)(d_5+\lambda)-HL\Big]\Big[(d_1+\lambda)(d_2+\lambda)(d_4+\lambda)-(d_4+\lambda)AC-BCK\Big] \\ &\quad -\Big[(d_1+\lambda)GK((d_5+\lambda)D+EL)\Big] = 0. \end{aligned} \tag{3.14}$$

It is clear that $\lambda = -d_6 < 0$ is a root of this characteristic equation. Thus, we now only focus on the stability of $P_2(\lambda)$ by using the Routh-Hurwitz stability criterion (see e.g. [Gantmacher et al., 1960]). This gives the following Theorem.

Theorem 3.1. *A steady state of the non-linear system (3.1) is locally asymptotically stable iff all the roots of the polynomial*

$$P_2(\lambda) = \lambda^5 + a_1\lambda^4 + a_2\lambda^3 + a_3\lambda^2 + a_4\lambda + a_5, \tag{3.15}$$

have negative real parts, that is iff the following conditions are satisfied,

$$\begin{gathered} a_i > 0, \quad i = 1, ..., 5, \\ a_1a_2a_3 + a_1a_5 > a_3^2 + a_1^2a_4, \quad \textit{and} \\ (a_1a_4 - a_5)(a_1a_2a_3 + a_1a_5 - a_3^2 - a_1^2a_4) > a_5(a_1a_2 - a_3)^2, \end{gathered}$$

where

$a_1 = d_1 + d_2 + d_3 + d_5 - F,$

$a_2 = -HL - d_5F + d_3d_5 + (d_3 + d_5 - F)(d_1 + d_2 + d_4) - AC + d_1d_2 + d_1d_4 + d_2d_4,$

$a_3 = -(d_1 + d_2 + d_4)(HL + d_5F - d_3d_5) - (d_3 + d_5 - F)(AC - d_1d_2 - d_1d_4 - d_2d_4) -$

$(d_4AC + BCK + DGK - d_1d_2d_4),$

$a_4 = (HL + d_5F - d_3d_5)(AC - d_1d_2 - d_1d_4 - d_2d_4) - (d_3 + d_5 - F)(d_4AC + BCK -$

$d_1d_2d_4) - (EGKL + (d_1 + d_5)DGK),$

$a_5 = (d_4AC + BCK - d_1d_2d_4)(HL + d_5F - d_3d_5) - (d_1d_5DGK + d_1EGKL).$

Otherwise, the steady state of the system is unstable.

For the stability condition, all roots of $P_2(\lambda)$ must have negative real part. By using the Routh-Hurwitz scheme [Saeed, 2008] for the 5-*th* degree characteristic polynomial $P_2(\lambda)$,

TABLE 3.5: 5-*th* degree Routh-Hurwitz scheme.

λ^5	λ^4	λ^3	λ^2	λ^1	λ^0
1	a_1	b_1	c_1	d_1	e_1
a_2	a_3	b_2	c_2	0	0
a_4	a_5	0	0	0	0

where b_1, b_2, c_1, c_2, d_1 and e_1 are as follows:

$$b_1 = \frac{a_1a_2 - a_3}{a_1}, \quad b_2 = \frac{a_1a_4 - a_5}{a_1}, \quad c_1 = \frac{b_1a_3 - a_1b_2}{b_1}, \quad c_2 = \frac{b_1a_5}{b_1} = a_5,$$
$$d_1 = \frac{c_1b_2 - b_1c_2}{c_1}, \quad e_1 = \frac{d_1c_2}{d_1} = c_2 = a_5.$$

All roots will have negative real part iff the coefficients a_i, $(i = 1, .., 5)$, b_1, b_2, c_1, c_2, d_1 and e_1, are all bigger than zero. Assuming $a_i > 0$, $(i = 1, .., 5)$, the stability conditions of $P_2(\lambda)$ can be derived as

$$a_1a_2 > a_3, \quad a_1a_4 > a_5, \quad a_1a_2a_3 + a_1a_5 > a_3^2 + a_1^2a_4, \quad \text{and}$$
$$(a_1a_4 - a_5)(a_1a_2a_3 + a_1a_5 - a_3^2 - a_1^2a_4) > a_5(a_1a_2 - a_3)^2.$$

These conditions show the validity of Theorem 3.1. For the parameters given in Table 3.2 and the initial input values in Table 3.3, the steady state (3.4) of the non-linear system (3.1) satisfies all conditions of Theorem 3.1;

where $a_1 = 0.9764,\ a_2 = 0.1026,\ a_3 = 0.0021,\ a_4 = 1.2003e-05,\ a_5 = 9.9659e-09,$ $a_1a_2 - a_3 = 0.098,\ a_1a_4 - a_5 = 1.171e-05,\ a_1a_2a_3 + a_1a_5 - a_3^2 - a_1^2a_4 = 1.9817e-04$ and $(a_1a_4 - a_5)(a_1a_2a_3 + a_1a_5 - a_3^2 - a_1^2a_4) - a_5(a_1a_2 - a_3)^2 = 2.2247e-09.$

3.5 Conclusion

In this chapter, we considered a dynamic model of Arabidopsis flowering introduced by Valentim et al. [2015]. This model is reconstructed with Hill functions to emphasise the importance of these functions and their effects on the concentrations. An analytical study of the steady state for the full system was performed. The steady states are calculated numerically with the estimated parameters taken from [Valentim et al., 2015]. The analysis results have shown that the system has only one positive stable steady state and that the time for which $AP1$ reaches the steady state is an agreement with the observed flowering has been finalised within the time around a month. The Routh-Hurwitz criterion has been used to provide local stability conditions which characterise the existence of this stable steady state.

In summary, the conditions in Theorem 3.1 show that the local stability of system (3.1) at the steady state depends on values of parameters and concentrations. Although explicit conditions for the presence of a stable steady state can be formulated, the task of identifying ranges on parameters where stability can occur remains difficult. To solve this issue, we now introduce a simpler system which reproduces the essential behaviour of system (3.1). For this purpose, we consider subsystems and analyse their stabilities in order to understand the behaviour of system (3.1).

Chapter 4

Deterministic model of the simplified Arabidopsis flowering GRNs

4.1 Introduction

Our stability analysis for system (3.1) produces conditions which include many biological parameters. Such parameters are difficult to determine from experiments and one of our objective is to provide specific ranges for individual coefficients that secure stable solutions. To overcome this issue of complexity, simplifying the system of differential equations by reducing the number of state variables is necessary to obtain more targeted regulatory networks. A simplified model then permits to better comprehend the functionality of gene expression in the regulatory system.

The most common and independent functions in floral transition are dominated by $AP1$, LFY, $SOC1$ in *Arabidopsis Thaliana* (see Figure 4.1) [Blázquez et al., 2001, Blázquez and Weigel, 2000, Welch et al., 2004, Yeap et al., 2014]. Indeed, it is known that the floral meristem identity genes have an important role to control the floral meristem specification while the flower development process is starting [Irish, 2010, Levy and Dean,

1998, Simon et al., 1996]. Thus, the minimal regulatory networks must consist of the main floral meristem identity genes of *Arabidopsis Thaliana*: $AP1$ and LFY, and the input variables of the meristem: FT and FD, where $AP1$ is the dominant regulatory concentration of floral initiation with LFY in *Arabidopsis Thaliana* [Irish, 2010, Wellmer and Riechmann, 2010]. Furthermore, $AP1$ has a key role between floral induction to flower formation, and it is being a junction of flowering in the GRN [Kaufmann et al., 2010]. On the other hand, FT induces flowering of Arabidopsis as an inhibitor and moves similar with LFY. Additionally, activation tagging isolates it [Kardailsky et al., 1999]. Moreover, FT and transcription factor FD affect each other in the meristem as a combined activator [Wang et al., 2014].

By considering the features of these floral meristem identity genes, we initially start reducing the six differential equations system by decoupling the external input variables SVP and FLC in the system (3.1) by using their initial values. Therefore, one of the main concentration, FT, will stay as a constant external input of the system as given in (3.3f). After this, we apply a further decoupling on $AGL24$ and FD on the network and we use their steady state values given in (3.3e) and (3.3d), respectively.

Finally, we need to apply this approach on $SOC1$ to obtain a differential equation system, depend on only $AP1$ and LFY. Unfortunately, this approach cannot be applied to reduce the system in two differential equations because of the complexity of the $SOC1$ equation. Therefore, we initially analyse the stability of three equations system with the concentrations $AP1$, LFY and $SOC1$.

Analytically, decoupling is possible to apply from six to three differential equations for the system (3.1). Therefore, we simplify the new system by using network motifs that capture essential characteristics of the floral transition. Examples of simplified *Arabidopsis Thaliana* GRN's can be seen in the study of Pullen et al. [2013], where a complex flowering time pathway included in the model of Jaeger et al. [2013] was simplified by focusing on essential flowering genes. Following these papers, we produce subsystems of the dynamic model of our network with two differential equations in three different motifs. The aim of these motifs is to construct parameter dependent stability conditions that reflect essential behaviour of the complex networks.

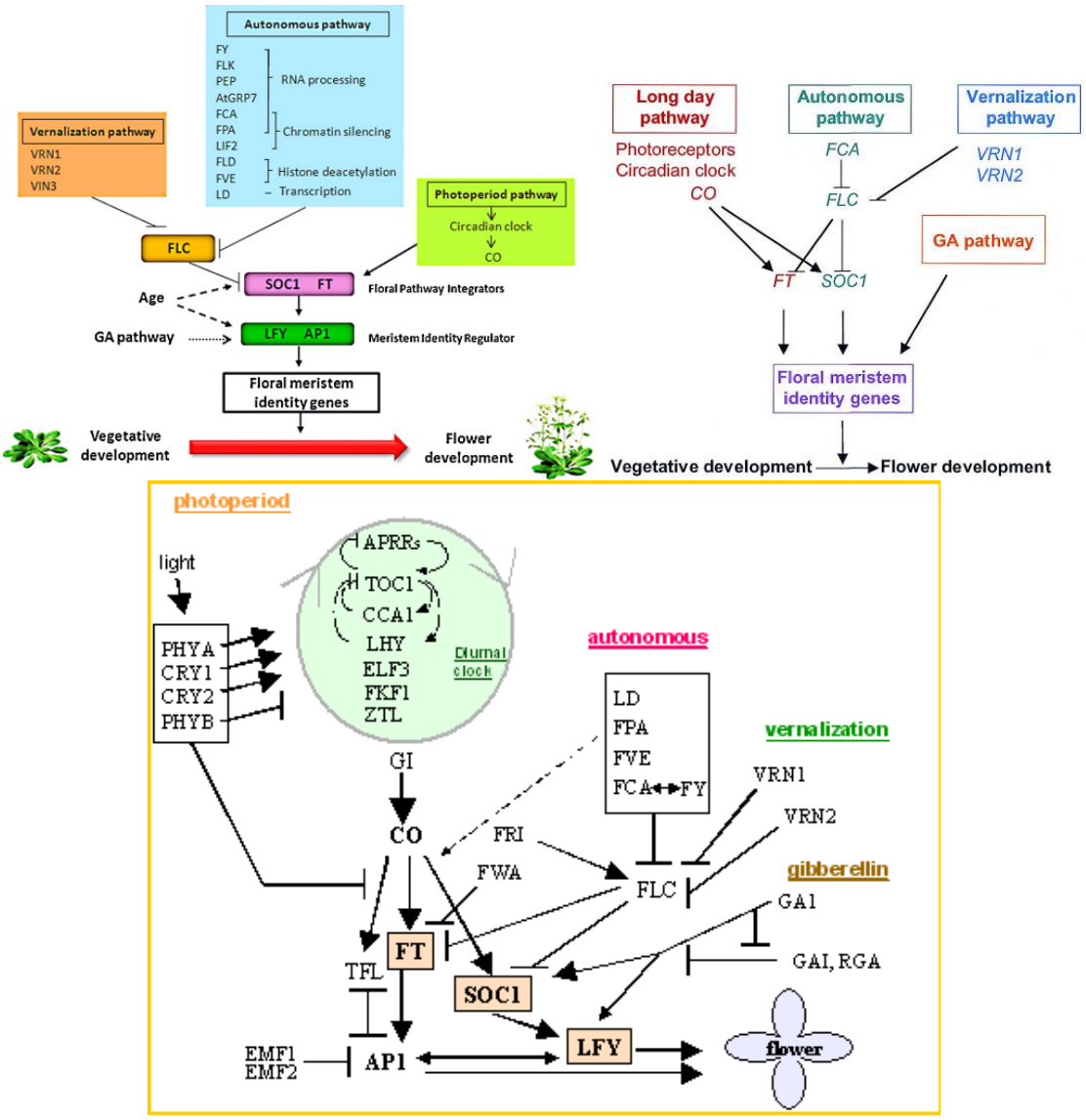

FIGURE 4.1: Figures, taken from [Yeap et al., 2014], [Blázquez et al., 2001] and [Welch et al., 2004], respectively, showing the important concentrations and their roles for the flowering of *Arabidopsis Thaliana*.

This chapter is organized as follows. Section 4.2 provides a decoupling approach to reduce the system (3.1) from six to three differential equations and introduces the numerical comparison of both systems. Then, simplified subsystems (motifs) of *Arabidopsis Thaliana* network with two equations are introduced. Steady states of the subsystems are analysed in section 4.3.1. In Section 4.3.2 and 4.3.3, numerical and analytical investigations of the steady state and stability of the simplified subsystems are introduced. Finally, this chapter is concluded in Section 4.4.

4.2 Deterministic model of the simplified network

As system (3.1) corresponds to a complex large regulatory network, it can be simplified while still saving its core structure. By decoupling some concentrations, it is possible to reduce the number of differential equations of the large system. One can see from the analysis of system (3.1) in the previous section that the main contribution to the dynamics is from concentrations $SOC1$, LFY and $AP1$. Hence, by considering $\frac{dx_i}{dt} = 0$ for $i = 4, 5$ and 6, the following system of differential equations can be obtained for the variables x_1, x_2 and x_3:

$$\begin{aligned}
\dot{x}_1 &= \frac{V_1 x_2^3}{x_2^3 + S_1^3} + \frac{V_2 x_2}{S_2 x_2 + S_3} + U_1 - d_1 x_1 \\
\dot{x}_2 &= \frac{V_3 x_1}{x_1 + S_4} + \frac{V_4 x_3}{x_3 + S_5} + \frac{V_5 x_3}{S_6 x_3 + S_7} - d_2 x_2 \\
\dot{x}_3 &= \frac{V_6 x_2 U_2}{S_8 x_2 + S_9} + \frac{V_7 x_3}{x_3 + S_{10}} + \frac{V_8 x_3}{S_{11} x_3 + S_{12}} - d_3 x_3.
\end{aligned} \tag{4.1}$$

where the parameters are defined by

$$\begin{aligned}
&V_1 = \beta_1,\ V_2 = \beta_2\beta_{10},\ V_3 = \beta_4,\ V_4 = \beta_5,\ V_5 = \beta_6\beta_{11},\ V_6 = \beta_9\beta_{10}\kappa_{11}\kappa_{12},\ V_7 = \beta_7\kappa_{11}\kappa_{12},\\
&V_8 = \beta_8\beta_{11}\kappa_{11}\kappa_{12},\ S_1 = K_1,\ S_2 = \beta_{10} + d_2K_2,\ S_3 = d_2K_2K_{13},\ S_4 = K_4,\ S_5 = K_5,\\
&S_6 = \beta_{11} + d_5K_6,\ S_7 = d_5K_6K_{14},\ S_8 = \beta_{10} + d_4K_9,\ S_9 = d_4K_9K_{13},\ S_{10} = K_7,\\
&S_{11} = \beta_{11} + d_5K_8,\ S_{12} = d_5K_8K_{14}.
\end{aligned}$$

Here, x_4, x_5 and x_6 remain constant in time, the constants u and U_1 at the steady state are defined in (3.3) and (3.4), respectively, and $U_2 = u(u + K_{10})^{-1}$. The scalar u represents the constant value of the FT concentration at the steady state, and U_1 and U_2 determine the effect of FT and FT-FD combination on $AP1$ and $SOC1$, respectively.

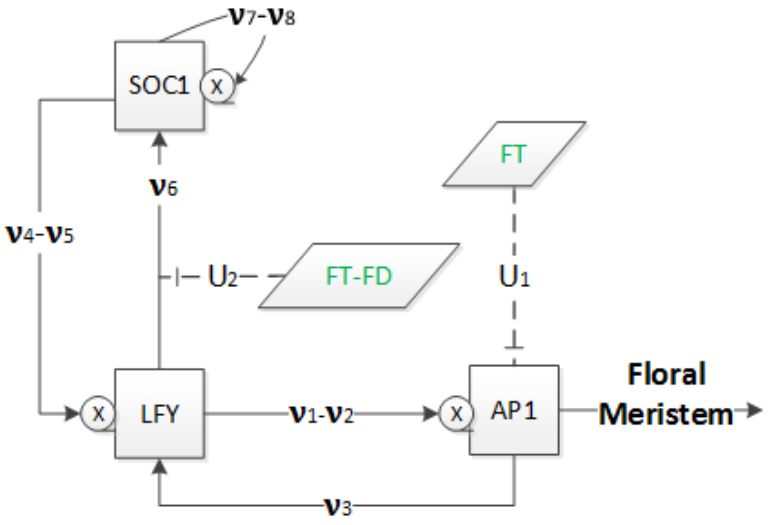

FIGURE 4.2: Flowchart of the system (4.1). Direction arrows represent activation or self-activation of dynamic input variables (in black) while dashed arrows illustrate the inhibition effect of the external input variables (in green). Junction symbols next to $AP1$, LFY and $SOC1$ show the multiple interactions from LFY to $AP1$, $SOC1$ to LFY and $SOC1$ to $SOC1$, respectively.

The network of system (4.1) is described in Figure 4.2. The difference with the model in Figure 3.4 is that $AGL24$ is not involved with the external input variables SVP and FLC as they are decoupled. This network consists of three internal state variables $SOC1$, LFY and $AP1$, which determine the main dynamics of system (4.1), and two external input variables FT and $FT\text{-}FD$ combination which are assumed constant, can be obtained from the steady state values.

The numerical solution of the non decoupled variables $SOC1$, LFY and $AP1$ in system (4.1) is compared with the numerical solution of system (3.1) in Figure 4.3. This result shows that decoupling some concentrations on the system can still capture the essential behaviour of complex network for these non-constant variables. On the other hand, the flowering time process for the reduced model is shorter than in full system and the desired time period can be increased or decreased with a feedback control design approach which will be given in Chapter 6.

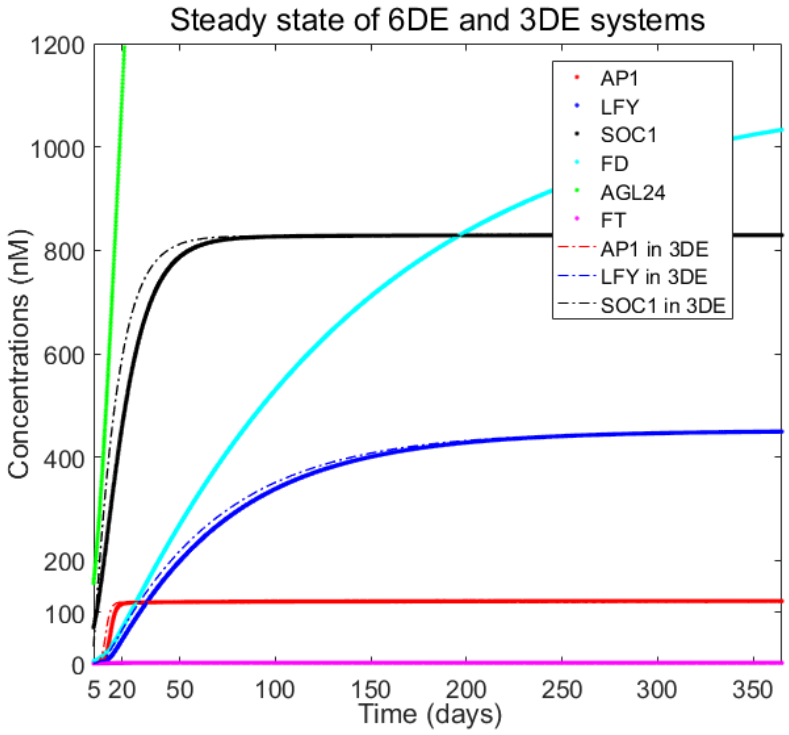

FIGURE 4.3: Comparison of the numerical solutions for steady state of the system (3.1) and (4.1) after decoupling. The figure on the left shows the numerical solutions of system (3.1) for one year where only FT is constant. The figure on the right represents the numerical solution of (4.1) for one year after decoupling of $AGL24$ and FD where they are constant with FT. The initial conditions are as in Figure 3.5.

4.3 Deterministic models of motifs

To further reduce the complexity of system (3.1), we use the approach in [Pullen et al., 2013], and reduce the system (4.1) from three to two equations to understand the essential characteristics of the floral transition by considering the two components, LFY and $AP1$, which constitute the minimal set for enabling the transition to floral meristem [Mandel et al., 1992]. Here, we model minimal regulatory networks of core components consisting of the concentrations LFY, $AP1$, FT and FD. We consider the simplified subsystem proposed in Figure 1(b) in [Pullen et al., 2013] to establish the essential characteristics of the floral transition. It can be obtained from system (4.1), represented in Figure 4.2, by considering constant $SOC1$ concentration ($\dot{x}_3 = 0$). The reason we use these four genes is: $AP1$ and LFY are key floral meristem identity genes in the

network of Arabidopsis flowering [Irish, 2010, Wellmer and Riechmann, 2010] and FT induces flowering through the activation of these two genes in a feed-forward circuit [Kardailsky et al., 1999] where FD has a significant role for FT signalling in meristem.

$AP1$ and LFY activate each other in the integration of flowering signals where they are mutual transcriptional activators [Liljegren et al., 1999]. As these concentrations are key floral meristem identity genes in the network, the subsystem is based on these two genes and takes into account the importance of the network activators and inhibitors. Additionally, we incorporate the action of FT-FD as a combined activator/inhibitor in meristem, as suggested in [Wang et al., 2014] and [Pullen et al., 2013]. Ignoring the change in $SOC1$ concentration in the network in Figure 4.2, we can redefine the simplified network as shown in Figure 4.4, where LFY and $AP1$ represent the main dynamics of this system. Furthermore, FT-FD and FT are the external input variables of meristem and leaves, respectively.

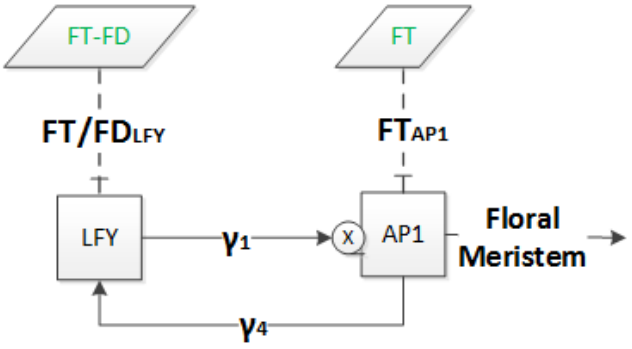

FIGURE 4.4: Flowchart of the simplified system (4.2). Direction arrows represent main activation where black labels describe the dynamic (internal) input variables, dashed ones inhibition/activation where the green labels represent the external input variables. Junction symbol next to $AP1$ shows the multiple interactions from LFY to $AP1$.

The analysis of the subsystem in Figure 4.4 allows us to investigate the activation and inhibition processes and provides ranges for input parameters which lead to the existence of stable solutions. Here, the inhibiting and activating effect of FT-FD in meristem and FT in leaves are described by F_1 for LFY and F_2 for $AP1$ in the system, respectively.

This gives the system

$$\begin{aligned} \frac{dx_1}{dt} &= \beta_1 \left(\frac{{x_2}^n}{{x_2}^n + {K_1}^n} \right) F_2 - d_1 x_1, \\ \frac{dx_2}{dt} &= \beta_4 \left(\frac{x_1}{x_1 + K_4} \right) F_1 - d_2 x_2. \end{aligned} \tag{4.2}$$

Here, F_1 and F_2 are joint inhibiting (when $F_i < 1$) and activating (when $F_i > 1$) constants, $\{i = 1, 2\}$. The variables x_1 and x_2 represent $AP1$ and LFY respectively, as defined before, and the parameters β_1, β_4, K_1, K_4, d_1 and d_2 are the same as previously (Table 3.2). We analyse subsystem (4.2) in three cases representing different $AP1$-LFY activation pathways. The first one shows the inhibition and activation of FT effect on $AP1$ while $F_1 = 1$; the second one, FT-FD effect on LFY while $F_2 = 1$. The third case shows the equal inhibition or activation effect of FT-FD and FT on LFY and $AP1$ ($F_1 = F_2$), respectively. The three realisations of the FT-FD and FT actions are given in Figure 4.5.

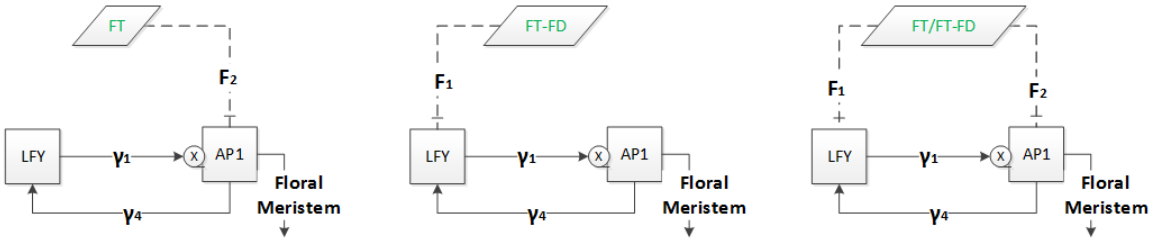

FIGURE 4.5: Effect of FT and combined effect of FT-FD inhibitor/activator actions on $AP1$ and LFY represented with F_2 and F_1 functions, respectively. Squares describe the floral meristem identity genes, LFY and AP1, which are the dynamic variables, and parallelograms describe the combination of external input variables, FT and FT-FD, which are repressor/activator of $AP1$ and LFY. Junction symbol next to AP1 shows the multiple interactions from $AP1$ and LFY, and γ_1 and γ_4 (Hill) functions are as in system (3.1). Subsystem 1, the action is on $AP1$ only ($F_1 = 1$, $F_2 \neq 1$), Subsystem 2, the action is on LFY only ($F_2 = 1$, $F_1 \neq 1$), and Subsystem 3, the action is on both $AP1$ and LFY.

The aim of the first and second subsystems is to analyse the effect of input variables on $AP1$ and LFY, respectively while one of them is exist but other one is not. The third subsystem is aimed to obtain the effect of input variables when they have an equal action on both main concentrations. The parameters in Table 3.2 are used to investigate

the behaviour of the input variables whether they play an inhibitor or an activator role. Note that the initial values of the concentrations are unknown in this system (4.5), and they can be obtained numerically from the steady state results by using the parameter values.

4.3.1 Steady states of motifs

The steady states $(\bar{x}_1, \bar{x}_2)$ of system (4.2) are found by considering the right-hand side of the equations equal to zero:

$$\begin{aligned} \beta_1 \left(\frac{\bar{x}_2^n}{\bar{x}_2^n + K_1^n} \right) F_2 - d_1 \bar{x}_1 &= 0, \\ \beta_4 \left(\frac{\bar{x}_1}{\bar{x}_1 + K_4} \right) F_1 - d_2 \bar{x}_2 &= 0. \end{aligned} \tag{4.3}$$

Here, it is easily shown that the trivial solution $(\bar{x}_1, \bar{x}_2) = (0, 0)$ is a stable steady state of the system (4.2). Although gene concentrations cannot formally be zero due to their biological meaning, the trivial steady state corresponds to a state where only small quantities are present due to non-modelled or stochastic effects. Hence we now focus on the non-trivial positive steady states of system (4.2), which can be obtained through the following process, where $\bar{x}_1 > 0$ and $\bar{x}_2 > 0$.

- From the first equality (4.3), we have

$$\bar{x}_1 = \frac{\beta_1 F_2}{d_1} \left(\frac{\bar{x}_2^n}{\bar{x}_2^n + {K_1}^n} \right). \tag{4.4}$$

- From the second equality (4.3), we have

$$\bar{x}_2 = \frac{\beta_4 F_1}{d_2} \left(\frac{\bar{x}_1}{\bar{x}_1 + K_4} \right), \tag{4.5}$$

  or equivalently

$$\bar{x}_1 = \frac{d_2 K_4 \bar{x}_2}{(\beta_4 F_1 - d_2 \bar{x}_2)}, \tag{4.6}$$

where $\beta_4 F_1 - d_2 \bar{x}_2 > 0$ as we only consider positive concentrations. This gives an upper bound for existence of $\bar{x}_2$ for all parameter values,

$$\bar{x}_2 < \frac{\beta_4 F_1}{d_2}. \tag{4.7}$$

Eliminating $\bar{x}_1$ from the equations (4.4) and (4.6),

$$\frac{\beta_1 F_2 \bar{x}_2^n}{d_1 \left(\bar{x}_2^n + {K_1}^n\right)} = \frac{d_2 K_4 \bar{x}_2}{(\beta_4 F_1 - d_2 \bar{x}_2)}, \tag{4.8}$$

we find the following polynomial equation in order to obtain all other non-trivial steady states of subsystem (4.2) for $\bar{x}_2$:

$$(\omega_1 + \omega_2 F_2)\bar{x}_2^n - \omega_3 F_1 F_2 \bar{x}_2^{n-1} + \omega_4 = 0. \tag{4.9}$$

where $\omega_1 = d_1 d_2 K_4$, $\omega_2 = d_2 \beta_1$, $\omega_3 = \beta_1 \beta_4$, $\omega_4 = d_1 d_2 K_1^n K_4$.

We focus only on positive solutions of $\bar{x}_1$ and $\bar{x}_2$ as they represent concentrations. These can be obtained by analysing the discriminant of the equation (4.9) which provides conditions on the roots. Descartes' rule of signs [Alina and Ionela-Rodica, 2011] indicates that for $n \geq 2$, equation (4.9) possesses either zero or two real positive roots due to two sign changes in the sequence of coefficients, while others are complex or negative.

As a consequence, system (4.2) has either zero or two positive steady states. We will analyse the conditions for positive real roots in further sections by using the parameter values in Table 3.2.

4.3.2 Deterministic stability of motifs

The dynamical subsystem (4.2) must have at least one stable steady state to represent the behaviour of the Arabidopsis flowering. In order to determine whether the positive equilibrium points $(\bar{x}_1, \bar{x}_2)$ are locally stable, we need to compute the eigenvalues of the Jacobian matrix evaluated at the equilibrium points.

The Jacobian matrix of the systems (4.2) is given as,

$$J_{(\bar{x}_1,\bar{x}_2)} = \begin{bmatrix} -d_1 & \dfrac{n\beta_1 K_1^n F_2 \bar{x}_2^{n-1}}{(\bar{x}_2^n + K_1^n)^2} \\ \dfrac{\beta_4 K_4 F_1}{(\bar{x}_1 + K_4)^2} & -d_2 \end{bmatrix}, \tag{4.10}$$

which gives the following characteristic equation,

$$P(\lambda) = \lambda^2 + (d_1 + d_2)\lambda + d_1 d_2 - \frac{n d_1 d_2 K_1^n K_4}{(\bar{x}_1 + K_4)(\bar{x}_2^n + K_1^n)}, \tag{4.11}$$

where $F_1 = \dfrac{d_2 \bar{x}_2 (\bar{x}_1 + K_4)}{\beta_4 \bar{x}_1}$ and $F_2 = \dfrac{d_1 \bar{x}_1 (\bar{x}_2^n + K_1^n)}{\beta_1 \bar{x}_2^n}$ are calculated from the equations (4.5) and (4.4), respectively.

If λ_1 and λ_2 are eigenvalues of J, we have

$$P(\lambda) = (\lambda - \lambda_1)(\lambda - \lambda_2).$$

Thus, we have the trace and determinant,

$$\mathrm{tr}(J) = \lambda_1 + \lambda_2 = -(d_1 + d_2), \quad \det(J) = \lambda_1 \lambda_2 = d_1 d_2 - \frac{n d_1 d_2 K_1^n K_4}{(\bar{x}_1 + K_4)(\bar{x}_2^n + K_1^n)}.$$

For asymptotic stability, we require that $Re\lambda < 0$. Therefore, the necessary and sufficient conditions for local stability are, $\mathrm{tr}(J) < 0$ and $\det(J) > 0$. The first condition is automatically satisfied while the second one gives

$$\det(J) = d_1 d_2 - \frac{n d_1 d_2 K_1^n K_4}{(\bar{x}_1 + K_4)(\bar{x}_2^n + K_1^n)} > 0. \tag{4.12}$$

If we substitute $\bar{x}_1$ from equation (4.4) into inequality (4.12), we find

$$\bar{x}_2^n > \frac{(n-1) d_1 K_1^n K_4}{(d_1 K_4 + \beta_1 F_2)}. \tag{4.13}$$

By substituting $\bar{x}_2^n$ from the equation (4.9), we obtain,

$$\bar{x}_2^n = \frac{\beta_1\beta_4 F_1 F_2 \bar{x}_2^{n-1} - d_1 d_2 K_1^n K_4}{d_2(d_1 K_4 + \beta_1 F_2)}. \tag{4.14}$$

By comparing the inequality (4.13) and equation (4.14), we obtain the necessary and sufficient condition for stability,

$$x_2^{n-1} > \frac{n d_1 d_2 K_1^n K_4}{\beta_1\beta_4 F_1 F_2}. \tag{4.15}$$

Combined with the inequality (4.7), a given steady state point $\bar{x}_2$ must satisfy the following ranges,

$$\bar{x}_2 < \frac{\beta_4 F_1}{d_2} \quad \text{and} \quad \bar{x}_2^{n-1} > \frac{n d_1 d_2 K_1^n K_4}{\beta_1\beta_4 F_1 F_2},$$

in order to be stable. The significance of this result is that the stability range is obtained in terms of the parameters of the system and the Hill coefficient n.

4.3.3 Numerical results for deterministic steady states and stability of the motifs

Steady states are explicitly important because they offer vital knowledge on the flowering state. They can be identified by the intersection of nullclines obtained from equations (4.4) and (4.6), leading to equation (4.8). They are plotted in $(\bar{x}_1, \bar{x}_2)$ space for the parameters in Table 3.2 and $n = 3$. The results for subsystem 1 and 2 are shown in Figures 4.6 and 4.7. In the graphs, reference points in the plane represent the values of $AP1$ and LFY for specific interactions. Points where the nullclines intersect represent the steady states of the system. The lack of intersection of the equations (4.4) and (4.6) indicates that there is no single steady state for the system (4.2) for the given values of F_1 and F_2.

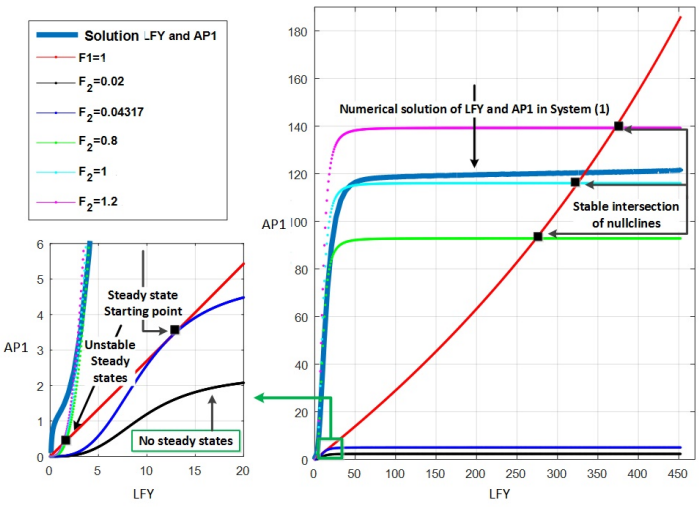

FIGURE 4.6: The nullclines (4.8) for subsystem 1 ($F_1 = 1$) with different values of F_2. The red curve represents LHS of (4.8), the other colours represent the RHS of (4.8). Intersections between red curve and other curves correspond to steady states. $F_2 = 0.02$ in black, shows there is no steady state point except trivial one $(0, 0)$. $F_2 = 0.04317$ in blue, corresponds to the lower bound for the existence of the steady state. $F_2 = 0.8$, $F_2 = 1$ and $F_2 = 1.2$ in green, cyan and magenta, respectively, each showing two steady states. The thick light blue line on the right of the figure represents the numerical solution of LFY and $AP1$ in (3.4), calculated in the steady state of system (3.1).

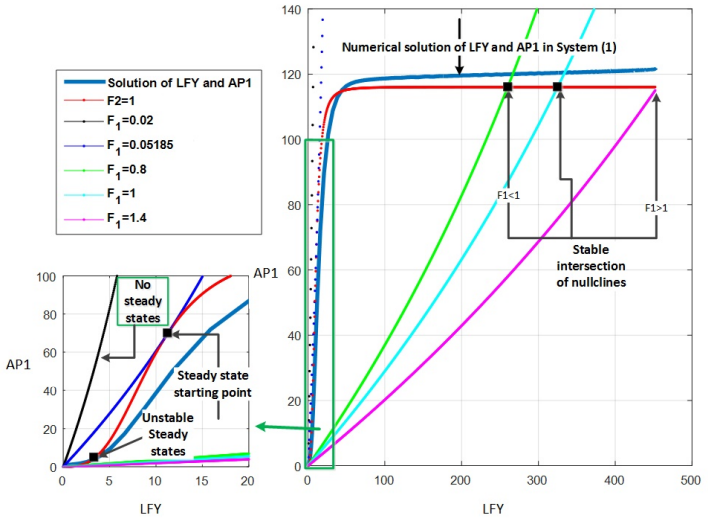

FIGURE 4.7: The nullclines (4.8) for subsystem 2 ($F_2 = 1$) with different values of F_1. The red curve represents RHS of (4.8), the other colours represent the LHS of (4.8). Intersections between red curve and other curves indicate steady states. $F_1 = 0.02$ in black, shows there is no steady state point except trivial one $(0, 0)$. $F_2 = 0.05185$ in blue, corresponds to the lower bound for the existence of the steady state. $F_2 = 0.8$, $F_2 = 1$ and $F_2 = 1.4$ in green, cyan and magenta, respectively, each showing two steady states. The thick light blue line on the right of the figure represents the numerical solution of LFY and $AP1$ in (3.4), calculated in the steady state of system (3.1).

Here, we analyse the occurrence of the steady states, and the condition for their convergence to the stable steady state. Let us now examine the stability of steady states of LFY and $AP1$ for the case $n = 3$, for which equation (4.9) becomes

$$(\omega_1 + \omega_2 F_2)\bar{x}_2^3 - \omega_3 F_1 F_2 \bar{x}_2^2 + \omega_4 = 0. \tag{4.16}$$

Remembering that all coefficients ω_j and F_i, $\{j = 1, \cdots, 4\}$, $\{i = 1, 2\}$, are strictly positive, it is readily seen from Viete's formulae that equation (4.16) always possesses a negative root along with either two strictly positive or complex roots. Therefore, to obtain strictly positive roots, the discriminant Δ_3 of the cubic (4.16) must be positive

$$\Delta_3 \;=\; \omega_4 \left[4(\omega_3 F_1 F_2)^3 - 27(\omega_1 + \omega_2 F_2)^2 \omega_4\right] \geq 0. \tag{4.17}$$

As values of ω_j can be calculated from the parameters in Table 3.2, the discriminant only depends on the unknown values of the external input variables F_i, which represent the inhibiting ($F_i < 1$) or activating ($F_i > 1$) actions of FT and FT/FD. From the minimum condition of discriminant ($\Delta_3 = 0$), we find the critical values of F_i for the existence of such roots. The plot in the (F_1, F_2) space given in Figure 4.8 represents the region for the existence of positive steady states, delimited by the degeneracy condition $\Delta_3 = 0$ which gives rise to double roots.

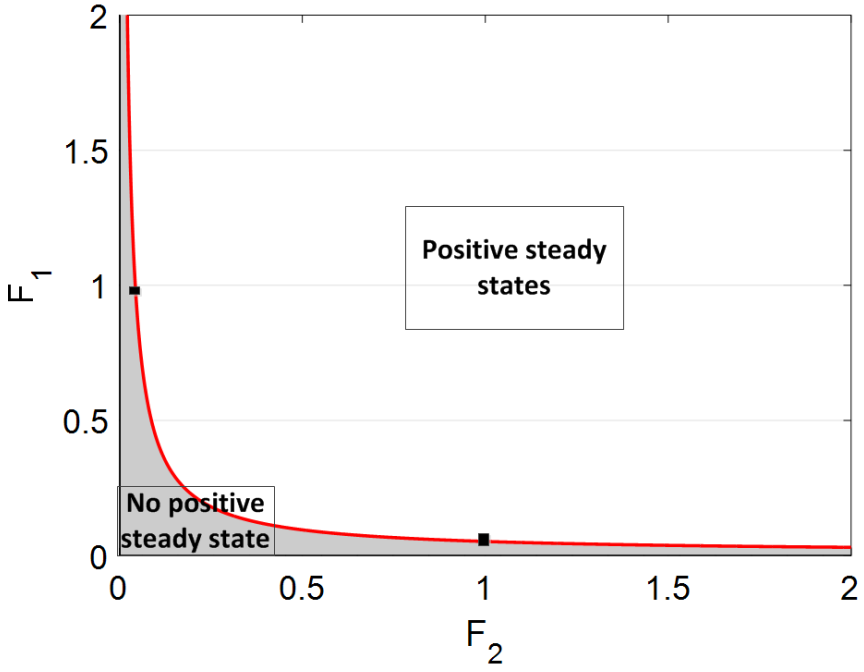

FIGURE 4.8: Minimum condition for steady states of simplified system (4.2) represented with red line which separates the region in white where steady states exist from the region in grey where there are no positive real steady states.

The points (1, 0.05185) and (0.04317, 1) given in Figure 4.8 indicate the lower bound for steady states of subsystem 1 on F_2 direction and subsystem 2 on F_1 direction, respectively, which are discussed in more details as follow.

1. For subsystem 1, $F_1 = 1$. (The changes in concentrations $\bar{x}_1$ and $\bar{x}_2$ in (4.4) depend on F_2, inhibition ($F_2 < 1$) and activation ($F_2 > 1$) actions of FT on $AP1$). Figure 4.6 shows the presence of a double root at $F_2 = 0.04317$ from which two distinct strictly positive equilibria emanate for $0.04317 < F_2 \leq max\{F_2\}$. Hence, when no action of FT-FD on LFY is present, the inhibition of FT on $AP1$ starts at the value of $F_2 = 0.04317$ and activation can be seen for $F_2 > 1$. Moreover, the behaviour of subsystem 1 is similar to system (3.1) for $F_2 \geq 0.04317$. The best match with the numerical solution of system (3.1) occurs for $F_2 > 1$, indicating an activation of FT on $AP1$. This result shows that F_2 can be considered as an activator of the system (4.2) instead of being inhibitor.

2. For subsystem 2, $F_2 = 1$. (The concentrations $\bar{x}_1$ and $\bar{x}_2$ in (4.6) depend on the F_1, inhibition ($F_1 < 1$) and activation ($F_1 > 1$) actions of FT-FD on LFY). A similar situation is seen in this case (Figure 4.7). The numerical result for this subsystem indicates

that in the absence of action of FT on $AP1$, the inhibition of FT-FD on LFY starts at the double root $F_1 = 0.05185$, from which originate one stable and one unstable positive steady states. The behaviour of subsystem 2 is similar to system (3.1) for $F_1 \geq 0.05185$, while the best match with the numerical solution of system (3.1) can be seen in the activation of FT-FD on LFY for $F_1 > 1$. In the view of such information, we use F_1 and F_2 external input variables as an activator of the LFY and $AP1$ in subsystem (4.2) to be able to obtain a compatible behaviour with system (3.1).

3. For subsystem 3, we distinguish two cases. In the first case, FT-FD and FT are assumed equally inhibit/activate LFY and $AP1$ by using the same maximum transcription rate ($F_1 = F_2$). The minimal value of the bifurcation parameter occurs at $F_1 = F_2 = 0.21156$, hence two distinct positive steady states for $F_1 > 0.21156$, as illustrated in Figures 4.9. The numerical solutions confirm that the actions of FT on $AP1$ and FT-FD on LFY do not start any interaction for the flowering of Arabidopsis until the inhibition value of $F_1 = 0.21156$. This situation is represented in the left-hand side of the trajectory line in Figure 4.9 where there is no steady state (the solutions of (4.16) for $\bar{x}_2$ are complex). The right-hand side of the trajectory line on this figure shows the stable and unstable steady states indicating that the Arabidopsis flowering is in process. This subsystem can capture the behaviour of the system (3.1) after the steady state occurs. The best match with the numerical solution of system (3.1) is estimated after FT and FT-FD start to activate $AP1$ and LFY, respectively. Details of stable and unstable steady states are given in second and third sub-figures of Figure 4.9.

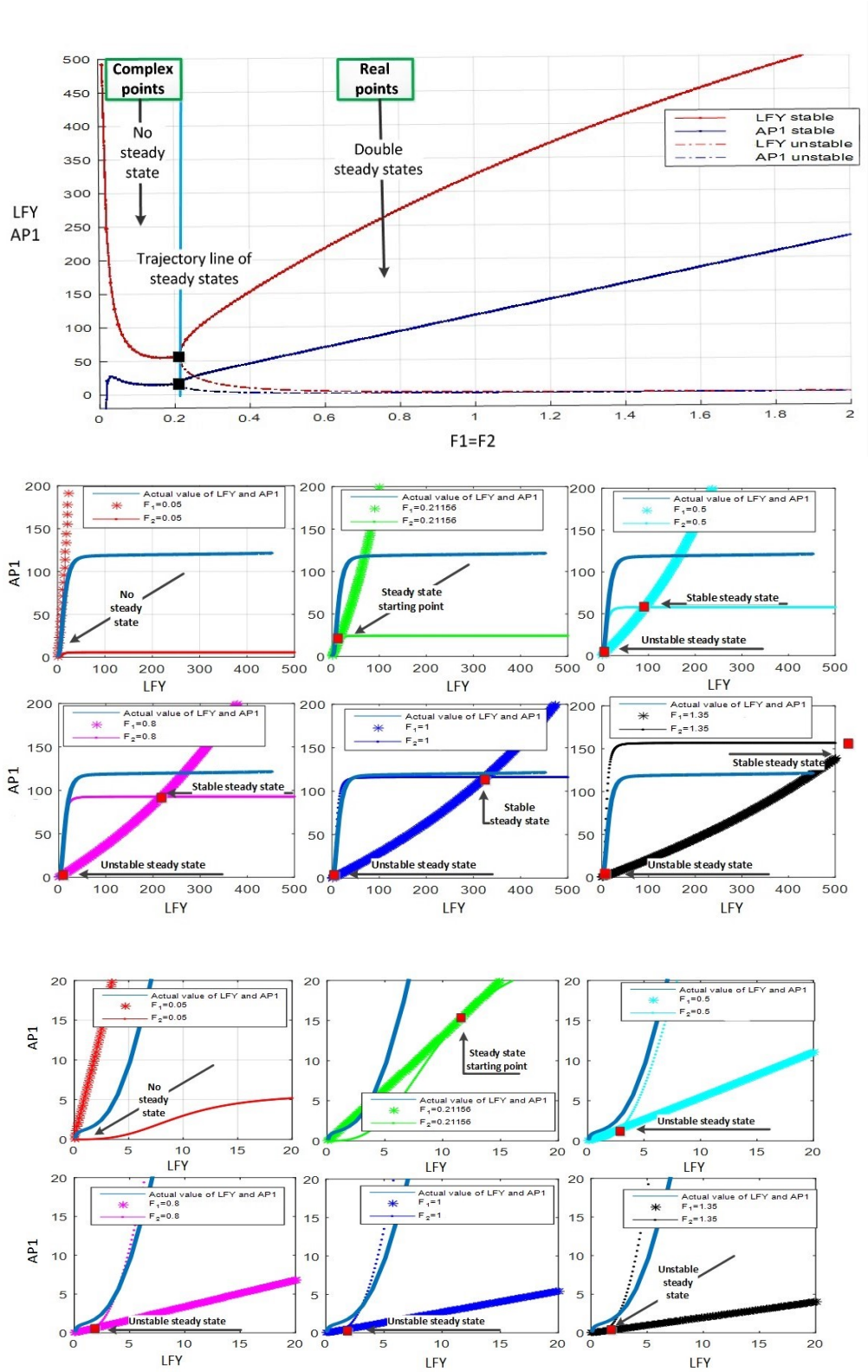

FIGURE 4.9: LFY and $AP1$ with values of F_i from 0 to 2 and ($F_1 = F_2$) in equation (4.8). The trajectory line, which is for $F_1 = 0.21156$, divides the existence of steady states into two regions. Two steady states occur right of the trajectory line for each value of F where one of them is a stable state, shown with solid line, and others are unstable, shown with dashed line. There are no positive steady states on the left of the trajectory line. The black points on the trajectory line show the degenerated stable steady state values of LFY and $AP1$. The details of unstable steady states and non-trivial stable ones can be seen in second and third Figures.

In the second case, we assume F_1 and F_2 may be different from each other. In this circumstance, the best match with system (3.1) is for $F_1 = 1.3445$ and $F_2 = 1.0476$. These results are obtained from (4.6) and (4.4) by using the estimated parameters from Table 3.2 and matching the steady state values of x_1 and x_2 from Table (3.4). Comparison with the solution of system (3.1) is given in Figure 4.10, showing that subsystem 3 captures well the behaviour of the full model (3.1) after FT-FD and FT start activating LFY and $AP1$, respectively. In this case, by considering the direction of the flow $\left(\frac{dx_1}{dt}, \frac{dx_2}{dt}\right)$ in the (x_1, x_2) phase plane of the system (4.2) for the obtained value $F1$ and $F2$ (Figure 4.11), it can be explicitly seen that the trivial and non-trivial upper steady states are stable, while the lower non-trivial one corresponds to a saddle node.

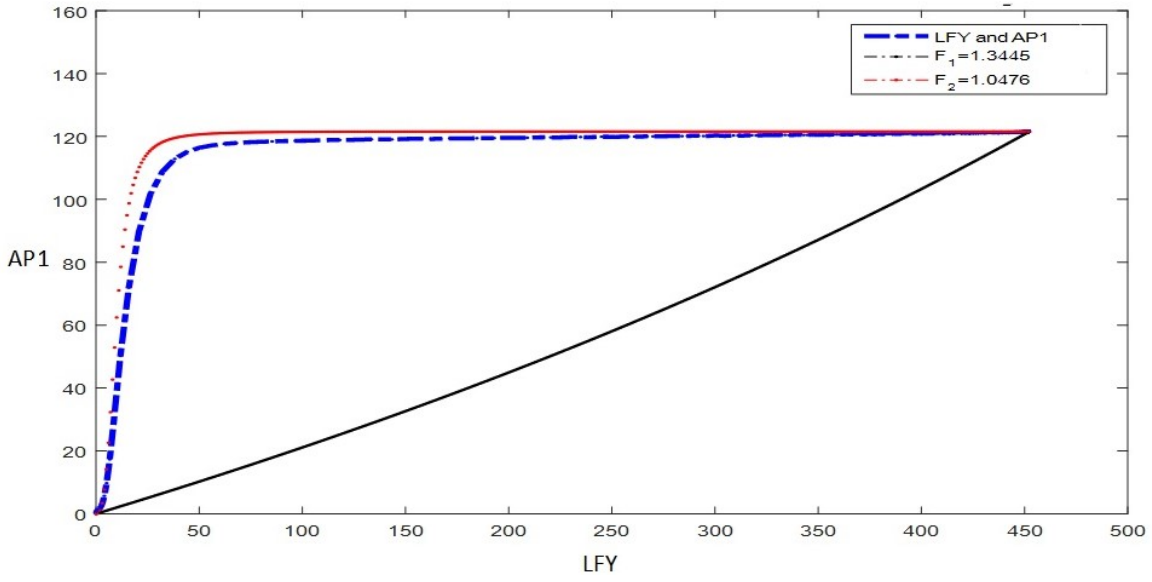

FIGURE 4.10: Intersection of nullclines (4.6) and (4.4) showing stable steady state for $F_1 = 1.3445$ and $F_2 = 1.0476$. Comparison with numerical solution of system (3.1) is also given in blue dashed line.

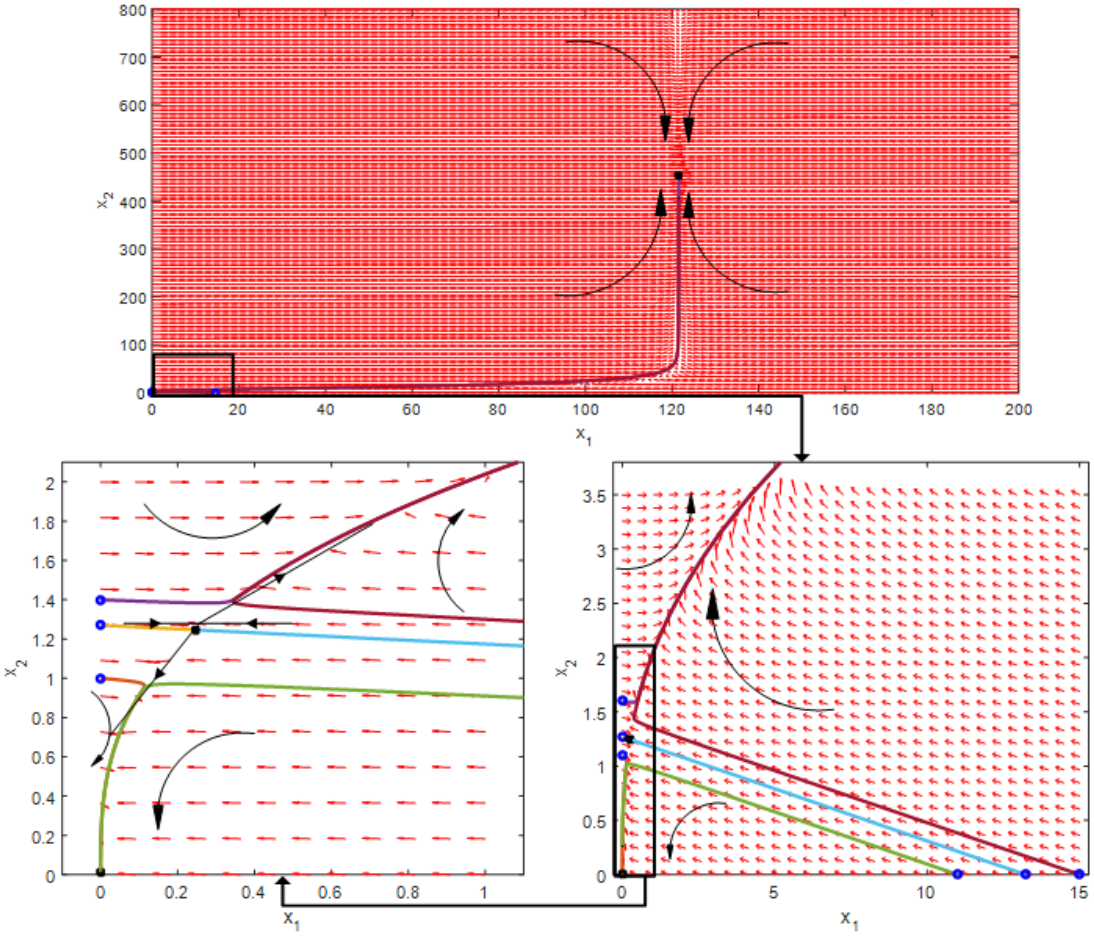

FIGURE 4.11: Phase plane of the $AP1(x_1)$ and $LFY(x_2)$ for the obtained values $F_1 = 1.3445$ and $F_2 = 1.0476$ in system (4.2). Black dots represent the steady states, and blue dots on the x-axis and y-axis represent the initial conditions ($AP1$, $LFY = 0$) and ($AP1 = 0$, LFY) for the coloured lines, respectively. Light blue and dark yellow lines show the eigenvectors of the unstable point (saddle nodes). Below and above these two lines the trivial and non-trivial stable steady states are reached, respectively. The curves with red and black colours show trajectories of the system, where their arrows represent the direction of the phase flow.

The unstable steady state can be regarded as the threshold values of the concentrations for the flowering of *Arabidopsis Thaliana*. As a consequence, if flowering is processing for some time which means the concentrations have already reached their threshold values for the flowering, then the concentrations can move away from an unstable steady state and converge to a non-trivial stable one.

In view of the control problem which will be developed in Chapter 6, the role of the components $AP1$, LFY and $SOC1$ can be summarised as in Table 4.1.

Components	Role of the components	Threshold
$AP1$	Floral meristem identity regulator. (Has key role between floral induction to flower formation)	0.24 nM
LFY	Floral meristem identity regulator. (Positive regulator of $AP1$)	1.24 nM
$SOC1$	Floral pathway integrator. (Activates LFY)	

TABLE 4.1: The role of the components $AP1$, LFY and $SOC1$. Threshold values of $AP1$ and LFY in the motifs (4.2) are obtained by using the parameter values in Table (3.2) and input values ($F_1 = 1.3445$ and $F_2 = 1.0476$).

4.4 Conclusion

In this chapter, we produced some simplified dynamical models of the full system of Arabidopsis flowering time GRN. Given the complexity of the system, more precise conditions have been formulated by considering subsystems which focus on the dynamics of essential elements. According to our analysis for the full system, three genes, $SOC1$, LFY and $AP1$, have a strong effect on the flowering of Arabidopsis. Therefore, decoupling for the other concentrations has been applied to simplify the system based on these three genes. Analytical solution of the simplified system is still difficult, however it illustrates specific pathways of inhibition and activation. By using these pathways, we reconstruct three different subsystems suggested in Pullen et al. [2013] and Jaeger et al. [2013]. This allowed us to derive necessary and sufficient conditions for the existence of the positive steady states of these subsystems with generalized expressions for Hill functions that represent the dynamics and cooperativity of the Arabidopsis flowering time regulation system. The most important floral identity genes, $AP1$ and LFY, are used to investigate the flowering where they are regulating each other, and the results are confirmed by experiments [Liljegren et al., 1999]. The necessary and sufficient conditions for the local stability have then been determined analytically and the stability ranges are established with the estimated parameters and compared with the numerical solutions. The numerical results have confirmed that these subsystems can capture the

essential behaviour of the full model by estimating the FT-FD and FT inhibition/activation effects on the concentration of LFY and $AP1$, respectively.

Our analyses, being in a good agreement with the experimental findings, bring further insights into the roles of LFY and $AP1$ and provide the opportunity to explore different pathways for flowering.

Chapter 5

Stochastic motifs

5.1 Introduction

The aim of this chapter is to investigate and compare the stability properties of simplified mathematical models of Arabidopsis flowering developed with stochastic perturbations. The motifs are reflecting the essential behaviour of the complex network and can capture the significant features of the full Arabidopsis flowering model. The advantage of this approach is based on the realistic description of gene effects and their interactions on flowering of Arabidopsis. New sufficient conditions of mean square stability are obtained analytically for this simplified model using Lyapunov function. Analytical and numerical investigations of the stability are performed with respect to gene concentration and noise term by using Ito stochastic formula within both additive and multiplicative white noise. For numerical implementations, Euler-Maruyama method is used to solve Ito SDEs systems.

5.2 Stochastic stability of motifs

In real life, most of the time-series behaviour of biological systems are not deterministic. To obtain more realistic representations of their behaviour, it is appropriate to work with

stochastic differential equations (SDEs), which can be obtained by incorporating noise terms into deterministic models. The aim of this section is to introduce and study for the first time SDEs for the behaviour of Arabidopsis flowering.

There are several ways for obtaining a SDEs model. Manninen et al. [2015, 2006] introduced a few different approaches in their papers for incorporating stochasticity into the deterministic models. For example, stochasticity can be incorporated into reaction rates, rate constants or into concentrations by using the chemical Langevin equation. In this study, we consider integrating stochasticity into reaction rates by taking into account both additive (stochasticity into rate of each variable) and multiplicative (stochasticity into each reaction rate) white noise by following Mackey and Nechaeva [1994].

Starting from the following general form of deterministic non-linear differential equations,

$$dX(t) = F(t, X(t))dt, \tag{5.1}$$

and, incorporating additive and multiplicative white noise into equations (5.1), we obtain two type of stochastic differential systems which will be studied in Subsections (5.2.1) and (5.2.2), respectively. The Ito forms of these SDEs systems are also introduced in these subsections.

5.2.1 Stochastic motifs with additive white noise

A general Ito formulation of a system of stochastic differential equations with additive white noise form can be written as

$$dX(t) = F(t, X(t))dt + GdW(t), \tag{5.2}$$

where the stochastic component GdW is added into the rate of each variable in deterministic model (5.1). Here, $G = diag[\sigma_1, \cdots, \sigma_m]$ describes non-negative real constant diagonal matrix with standard deviation parameters σ_j, $j = 1, \ldots, m$, and $W(t)$ is a

random variable which represents m-dimensional standard Brownian motion or Wiener process over $t \in [0, T]$.

The general solution of equations (5.2) can be written as

$$X(t) = X(0) + \int_0^t F(s, X(s))ds + \sum_{j=1}^{m} \int_0^t G_j dW_j(s),$$

where $X(0)$ is the initial condition of the system and t is taken in the interval $[0, T]$. By modifying system (4.2), we obtain the following stochastic differential equations,

$$\begin{aligned} dx_1(t) &= [f_1(x_2(t)) - d_1 x_1(t)]\, dt + \sigma_1 dW_1(t), \\ dx_2(t) &= [f_2(x_1(t)) - d_2 x_2(t)]\, dt + \sigma_2 dW_2(t), \end{aligned} \tag{5.3}$$

where σ_1, σ_2 are real constants and, W_1 and W_2 are independent standard Wiener processes with increments $dW_i(t) = W_i(t + \Delta_t) - W_i(t)$, $i = 1, 2$, and each independent random variables satisfy $dW_i \sim \sqrt{\Delta t}\mathcal{N}(0, 1)$. Hill functions f_1 and f_2 are defined as

$$f_1(x_2) = \frac{\beta_1 F_2 x_2^3}{x_2^3 + K_1^3}, \qquad f_2(x_1) = \frac{\beta_4 F_1 x_1}{x_1 + K_4},$$

and the parameters are the same as in previous sections. For numerical implementations with additive white noise, the Euler-Maruyama method with fixed time step Δt is used to solve this Ito SDEs model,

$$x_i(t + \Delta t) = x_i(t) + F_i(t, x(t))\Delta t + \sigma_i dW_i. \tag{5.4}$$

The deterministic model of system (4.2) has three steady states: two of them are stable with a trivial and a non-trivial solution, and one is an unstable, trapped between these two stable steady states. The behaviour of this system depends on the initial conditions of the concentrations. If their initial values are lower than the unstable steady state (sub-threshold value of the system (4.2) for flowering of Arabidopsis), then system will certainly reach the trivial solution which means values are insufficient for triggering process of Arabidopsis flowering. Therefore, flowering of the Arabidopsis will not occur. If their initial values are larger than the unstable steady state, the flowering

of this seed will proceed, being attached by the non-trivial stable steady states of the concentrations.

On the other hand, the behaviour of the stochastic model for system (4.2), which is given in (5.3), is more complex and depends on the initial conditions and the amount of noise in each of the concentrations. So, it is not certain whether it reaches non-trivial (passing the sub-threshold for the flowering) or trivial (non-flowering) stable equilibria. This is a random process and this kind of behaviour is known as "stochastic switching" [Ullah and Wolkenhauer, 2011]. We show the behaviour of stochastic model (5.3) with a time-varying histogram to see the changes of the behaviour. The initial values are fixed as $(0.2, 1.2)$, which lie between unstable and trivial stable steady states for the parameter values from Table 3.2. The implementation has been performed 100 times with a fixed constant noise of 5% ($\sigma_i = 0.05$).

As can be seen from Figures 5.1 and 5.2, stochasticity can change the behaviour of the system. The solutions are initially concentrated around the initial values and then diverted to two different directions. At the end, they converged around either trivial or non-trivial stable solutions with a considerable proportion. This shows that successful solutions for the Arabidopsis flowering can be obtained by using stochastic equations system even if the initial values are under the threshold value.

We also consider the effect of the different σ values on the stochastic system (5.3). If we look at the initial values of the concentrations (x_{init}) around the unstable steady state within 5% range, $0.95\bar{x} < x_{init} < 1.05\bar{x}$, we obtain the results presented in Figure 5.3.

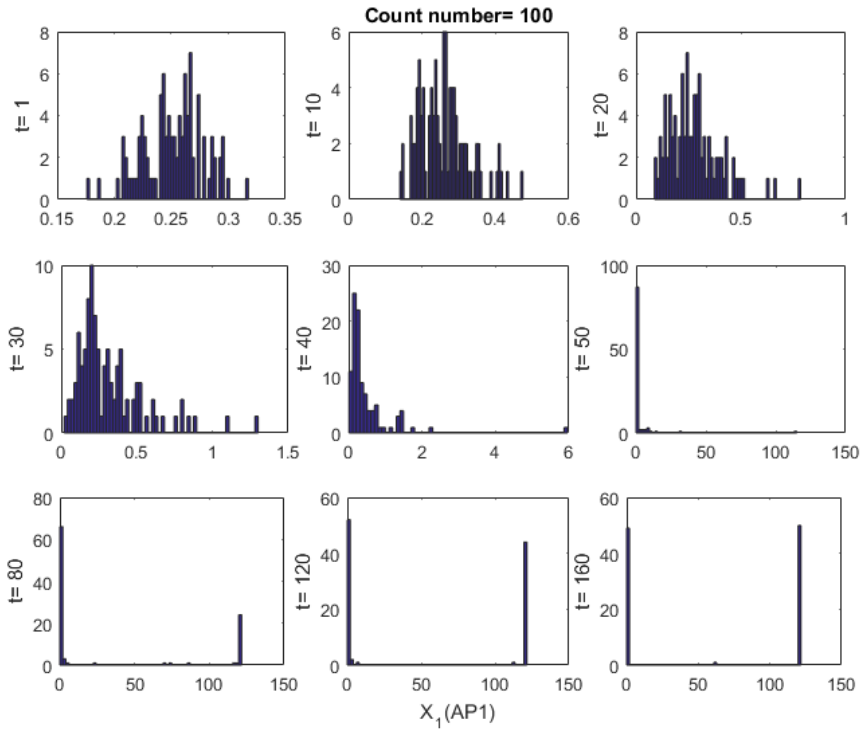

FIGURE 5.1: Temporal histogram progress for the Arabidopsis flowering stochastic model for $AP1$.

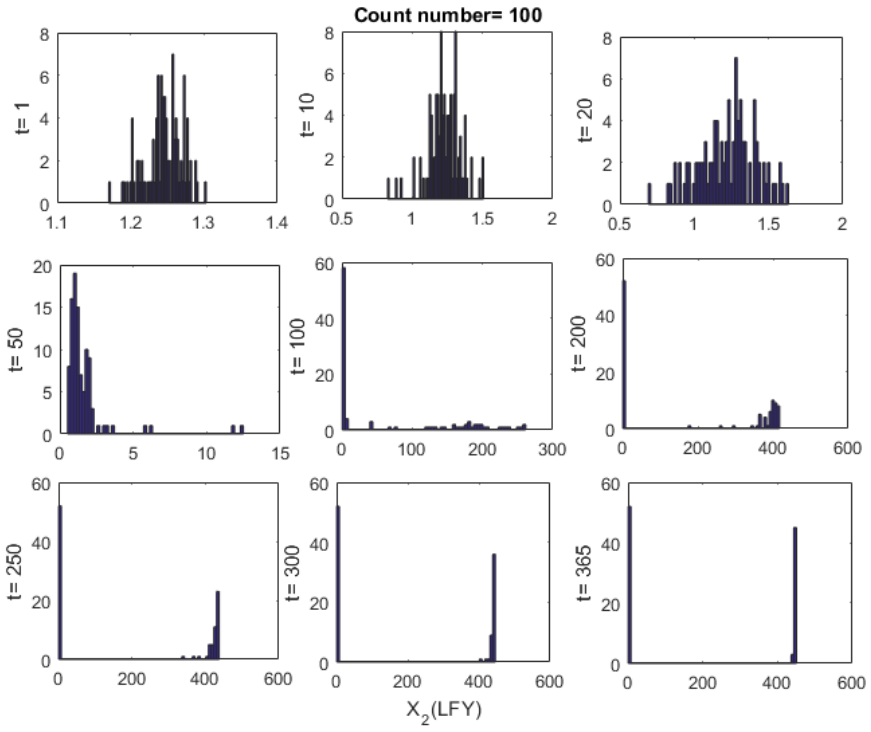

FIGURE 5.2: Temporal histogram progress for the Arabidopsis flowering stochastic model for LFY.

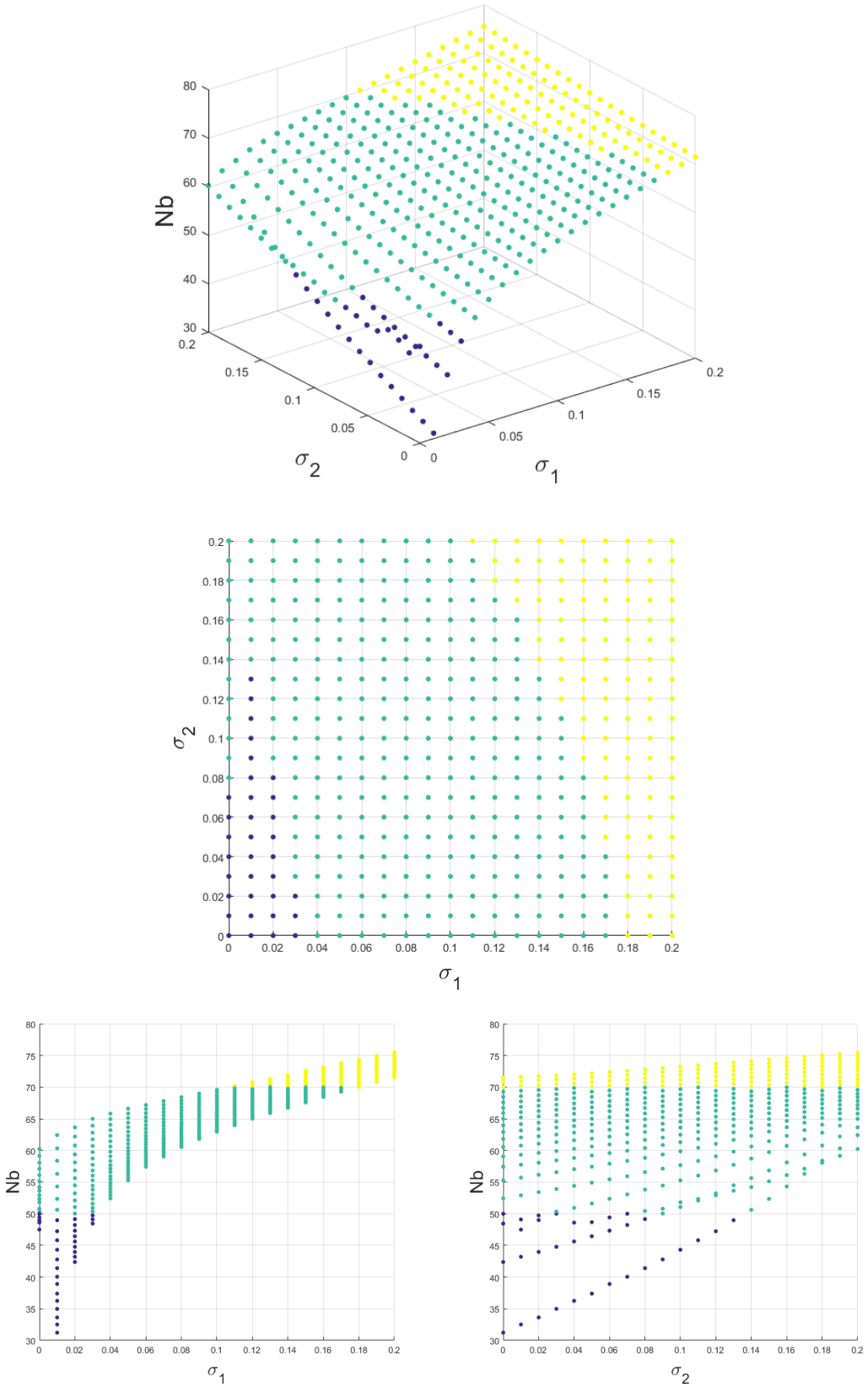

FIGURE 5.3: Proportion of successful solutions (Nb) of the SDEs of Arabidopsis flowering model (5.3) with random initial condition within 5% of the unstable solution, depending on the noise parameter σ_i. Blue, green and yellow dots represent success rations of the flowering process for less than 50%, between 50% and 70%, and more than 70%, respectively.

5.2.2 Stochastic motifs with multiplicative white noise

In contrast with the previous subsection, where the possibility of successful flowering was depending only on the amount of noise terms and initial values of the concentrations, here we assume that the amplitude of noise also depends on the state of the system. The aim of this study is to determine the flowering and non-flowering domain of the stochastic motifs with multiplicative white noise. These can be obtained by using a Lyapunov function approach, centered at the origin or at a non-trivial steady state of the system. This allows to obtain necessary stability conditions which depend on the noise parameters σ_i.

First, we start by introducing the Ito formula of a system of stochastic differential equations with multiplicative white noise in the form

$$dX(t) = F(t, X(t))dt + G(t, X(t))dW(t). \tag{5.5}$$

This can be obtained by integrating the stochastic component $G(X)dW$ into each reaction rate of the deterministic model (5.1), where $F(t, X(t)) = (F_i(t, X(t))) \in \mathbb{R}^n$, $G(t, X(t)) = (G_{ij}(t, X(t)) \in \mathbb{R}^{n\times m}$, is a matrix of measurable functions, and $W(t) = (W_i(t)) \in \mathbb{R}^m$ is an m-dimensional independent Wiener process, or equivalently an m-dimensional vector of standard Brownian motions.

The solution $X(t)$ of the SDE can be obtained after the integration of equation (5.5) as

$$X(t) = X(0) + \int_0^t F(s, X(s))ds + \sum_{j=1}^{m} \int_0^t G_j(s, X(s))dW_j(s),$$

for $j = 1, \cdots, m$ and $0 \leq t \leq T$.

More precisely, stochastic perturbations of the variables around their equilibrium values are assumed to be of white noise type and proportional to the distances of $AP1(x_1)$ and $LFY(x_2)$ from the steady state values $\bar{x}_1$ and $\bar{x}_2$. The question whether the dynamical behaviour of model (4.2) is influenced by stochastic effects is investigated by looking at the asymptotic stochastic stability of equilibrium points. By considering an explicit stochasticity in the deterministic differential equations system (4.2), we obtain an Ito

stochastic differential equations system of the Arabidopsis flowering with the stochastic perturbations of x_1 and x_2 from the equilibrium point $(\bar{x}_1, \bar{x}_2)$, given by

$$\begin{aligned} dx_1(t) &= \left[f_1(x_2(t)) - d_1 x_1(t)\right] dt + \sigma_1(x_1(t) - \bar{x}_1) dW_1(t), \\ dx_2(t) &= \left[f_2(x_1(t)) - d_2 x_2(t)\right] dt + \sigma_2(x_2(t) - \bar{x}_2) dW_2(t), \end{aligned} \tag{5.6}$$

where again σ_i are positive constants and W_i are independent standard Wiener process components with increments $\Delta W_i(t) = W_i(t + \Delta_t) - W_i(t)$, $i = 1, 2$, and Gaussian random variables $dW_i \sim \Delta(t)\mathcal{N}(0, 1)$. As mentioned before, $x_i, \bar{x}_i \in R_0^+$ are non-negative real numbers.

Let us investigate that the trivial solution $x(t) = 0$ of system (5.6) is locally asymptotically stable in probability while there exists a domain which is neighbourhood of $\bar{x} \equiv 0$. The importance of this domain is being the non-flowering domain of the *Arabidopsis Thaliana* GRN for system (5.6).

Theorem 5.1 (Barbashin-Krasovskii theorem for stochastic differential equations [Ignatyev and Mandrekar, 2010])**.** *Let the origin $x = 0$ be an equilibrium point for a stochastic differential equation system of the form*

$$dX(t) = f(X)dt + \sum_{i=1}^{n} g_i(X) dW_i(t), \;\; X \in \mathbb{R}^n, \;\; f(0) = g_i(0) = 0,$$

where f, $g_i \in \mathbb{R}^n$ satisfy Lipschitz conditions and $W_i(t)$ are independent Wiener processes. Let $V : D \longrightarrow \mathbb{R}$ be a continuously differentiable positive definite function on a domain $D \subset \mathbb{R}^n$ containing the origin, such that $LV(x(t)) \leq 0$ in D, where L is a differential operator acting on the function V as

$$LV(x(t)) = \sum_{i=1}^{n} f_i \frac{\partial V}{\partial x^i} + \frac{1}{2} \sum_{i,j=1}^{n} G_{ij} \frac{\partial^2 V}{\partial x^i x^j}, \; G_{ij} = \sum_{i=1}^{k} g_{im} g_{jm}. \tag{5.7}$$

Let $S = \{x \in D : LV(x) = 0\}$ be set of all points where $LV = 0$ and suppose that no other solution can stay in S, other than the trivial solution $x(t) \equiv 0$. Then the origin is locally asymptotically stable in probability.

Theorem 5.2. *The equilibrium point $\bar{x} = 0$ of system (5.6) is locally asymptotically stable in probability if the conditions*

- $0 \leq \sigma_i < \sqrt{2d_i}, \quad i = 1, 2,$

are satisfied.

Proof. 5.2. Let $\bar{x} = 0 \in D \subset \mathbb{R}^2$ be an equilibrium point of the stochastic differential equations system (5.6) where D is defined as a positive neighbourhood of this point. Let us define a positive definite function V with a strictly positive arbitrary constant θ such that

$$V(x) = \frac{1}{2}(\theta x_1^2 + x_2^2), \quad \theta > 0, \tag{5.8}$$

where $V : D \longrightarrow \mathbb{R}$ is a continuous differentiable and satisfies that $V(0) = 0$ for only $x = 0$ and $V(x) > 0$ for all $x \in D \setminus \{0\}$.

Applying the L operator (5.7) to $V(x)$ in (5.8) gives the following expression for system (5.6),

$$\begin{aligned} LV(x) &= \theta x_1(f_1(x_2) - d_1 x_1) + x_2(f_2(x_1) - d_2 x_2) + \frac{1}{2}(\theta\sigma_1^2(x_1 - \bar{x}_1)^2 + \sigma_2^2(x_2 - \bar{x}_2)^2), \\ &= \theta x_1(f_1(x_2) - d_1 x_1) + x_2(f_2(x_1) - d_2 x_2) + \frac{1}{2}(\theta\sigma_1^2 x_1^2 + \sigma_2^2 x_2^2), \end{aligned} \tag{5.9}$$

where $\bar{x}_1 = \bar{x}_2 = 0$. It is clear that $x = 0$ is a solution of $LV(x) = 0$. Hence, it is necessary to find a domain D around a positive neighbourhood of $x = 0$, which satisfies $LV < 0$ and $LV = 0$ for only $x = 0$ that means there is no other solution except the zero one while $LV = 0$.

Taking a second-order Taylor series in some positive neighbourhood around $(x_1, x_2) = (0, 0)$ for $LV(x)$ in (5.9) gives

$$LV(x) \approx -\frac{\theta(2d_1 - \sigma_1^2)}{2}x_1^2 - \frac{(2d_2 - \sigma_2^2)}{2}x_2^2 + \frac{\beta_4 F_1}{K_4}x_1 x_2. \tag{5.10}$$

Using Young's inequality in (5.10), for any sufficiently small constant $\varepsilon > 0$,

$$\pm x_1 x_2 \leq \frac{1}{2}(\varepsilon x_1^2 + \frac{1}{\varepsilon}x_2^2),$$

we obtain,

$$LV(x) \leq -\frac{\theta(2d_1 - \sigma_1^2)}{2}x_1^2 - \frac{(2d_2 - \sigma_2^2)}{2}x_2^2 + \frac{\beta_4 F_1}{K_4}\frac{1}{2}\left(\varepsilon x_1^2 + \frac{1}{\varepsilon}x_2^2\right). \tag{5.11}$$

By grouping x_1^2 and x_2^2 for $\theta > 0$, we find

$$LV(x) \quad \leq \quad -x_1^2\left[\frac{(2d_1 - \sigma_1^2)\theta}{2} - \frac{\beta_4 F_1}{2K_4}\epsilon\right] - x_2^2\left[\frac{(2d_2 - \sigma_2^2)}{2} - \frac{\beta_4 F_1}{2K_4\epsilon}\right]. \tag{5.12}$$

This is locally and asymptotically stable in probability if $LV(x) < 0$, therefore, the following inequalities are required,

$$\left(2d_1 - \sigma_1^2\right)\theta - \left(\frac{\beta_4 F_1}{K_4}\right)\epsilon \quad > \quad 0 \tag{5.13}$$

$$(2d_2 - \sigma_2^2)\epsilon - \left(\frac{\beta_4 F_1}{K_4}\right) \quad > \quad 0, \tag{5.14}$$

In particular, this implies that

$$\sigma_1^2 < 2d_1 \quad \text{and} \quad \sigma_2^2 < 2d_2,$$

where θ, ϵ and parameter values are all positive.

It is clear that if the ranges (5.13) and (5.14) are satisfied than $LV(x)$ in (5.12) equals to zero for only $x = 0$.

Combining the inequalities (5.13) and (5.14), we find,

$$\frac{\beta_4 F_1}{\left(2d_2 - \sigma_2^2\right)K_4} < \epsilon < \frac{\theta K_4\left(2d_1 - \sigma_1^2\right)}{\beta_4 F_1}. \tag{5.15}$$

To obtain the sufficient conditions for the mean square stability, we consider the left and right hand-sides of the inequality (5.15) while all parameters are positive. Multiplying and dividing both of side by $\beta_4 F_1$ and $K_4\left(2d_1 - \sigma_1^2\right)$, respectively, gives the following

conditions,

$$\theta > \left(\frac{\beta_4 F_1}{K_4}\right)^2 \frac{1}{\left(2d_1 - \sigma_1^2\right)\left(2d_2 - \sigma_2^2\right)} > 0, \tag{5.16}$$

which shows that for any σ_1, σ_2 satisfying $\sigma_i < \sqrt{2d_i}$ one can choose a suitable positive value of θ such that V is a local Lyapunov function of the system. Thus, the origin is locally asymptotically stable in probability.

□

Sufficient conditions for the mean square stability of the stochastic differential equations system (5.6) with a defined Lyapunov function (5.8) around trivial stable state have been obtained from the Theorem 5.2. The result represents the stability domain of the system around origin which gives non-flowering area of it depends on noise. As a result, stability of the non-negative equilibrium not only depend on concentrations and the parameters of the system but also depend on the noise terms. By using the parameter values in Table 3.2, the minimum θ value has been obtained as $\theta > 0.125$, which means Lyapunov function (5.8) satisfies stability of the trivial solution of stochastic system (5.6) if θ is chosen larger than 0.125.

5.3 Conclusions

In this chapter, stochastic motif was initially studied around the unstable steady state with an additive white noise to show how the flowering and non-flowering process can change with the effect of the noise term. Numerical simulations of the Ito stochastic differential equations system (5.3) was performed with fixed initial values and constant noise in the time-varying histogram. Moreover, it was simulated with different initial values around the unstable steady state within 5% range and different noise within 20% range, and the possibilities of the successful flowering process was illustrated.

Then, stability of the stochastic motif was studied around trivial stable steady state with a multiplicative white noise to obtain sufficient conditions of mean square stability

by using Lyapunov function for non-flowering domain. The Ito stochastic differential equations system (5.6) was performed to investigate analytical and numerical solutions. The sufficient conditions for non-flowering stability area was investigated around the origin within a range depends on the noise terms and defined Lyapunov function (5.8).

As a result of both approaches, it is demonstrated that the stochasticity can change the behaviour of the stability region which cannot be obtained in the case of deterministic model of the Arabidopsis.

Chapter 6

Control theory and observer design of Arabidopsis flowering GRN

6.1 Introduction

In previous chapters, the stability analysis and behaviour of the motif models have been studied within the deterministic and stochastic perspectives. However, the stability analysis of the full model and simplified one is not an easy task analytically. Moreover, similar behaviour of the full model can be observed in the simplified model, which is obtained by decoupling some concentrations, but some of the concentrations cannot be exactly measured in the simplified model. Therefore, an observer has to be designed and applied numerically to estimate these unmeasured variables by using the measured ones (inputs and outputs). Furthermore, by doing some modifications on the simplified model, feedback control laws can be designed and the behaviour of this model can be regulated by controlling the input of the system related to reference value of output [Dibiasio et al., 1978, Ma et al., 2016, Oyarzún and Chaves, 2015].

In this chapter, observability and controllability of the dynamical models of Arabidopsis flowering is studied. The simplified dynamic model of Arabidopsis flowering time GRN system constructed with three differential equations based on $SOC1$, LFY and $AP1$ is considered. The validity of this simplified system, which is obtained by decoupling some concentrations in the original model, is controlled by using control feedback theory, and this system is regulated by controlling the inputs to obtain the desired behaviour. Recall that the simplified system with three equations is still complex and cannot be reduced directly into the system with two differential equations by decoupling $SOC1$ or LFY, which are not measurable variables. For this reason, the observer design of this system is employed in two different gain observer examples; constant and high gain observer. The constant gain observer approach is an easy task and does not depend on the state variables. On the other hand, high gain observer depends on the state variable and estimation of this observer is more difficult than the constant one.

In the simplified system of equations, $AP1$ represents an output measured concentration while estimated of the variables $SOC1$ and LFY are non-measured. We have a single input variable FT, which is given as u in U_1 and U_2 input functions. We recall that the three equation system was given in system (4.1) as

$$\begin{aligned} \dot{x}_1 &= f_1(x_2) + U_1(u) - d_1 x_1 \\ \dot{x}_2 &= f_2(x_1) + f_3(x_3) - d_2 x_2 \\ \dot{x}_3 &= f_4(x_2) U_2(u) + f_5(x_3) - d_3 x_3, \\ y &= x_1, \end{aligned} \tag{6.1}$$

where the f functions are defined as

$$f_1(x_2) = \frac{V_1 x_2^3}{x_2^3 + S_1^3} + \frac{V_2 x_2}{S_2 x_2 + S_3}, \quad f_2(x_1) = \frac{V_3 x_1}{x_1 + S_4}, \quad f_3(x_3) = \frac{V_4 x_3}{x_3 + S_5} + \frac{V_5 x_3}{S_6 x_3 + S_7},$$
$$f_4(x_2) = \frac{V_6 x_2}{S_8 x_2 + S_9}, \quad f_5(x_3) = \frac{V_7 x_3}{x_3 + S_{10}} + \frac{V_8 x_3}{S_{11} x_3 + S_{12}},$$

and the input functions $U_1(u) = \dfrac{\beta_3 u}{d_1(K_3 + u)}$ and $U_2(u) = \dfrac{u}{K_{10} + u}$ were given in (3.3) and (4.1) before, respectively. These input functions consist of a single input u and constant parameters. Here, x_1, x_2 and x_3 represent $AP1$, LFY and $SOC1$ concentrations,

respectively. The constants are the same as in system (4.1). The network of the system is illustrated in Figure 6.1.

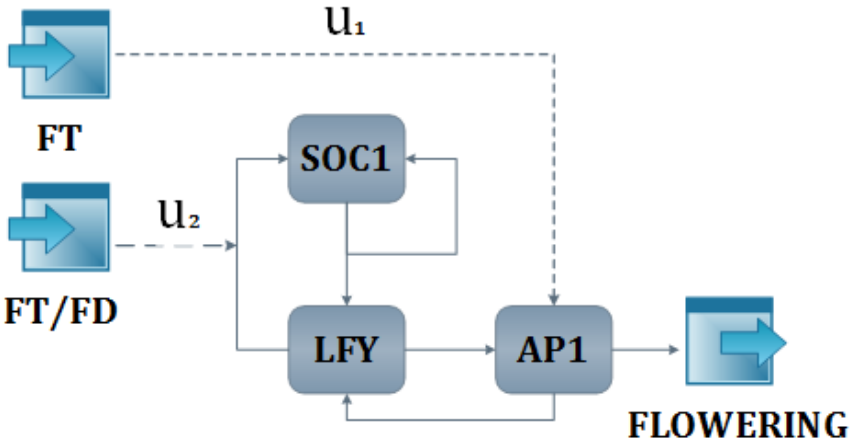

FIGURE 6.1: Gene regulatory network of the Arabidopsis flowering. FT is the input of system as (6.1), also through a combined action with FD, with an effect on $SOC1$ and $AP1$, as shown with dashed lines.

6.2 Observer design for the dynamic model of Arabidopsis flowering

System (6.1) is represented in the following form

$$h(x) = x_1, \quad f(x,u) = \left\{ \begin{array}{rcl} f^1(x_1,x_2,u) & = & f_1(x_2) + U_1(u) - d_1x_1 \\ f^2(x_1,x_2,x_3,u) & = & f_2(x_1) + f_3(x_3) - d_2x_2 \\ f^3(x,u) & = & f_4(x_2)U_2(u) + f_5(x_3) - d_3x_3 \end{array} \right\},$$

which can be formulated by setting $x = [x_1\ x_2\ x_3]^T$ and $y = x_1$ as

$$\begin{array}{rcl} \dot{x}(t) & = & f(x(t),u(t)) \\ y(t) & = & h(x(t)) = x_1. \end{array} \tag{6.2}$$

In the first part of this section, we aim to design constant and state-dependent high gain observers for the system (6.2). To achieve this, the f and h functions must be smooth

and continuously differentiable with respect to x, and they must satisfy a Lipschitz continuity condition which is given in the following assumption.

Assumptions 1. $f(x,u)$ is Lipschitz with respect to the state x, uniformly in the control u, that is, there exists a Lipschitz constant $\lambda_u > 0$ such that

$$\|f(x,u) - f(\hat{x},u)\| \leq \lambda_u \|x - \hat{x}\| \text{ for any } x, \hat{x} \in R^n, u \in R^m.$$

Unfortunately, for the system (6.2), the expression of the gain is very complicated. The complexity comes from the Hill functions which are non-linear and not globally Lipschitz continuous. To overcome this issue, we replace these functions with exponential ones by using Pade approximation up to some adjustment to satisfies the Lipschitz condition. Then, we compare the observer results of the systems with Hill and exponential functions to see the differences and similarities. The following remarks will be used to convert the systems from Hill functions to exponential ones in Pade form.

Remarks 2. Assume that a Hill function is of the form

$$f(x) = \left(\frac{Vx^n}{S_1 x^n + S_2}\right),$$

where V and S_i are positive constants and n is positive integer. This function can be written as

$$f(x) = \gamma_1 - \left(\frac{\gamma_1}{\gamma_2 x^n + 1}\right),$$

where $\gamma_1 = \dfrac{V}{S_1}$ and $\gamma_2 = \dfrac{S_1}{S_2}$.

Remarks 3. Assume that a Hill function is of the form

$$f(x) = \left(\frac{\gamma_1}{\gamma_2 x^n + 1}\right),$$

This kind of function can be approximated by using the following Pade approximants. For all $i, j > 0$ and positive integer n,

$$\left(\frac{\gamma_i}{\gamma_j x^n + 1}\right) \approx \gamma_i e^{-\gamma_j x^n}.$$

In practice, we want to design an observer that is as simple as possible for implementation purposes. Therefore, we reconstruct the equations system (6.1) by using the Remark (2) to write a simpler system as given below,

$$\begin{aligned}
\dot{x}_1 &= -d_1 x_1 - \left(\frac{\gamma_1}{\gamma_2 {x_2}^3 + 1}\right) - \left(\frac{\gamma_3}{\gamma_4 x_2 + 1}\right) + U_1 + \gamma_1 + \gamma_3, \\
\dot{x}_2 &= -d_2 x_2 - \left(\frac{\nu_1}{\nu_2 x_1 + 1}\right) - \left(\frac{\nu_3}{\nu_4 x_3 + 1}\right) - \left(\frac{\nu_5}{\nu_6 x_3 + 1}\right) + \nu_1 + \nu_3 + \nu_5, \\
\dot{x}_3 &= -d_3 x_3 - \left(\frac{\alpha_1 U_2}{\alpha_2 x_2 + 1}\right) - \left(\frac{\alpha_3}{\alpha_4 x_3 + 1}\right) - \left(\frac{\alpha_5}{\alpha_6 x_3 + 1}\right) + \alpha_1 U_2 + \alpha_3 + \alpha_5, \\
y &= x_1, \qquad (6.3)
\end{aligned}$$

where the parameters are

$$\begin{gathered}
\gamma_1 = V_1,\ \gamma_2 = \frac{1}{S_1^3},\ \gamma_3 = \frac{V_2}{S_2},\ \gamma_4 = \frac{S_2}{S_3}, \\
\nu_1 = V_3,\ \nu_2 = \frac{1}{S_4},\ \nu_3 = V_4,\ \nu_4 = \frac{1}{S_5},\ \nu_5 = \frac{V_5}{S_6},\ \nu_6 = \frac{S_6}{S_7}, \\
\alpha_1 = \frac{V_6}{S_8},\ \alpha_2 = \frac{S_8}{S_9},\ \alpha_3 = V_7,\ \alpha_4 = \frac{1}{S_{10}}, \alpha_5 = \frac{V_8}{S_{11}}, \alpha_6 = \frac{S_{11}}{S_{12}}.
\end{gathered}$$

System (6.3) with Hill functions has a unique stable steady state solution which is obtained as $(\bar{x}_1, \bar{x}_2, \bar{x}_3) = (120.7, 450.63, 827.83)$ for the parameter values in Table A.1 (see Appendix A). By using Remark (3), the Hill functions can be replaced with the Pade approximation and x_i with ω_i, {i=1,2,3},

$$\begin{aligned}
\dot{\omega}_1 &= -d_1\omega_1 - \gamma_1 e^{-\gamma_2\omega_2^3} - \gamma_3 e^{-\gamma_4\omega_2} + U_1 + \gamma_1 + \gamma_3, \\
\dot{\omega}_2 &= -d_2\omega_2 - \nu_1 e^{-\nu_2\omega_1} - \nu_3 e^{-\nu_4\omega_3} - \nu_5 e^{-\nu_6\omega_3} + \nu_1 + \nu_3 + \nu_5, \\
\dot{\omega}_3 &= -d_3\omega_3 - \alpha_1 U_2 e^{-\alpha_2\omega_2} - \alpha_3 e^{-\alpha_4\omega_3} - \alpha_5 e^{-\alpha_6\omega_3} + \alpha_1 U_2 + \alpha_3 + \alpha_5, \\
y &= \omega_1, \qquad (6.4)
\end{aligned}$$

where the new steady state is obtained as $(\bar{\omega_1}, \bar{\omega_2}, \bar{\omega_3}) = (120.7, 522.22, 943.064)$.

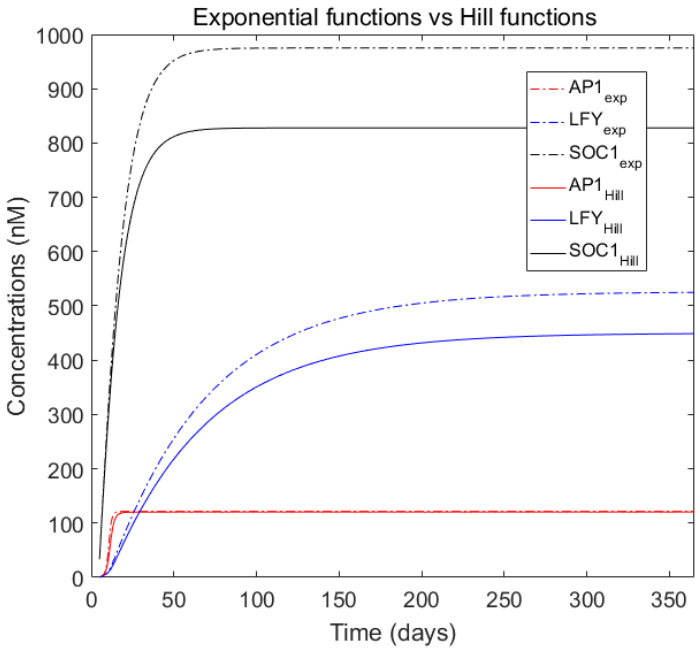

FIGURE 6.2: Comparison of the exponential (with dashed lines) and Hill functions.

By writing $\omega_1 = \rho_1 x_1$, $\omega_2 = \rho_2 x_2$ and $\omega_3 = \rho_3 x_3$, we obtain the following equations system:

$$\begin{aligned}
\dot{x}_1 &= -d_1 x_1 - \frac{\gamma_1}{\rho_1} e^{-\gamma_2 \rho_2^3 x_2^3} - \frac{\gamma_3}{\rho_1} e^{-\gamma_4 \rho_2 x_2} + \frac{U_1}{\rho_1} + \frac{\gamma_1}{\rho_1} + \frac{\gamma_3}{\rho_1}, \\
\dot{x}_2 &= -d_2 x_2 - \frac{\nu_1}{\rho_2} e^{-\nu_2 \rho_1 x_1} - \frac{\nu_3}{\rho_2} e^{-\nu_4 \rho_3 x_3} - \frac{\nu_5}{\rho_2} e^{-\nu_6 \rho_3 x_3} + \frac{\nu_1}{\rho_2} + \frac{\nu_3}{\rho_2} + \frac{\nu_5}{\rho_2}, \\
\dot{x}_3 &= -d_3 x_3 - \frac{\alpha_1 U_2}{\rho_3} e^{-\alpha_2 \rho_2 x_2} - \frac{\alpha_3}{\rho_3} e^{-\alpha_4 \rho_3 x_3} - \frac{\alpha_5}{\rho_3} e^{-\alpha_6 \rho_3 x_3} + \frac{\alpha_1 U_2}{\rho_3} + \frac{\alpha_3}{\rho_3} + \frac{\alpha_5}{\rho_3}, \\
y &= \rho_1 x_1,
\end{aligned} \tag{6.5}$$

where ρ_1, ρ_2, and ρ_3 are found such that, $\rho_1 = \dfrac{\bar{\omega}_1}{\bar{x}_1} = 1$, $\rho_2 = \dfrac{\bar{\omega}_2}{\bar{x}_2} = 1.15911$, $\rho_3 = \dfrac{\bar{\omega}_3}{\bar{x}_3} = 1.13919$.

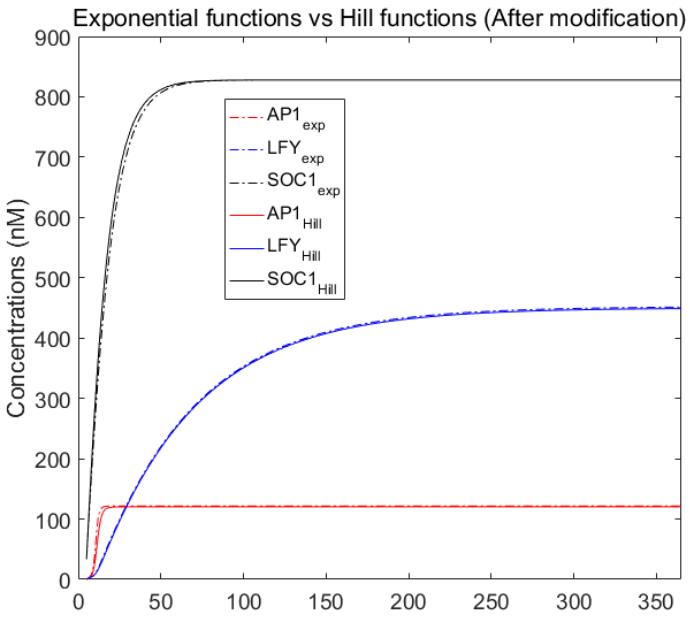

FIGURE 6.3: Comparison of the exponential (with dashed lines) and Hill functions after modification.

As a result, it is found that the exponential functions, which are obtained as Pade approximants, make the process faster than Hill functions. This also means that the error using exponential functions goes to zero faster than for Hill functions.

The system (6.5) can be represented in the form :

$$\begin{aligned} \dot{x}(t) &= g(x(t), u(t)) + \varphi(u(t)) + R, \\ y(t) &= h(x(t)) = \bar{C}x(t), \end{aligned} \tag{6.6}$$

where $\bar{C} = [\rho_1\ 0\ 0]$ is a vector matrix, and $f(x(t), u(t))$ in system (6.2) is represented as $f(x(t), u(t)) = g(x(t), u(t)) + \varphi(u(t)) + R$. Here, R is a constant vector of appropriate dimension, and $\varphi(u)$ is the input vector, represented as

$$R = \begin{bmatrix} (\gamma_1 + \gamma_3)/\rho_1 \\ (\nu_1 + \nu_3 + \nu_5)/\rho_2 \\ (\alpha_3 + \alpha_5)/\rho_3 \end{bmatrix}, \quad \varphi(u) = \begin{bmatrix} U_1/\rho_1 \\ 0 \\ \alpha_1 U_2/\rho_3 \end{bmatrix},$$

and $g(x, u)$ is defined as

$$g(x,u)=\begin{bmatrix} g^1(x_1,x_2)\\ g^2(x_1,x_2,x_3)\\ g^3(x_2,x_3,u)\end{bmatrix}=\begin{bmatrix} -d_1x_1-(\gamma_1e^{-\gamma_2\rho_2^3x_2^3}+\gamma_3e^{-\gamma_4\rho_2x_2})/\rho_1\\ -d_2x_2-(\nu_1e^{-\nu_2\rho_1x_1}+\nu_3e^{-\nu_4\rho_3x_3}+\nu_5e^{-\nu_6\rho_3x_3})/\rho_2\\ -d_3x_3-(\alpha_1U_2e^{-\alpha_2\rho_2x_2}+\alpha_3e^{-\alpha_4\rho_3x_3}+\alpha_5e^{-\alpha_6\rho_3x_3})/\rho_3\end{bmatrix}.$$

As mentioned before, to design a high gain observer, it is necessary that the functions, f (now we consider g) and h, must be smooth and continuously differentiable with respect to x, and they must be Lipschitz continuous which means they are globally Lipschitz with respect to x uniformly in u. Moreover, their partial and respective time derivatives must be bounded and the following assumption and notation, taken from the papers [Busawon et al., 1998a, Busawon and De Leon-Morales, 1999], must be considered:

Assumptions 2. There exists positive constants a, b, $\{0<a\leq b<\infty\}$ such that for all $z\in R^n$ and $u\in R$:

$$0<a\leq\left|\frac{\partial g^i(x,u)}{\partial x_{i+1}}\right|_{x=z},\ \left|\frac{\partial h(x)}{\partial x_i}\right|_{x=z}\leq b<\infty,\quad i=1,\ldots,n-1.$$

Notations 1. Let denote the Jacobian matrices of g and h calculated at the point $z\in R^n$ with respect to x as $\dfrac{\partial g}{\partial x}(z,u)$ and $\dfrac{\partial h}{\partial x}(z)$, respectively. By using them, the observability (Jacobian) matrix $\Omega(z,u)$ can be represented as follows

$$\Omega(z,u)=\left(\frac{d\Theta(x,u)}{dx}\bigg|_{x=z}\right)=\begin{pmatrix}\nabla h(x,u)\\ \nabla L_gh(x,u)\\ \vdots\\ \nabla L_g^{n-1}h(x,u)\\ \vdots\end{pmatrix}\bigg|_{x=z}.$$

By defining $G(z,u)$ and $H(z)$ as $G_{ij}(z,u)=\dfrac{\partial g^i}{\partial x_j}(z,u)$ and $H_i(z)=\dfrac{\partial h}{\partial x_i}(z)$, $i,j=1,\ldots,n$, the observability matrix can be written as

$$\Omega(z,u)=\begin{pmatrix}H(z,u)\\ H(z,u)G(z,u)\\ \vdots\\ H(z,u)G^{n-1}(z,u)\\ \vdots\end{pmatrix}.$$

Note that the function $g(x,u)$, which is consisted with Pade approximants, is globally Lipschitz (see Appendix B).

Before starting the observer design, it is necessary to show that this non-linear system satisfies the observability condition, which means the Jacobian matrix must be of full rank. By considering the Notation (1), the following matrices can be obtained,

$$H(z) = \bar{C} = \rho_1 \begin{bmatrix} 1 & 0 & 0 \end{bmatrix}, \quad G(z,u) = \begin{bmatrix} G_{11} & G_{12} & 0 \\ G_{21} & G_{22} & G_{23} \\ 0 & G_{32} & G_{33} \end{bmatrix},$$

where the defined G functions are calculated as

$$G_{11} = -d_1, \quad G_{12} = (3\gamma_1\gamma_2\rho_2^3 z_2^2 e^{-(\gamma_2\rho_2^3 z_2^3)} + \gamma_3\gamma_4\rho_2 e^{-(\gamma_4\rho_2 z_2)})/\rho_1,$$
$$G_{21} = (\nu_1\nu_2\rho_1 e^{-(\nu_2\rho_1 z_1)})/\rho_2, \quad G_{22} = -d_2, \quad G_{23} = (\nu_3\nu_4\rho_3 e^{-(\nu_4\rho_3 z_3)} + \nu_5\nu_6\rho_3 e^{-(\nu_6\rho_3 z_3)})/\rho_2,$$
$$G_{32} = (\alpha_1\alpha_2 U_2\rho_2 e^{-(\alpha_2\rho_2 z_2)})/\rho_3, \quad G_{33} = -d_3 + (\alpha_3\alpha_4\rho_3 e^{-(\alpha_4\rho_3 z_3)} + \alpha_5\alpha_6\rho_3 e^{-(\alpha_6\rho_3 z_3)})/\rho_3.$$

The observability (Jacobian) matrix can be written as

$$\Omega(z,u) = \begin{pmatrix} H(z) \\ H(z)G(z,u) \\ H(z)G^2(z,u) \end{pmatrix} = \rho_1 \begin{pmatrix} 1 & 0 & 0 \\ G_{11} & G_{12} & 0 \\ G_{11}^2 + G_{12}G_{21} & (G_{11} + G_{22})G_{12} & G_{12}G_{23} \end{pmatrix},$$

where $\Omega(z,u)$ is a lower triangular matrix and nonsingular for all $z \in \mathbb{R}^3$ and $u \in \mathbb{R}$ which means it is full rank and invertible matrix. Therefore, the system (6.5) is said to be uniformly observable with a single output.

A high gain observer of the system (6.6) can be written as

$$\begin{aligned} \dot{\hat{x}}(t) &= g(\hat{x}(t), u(t)) + \varphi(u(t)) + R + K_\theta(y(t) - \hat{y}(t)) \\ \hat{y}(t) &= h(\hat{x}(t)) = \bar{C}\hat{x}(t) = \rho_1\hat{x}_1(t). \end{aligned} \tag{6.7}$$

In the observer system (6.7), $\hat{x}$ denotes the estimate of state x, and the gain matrix K_θ can be chosen in many different ways. In this study, we apply and compare two different high gain matrices, namely constant and state-dependent.

The first one is, $K_\theta = S^{-1}(\theta)\bar{C}^T$, which can also be defined in the form $K_\theta = \Delta_\theta^{-1}K$, where the Δ_θ is block-diagonal as $\Delta_\theta = diag\left[\frac{1}{\theta}, \frac{1}{\theta^2}, \frac{1}{\theta^3}\right]$ and K is chosen a column vector as $K = col(C_3^1, C_3^2, C_3^3)$, as defined in Subsection 2.5.1. A symmetric positive definite matrix S_θ, which is the solution of the algebraic equation,

$$-\theta S_\theta - A^T S_\theta - S_\theta A + C^T C = 0,$$

for θ large enough, $\theta \geq 1$, is of the same format as given in Subsection 2.5.1.

Note that the vector K does not have to be of the form defined above. However, the selected vector K should ensure the stability of the matrix $(\mathcal{A} - K\bar{C})$, where $\bar{C}$ and $\mathcal{A}$ matrices are

$$\bar{C} = \rho_1 \begin{bmatrix} 1 & 0 & 0 \end{bmatrix} \quad \text{and} \quad \mathcal{A} = \begin{bmatrix} 0 & \frac{\partial g^1}{\partial x_2} & 0 \\ 0 & 0 & \frac{\partial g^2}{\partial x_3} \\ 0 & 0 & 0 \end{bmatrix} = \begin{bmatrix} 0 & G_{12} & 0 \\ 0 & 0 & G_{23} \\ 0 & 0 & 0 \end{bmatrix}.$$

By choosing the column vector K as $K = col(C_3^1, C_3^2, C_3^3)$ and $\theta = 3$, we obtain the simulations as shown in Figure 6.4 and 6.5.

Figure 6.4 shows that high gain observer system (6.7) with a constant gain can capture behaviour of both systems (6.1) and (6.5), which means that systems with Hill and exponential functions behave similarly. The concentrations $AP1$ and LFY and their observers are compared in Figure 6.5, where the convergence time of the observers can be seen in detail.

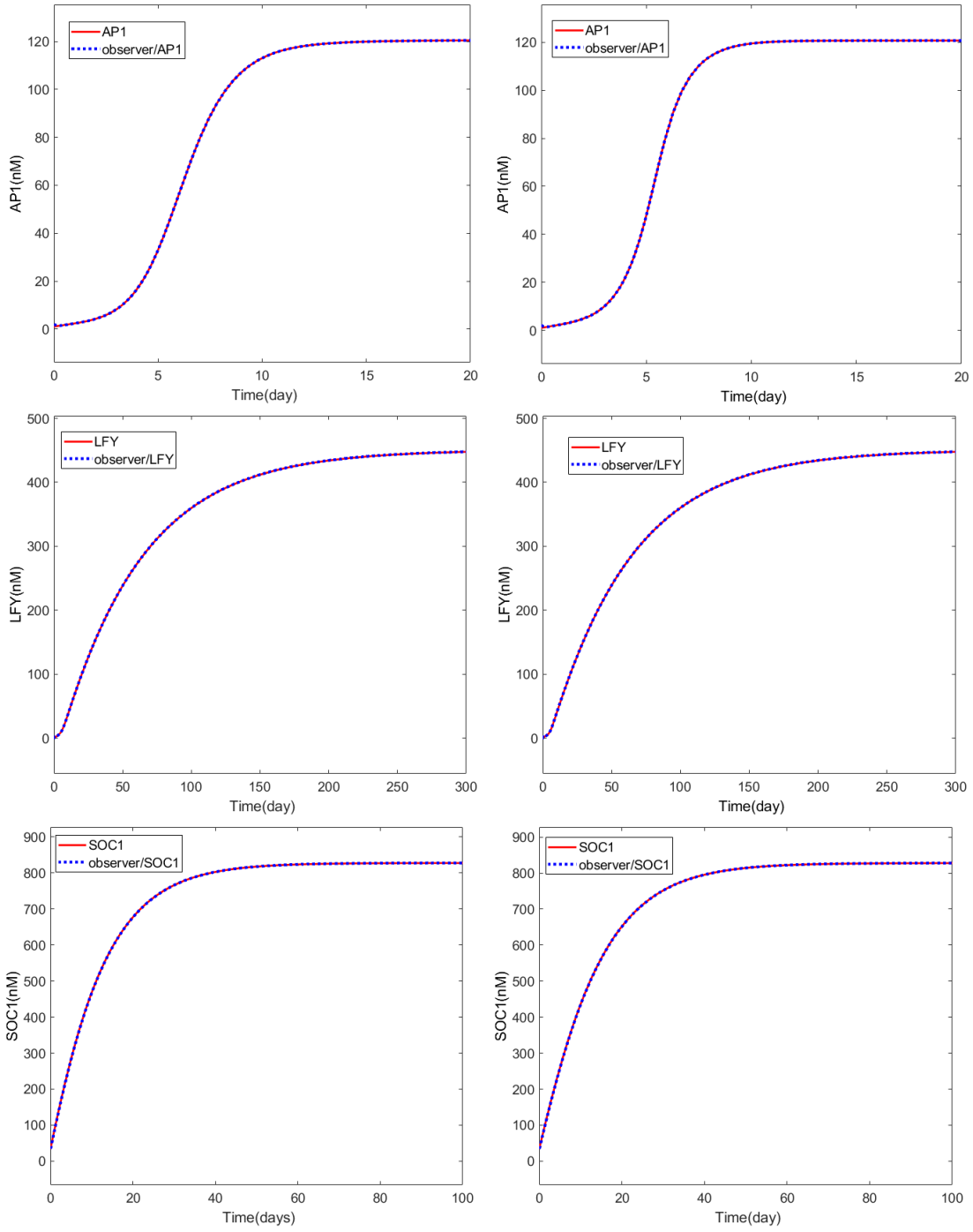

FIGURE 6.4: Observer design of $AP1$, LFY and $SOC1$ in system (6.1) on the left and (6.5) on the right.

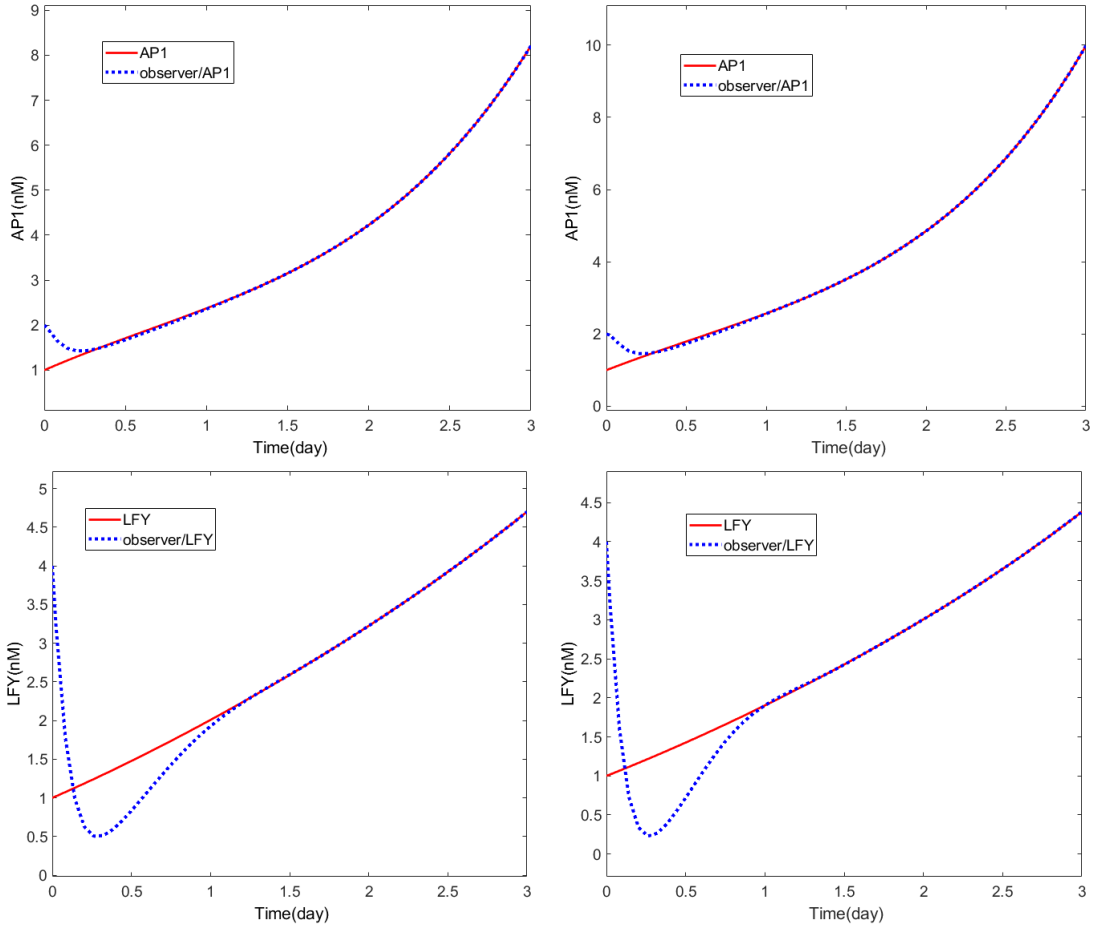

FIGURE 6.5: Observer design of $AP1$ and LFY in system (6.1) on the left and (6.5) on the right.

Indeed, the observer error $\varepsilon(t) = x(t) - \hat{x}(t)$ is calculated as

$$\begin{aligned}\dot{\varepsilon} = \dot{x} - \dot{\hat{x}} =& g(x,u) - g(\hat{x},u) - K_\theta(y - \hat{y}) \\ =& g(x,\hat{x},u) - \Delta_\theta^{-1} K\bar{C}\varepsilon,\end{aligned} \tag{6.8}$$

where $g(x,\hat{x},u) = g(x,u) - g(\hat{x},u)$, $(y - \hat{y}) = (h(x) - h(\hat{x})) = \bar{C}(x - \hat{x})$ and the observer error converges exponentially and asymptotically towards zero.

Now, we show that system (6.7) is an exponential observer for the system (6.6)

Theorem 6.1. *Assume that system (6.6) is bounded and satisfies the Lipschitz condition. Then, system (6.7) is an exponential observer for the system (6.6) for θ large enough.*

Proof. By setting, $\varepsilon = (x - \hat{x})$ and considering the assumption (2), we have

$$\begin{aligned} g^i(x, \hat{x}, u) &= g^i(x_{i+1}, z_i, u) - g^i(\hat{x}_{i+1}, \hat{z}_i, u) \\ &= g^i(x_{i+1}, z_i, u) - g^i(\hat{x}_{i+1}, z_i, u) + g^i(\hat{x}_{i+1}, z_i, u) - g^i(\hat{x}_{i+1}, \hat{z}_i, u) \\ &= \frac{\partial g^i}{\partial x_{i+1}}(\delta_i, z^i, u)(x_{i+1} - \hat{x}_{i+1}) + g^i(\hat{x}_{i+1}, z_i, u) - g^i(\hat{x}_{i+1}, \hat{z}_i, u) \\ &= \mathcal{A}\varepsilon + \bar{G}, \quad i = \{1, 2\}, \end{aligned} \tag{6.9}$$

where g is continuous on $[\hat{x}, x]$ and differentiable on $Co(\hat{x}, x)$ defines the convex hull of the set $\{\hat{x}, x\}$ as

$$z \in Co(\hat{x}, x) = \{\hat{x} + \delta\varepsilon, \delta \in [0, 1]\},$$

which means $\lim_{\hat{x} \to x} \delta = 0$. Here, $\mathcal{A}$ and $\bar{G}$ are the form

$$\mathcal{A} = \begin{bmatrix} 0 & \frac{\partial g^1}{\partial x_2} & 0 \\ 0 & 0 & \frac{\partial g^2}{\partial x_3} \\ 0 & 0 & 0 \end{bmatrix} \quad \text{and} \quad \bar{G} = \begin{bmatrix} h(\hat{x}_1, z_0, u) - h(\hat{x}_1, \hat{z}_0, u) \\ g^1(\hat{x}_2, z_1, u) - g^1(\hat{x}_2, \hat{z}_1, u) \\ g^2(\hat{x}_3, z_2, u) - g^2(\hat{x}_3, \hat{z}_2, u) \end{bmatrix}.$$

By substituting this result into equation (6.8), we find

$$\begin{aligned} \dot{\varepsilon} =& \mathcal{A}\varepsilon + \bar{G} - \Delta_\theta^{-1} K \bar{C} \varepsilon \\ =& (\mathcal{A} - \Delta_\theta^{-1} K \bar{C})\varepsilon + \bar{G}. \end{aligned} \tag{6.10}$$

Transforming the error term as $\bar{\varepsilon} = \Delta_\theta \varepsilon$, which yields

$$\dot{\bar{\varepsilon}} = \Delta_\theta \dot{\varepsilon} = \Delta_\theta (\mathcal{A} - \Delta_\theta^{-1} K \bar{C}) \Delta_\theta^{-1} \bar{\varepsilon} + \Delta_\theta \bar{G}, \tag{6.11}$$

where, $\varepsilon = \Delta_\theta^{-1} \bar{\varepsilon}$. Since, $\Delta_\theta \mathcal{A} \Delta_\theta^{-1} = \theta \mathcal{A}$ and $\bar{C} \Delta_\theta^{-1} = \theta \bar{C}$, we find

$$\dot{\bar{\varepsilon}} = \theta(\mathcal{A} - K\bar{C})\varepsilon + \Delta_\theta \bar{G}. \tag{6.12}$$

Since K is selected for $(\mathcal{A} - K\bar{C})$ to be Hurwitz, there exists a SPD matrix P such that

$$(\mathcal{A} - K\bar{C})^T P + P(\mathcal{A} - K\bar{C}) = -I.$$

If we consider a Lyapunov function $V(\bar{\varepsilon}) = \bar{\varepsilon}^T P\dot{\bar{\varepsilon}}$, we find

$$\begin{aligned} \dot{V(\bar{\varepsilon})} =& \dot{\bar{\varepsilon}}^T P\bar{\varepsilon} + \bar{\varepsilon}^T P\dot{\bar{\varepsilon}} = 2\bar{\varepsilon}^T P\dot{\bar{\varepsilon}} \\ =& -\theta\|\bar{\varepsilon}\|^2 + 2\bar{\varepsilon}^T P(\Delta_\theta \bar{G}). \end{aligned} \tag{6.13}$$

From the assumption (2), it is known that the matrix $\bar{G}$ is bounded . Hence for θ large enough, there exist a positive constant c_0, independent of θ such that

$$\|\Delta_\theta \bar{G}\| \leq c_0\bar{\varepsilon},$$

which gives,

$$\begin{aligned} \dot{V(\bar{\varepsilon})} \leq& -\theta\|\bar{\varepsilon}\|^2 + 2c_0\lambda_{max}(P)\|\bar{\varepsilon}\|^2 \\ =& (2c_0\lambda_{max}(P) - \theta)\|\bar{\varepsilon}\|^2, \end{aligned} \tag{6.14}$$

where $\lambda_{max}(P)$ is assumed to be the largest eigenvalue of P. By choosing $2c_0\lambda_{max}(P) < \theta$, we find $\dot{V(\bar{\varepsilon})} < 0$, which verifies the assertion that system (6.7) is an exponential observer for system (6.6), with $K_\theta = \Delta_\theta^{-1}K$. □

The following simulations are obtained by considering the observer errors (6.8) of system (6.5) and comparison with the errors of system (6.1) for the concentrations $AP1$, LFY and $SOC1$.

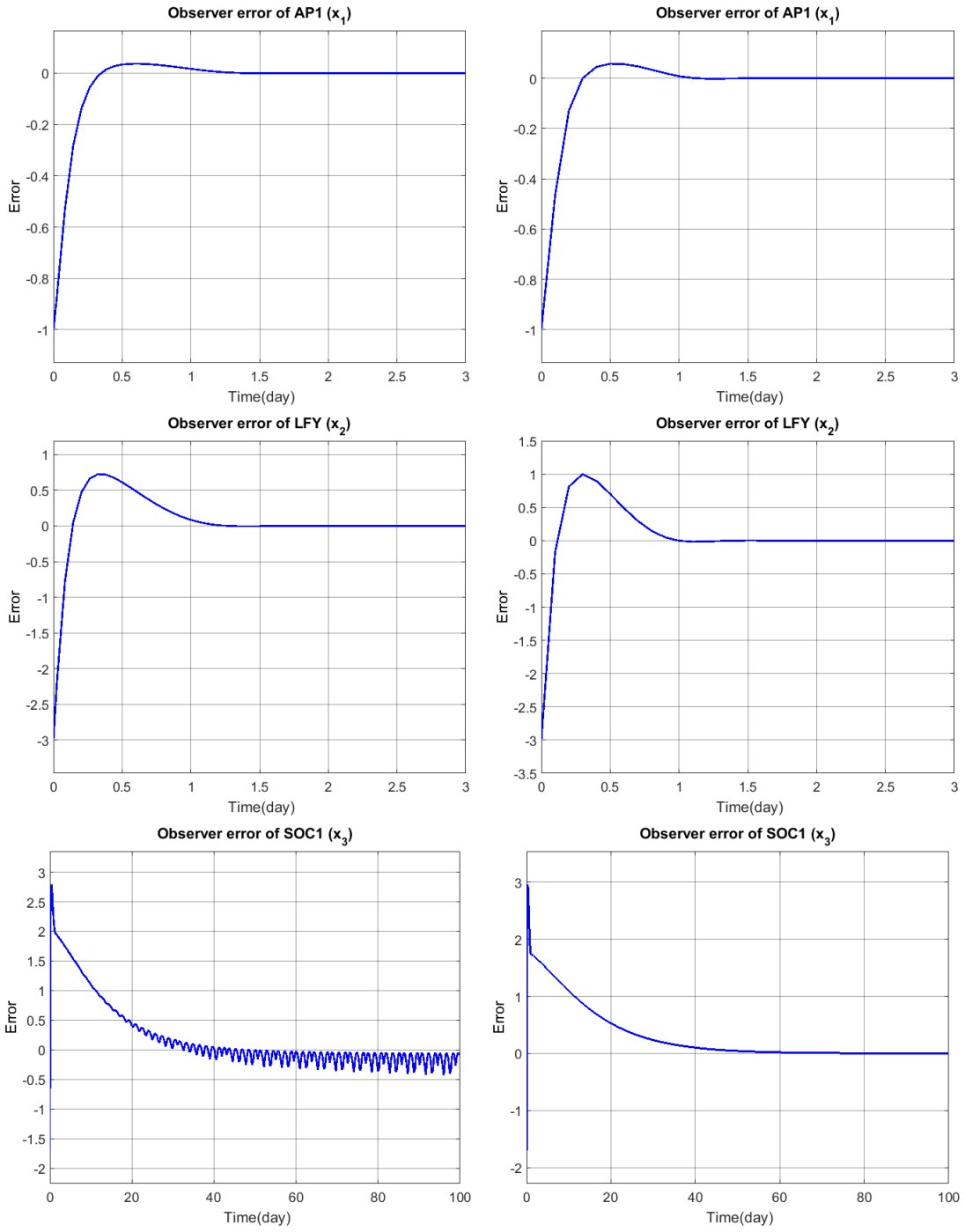

FIGURE 6.6: Observer error of $AP1$, LFY and $SOC1$ in system (6.1) on the left and (6.5) on the right. The magnitute of errors are in nM.

As can be seen in Figure 6.6, errors between systems and their observers converge to zero around 1.5 days for both Hill and exponential functions of the variable $AP1$ and LFY, but the convergence takes around 60 days for the variable $SOC1$. This results,

obtained with a constant high gain observer, will be compared with the state-dependent high gain observer.

The second type of gain matrix K_θ, which gives a state-dependent high gain observer, can be chosen as

$$K_\theta = \Omega^{-1}(\hat{x}, u)\Delta_\theta^{-1}K,$$

where the $\Omega^{-1}(\hat{x}, u)$ is the inverse of the observability matrix. This gives a new observer error of the system (6.6) as

$$\begin{aligned}\dot{\varepsilon} =& g(x, u) - g(\hat{x}, u) - K_\theta(y - \hat{y}) \\ =& g(x, \hat{x}, u) - \Omega^{-1}(\hat{x}, u)\Delta_\theta^{-1}KH\varepsilon \\ =& (G(\hat{x}, u) + r - \Omega^{-1}(\hat{x}, u)\Delta_\theta^{-1}KH)\varepsilon, \end{aligned} \tag{6.15}$$

where this observer error must also converges exponentially and asymptotically towards zero. Here, $G(\hat{x}, u)$ and r are obtained as

$$\begin{aligned} g(x, u) - g(\hat{x}, u) =& g(x, \hat{x}, u) \\ =& G(z, u)\varepsilon - G(\hat{x}, u)\varepsilon + G(\hat{x}, u)\varepsilon \\ =& r\varepsilon + G(\hat{x}, u)\varepsilon, \end{aligned}$$

where $G(z, u)$ comes from the differential mean value theorem,

$$g(x, \hat{x}, u) = g'(z, u)\varepsilon = G(z, u)\varepsilon.$$

Note that g is continuous on $[\hat{x}, x]$ and differentiable on $Co(\hat{x}, x)$ defines the convex hull of the set $\{\hat{x}, x\}$

$$z \in Co(\hat{x}, x) = \{\hat{x} + r\varepsilon, r \in [0, 1]\},$$

which means $\lim_{\hat{x}\to x} r = 0$ for $r = G(z, u) - G(\hat{x}, u)$.

Let us show that the system (6.7) is an exponential observer for the system (6.6) while $K_\theta = \Omega^{-1}(\hat{x}, u)\Delta_\theta^{-1}K$. Transforming the error term as $\bar{\varepsilon} = \Delta_\theta \Omega \varepsilon$, the new error can be written as

$$\begin{aligned}
\dot{\bar{\varepsilon}} &= \Delta_\theta \dot{\Omega}(\hat{x}, u)\varepsilon + \Delta_\theta \Omega(\hat{x}, u)\dot{\varepsilon} \\
&= \Delta_\theta \dot{\Omega}(\hat{x}, u)\Omega^{-1}(\hat{x}, u)\Delta_\theta^{-1}\bar{\varepsilon} + \Delta_\theta \Omega(\hat{x}, u)G(\hat{x}, u)\Omega^{-1}(\hat{x}, u)\Delta_\theta^{-1}\bar{\varepsilon} \\
&\quad + \Delta_\theta \Omega(\hat{x}, u)r\Omega^{-1}(\hat{x}, u)\Delta_\theta^{-1}\bar{\varepsilon} - KH\Omega^{-1}(\hat{x}, u)\Delta_\theta^{-1}\bar{\varepsilon} \\
&= \Delta_\theta \dot{\Omega}(\hat{x}, u)\Omega^{-1}(\hat{x}, u)\Delta_\theta^{-1}\bar{\varepsilon} + \Delta_\theta \mathcal{A}\Delta_\theta^{-1}\bar{\varepsilon} + \Delta_\theta B(\hat{x}, u)\Delta_\theta^{-1}\bar{\varepsilon} \\
&\quad + \Delta_\theta \Omega(\hat{x}, u)r\Omega^{-1}(\hat{x}, u)\Delta_\theta^{-1}\bar{\varepsilon} - K\bar{C}\Delta_\theta^{-1}\bar{\varepsilon},
\end{aligned}$$

where $\Omega(\hat{x}, u)G(\hat{x}, u)\Omega^{-1}(\hat{x}, u) = \mathcal{A} + B(\hat{x}, u)$ and $H\Omega^{-1}(\hat{x}, u) = \bar{C}$.

Since, $\Delta_\theta \mathcal{A}\Delta_\theta^{-1} = \theta\mathcal{A}$ and $\bar{C}\Delta_\theta^{-1} = \theta\bar{C}$, we find

$$\begin{aligned}
\dot{\bar{\varepsilon}} &= \theta(\mathcal{A} - K\bar{C})\bar{\varepsilon} + \Delta_\theta \dot{\Omega}(\hat{x}, u)\Omega^{-1}(\hat{x}, u)\Delta_\theta^{-1}\bar{\varepsilon} + \Delta_\theta B(\hat{x}, u)\Delta_\theta^{-1}\bar{\varepsilon} \\
&\quad + \Delta_\theta \Omega(\hat{x}, u)r\Omega^{-1}(\hat{x}, u)\Delta_\theta^{-1}\bar{\varepsilon}.
\end{aligned}$$

Remember that $(\mathcal{A} - K\bar{C})$ is Hurwitz and therefore, there exists a SPD matrix P such that

$$(\mathcal{A} - K\bar{C})^T P + P(\mathcal{A} - K\bar{C}) = -I.$$

Now, if we consider a Lyapunov function $V(\bar{\varepsilon}) = \bar{\varepsilon}^T P\dot{\bar{\varepsilon}}$, we find

$$\begin{aligned}
\dot{V(\bar{\varepsilon})} =& \dot{\bar{\varepsilon}}^T P\bar{\varepsilon} + \bar{\varepsilon}^T P\dot{\bar{\varepsilon}} = 2\bar{\varepsilon}^T P\dot{\bar{\varepsilon}} \\
=& -\theta\|\bar{\varepsilon}\|^2 \\
&+ 2\bar{\varepsilon}^T P\left(\Delta_\theta \dot{\Omega}(\hat{x}, u)\Omega^{-1}(\hat{x}, u)\Delta_\theta^{-1} + \Delta_\theta B(\hat{x}, u)\Delta_\theta^{-1} + \Delta_\theta \Omega(\hat{x}, u)r\Omega^{-1}(\hat{x}, u)\Delta_\theta^{-1}\right)\bar{\varepsilon} \\
\leq& -\theta\|\bar{\varepsilon}\|^2 \\
&+ 2\|P\bar{\varepsilon}\|\left(\|\Delta_\theta \dot{\Omega}(\hat{x}, u)\Omega^{-1}(\hat{x}, u)\Delta_\theta^{-1}\| + \|\Delta_\theta B(\hat{x}, u)\Delta_\theta^{-1}\| + \|\Delta_\theta \Omega(\hat{x}, u)r\Omega^{-1}(\hat{x}, u)\Delta_\theta^{-1}\|\right)\|\bar{\varepsilon}\|.
\end{aligned} \tag{6.16}$$

The matrices $\dot{\Omega}(\hat{x},u)\Omega^{-1}(\hat{x},u)$ and $\Omega(\hat{x},u)r\Omega^{-1}(\hat{x},u)$ are lower triangular. Therefore, $\dot{\Omega}(\hat{x},u)\Omega^{-1}(\hat{x},u) + \Omega(\hat{x},u)r\Omega^{-1}(\hat{x},u)$ is also lower triangular. Moreover, $B(\hat{x},u)$ and $\dot{\Omega}(\hat{x},u)$ are bounded. Hence, by assuming $\theta \geq 1$, there exist a positive constant c_1, independent of θ such that

$$\|\Delta_\theta \dot{\Omega}(\hat{x},u)\Omega^{-1}(\hat{x},u)\Delta_\theta^{-1}\| + \|\Delta_\theta B(\hat{x},u)\Delta_\theta^{-1}\| + \|\Delta_\theta \Omega(\hat{x},u)r\Omega^{-1}(\hat{x},u)\Delta_\theta^{-1}\| \leq c_1.$$

This gives,

$$\begin{aligned} \dot{V(\bar{\varepsilon})} &\leq -\theta\|\bar{\varepsilon}\|^2 + 2c_1\|P\bar{\varepsilon}\|\|\bar{\varepsilon}\| \\ &\leq -\theta\|\bar{\varepsilon}\|^2 + 2c_1\lambda_{max}(P)\|\bar{\varepsilon}\|^2, \end{aligned} \tag{6.17}$$

where $\lambda_{max}(P)$ is assumed to be the largest value of P. While $K_\theta = \Omega^{-1}(\hat{x},u)\Delta_\theta^{-1}K$, the system (6.7) is an exponential observer for system (6.6) if and only if the inequality above is less than zero, which can be obtained by assuming $2c_1\lambda_{max}(P) < \theta$.

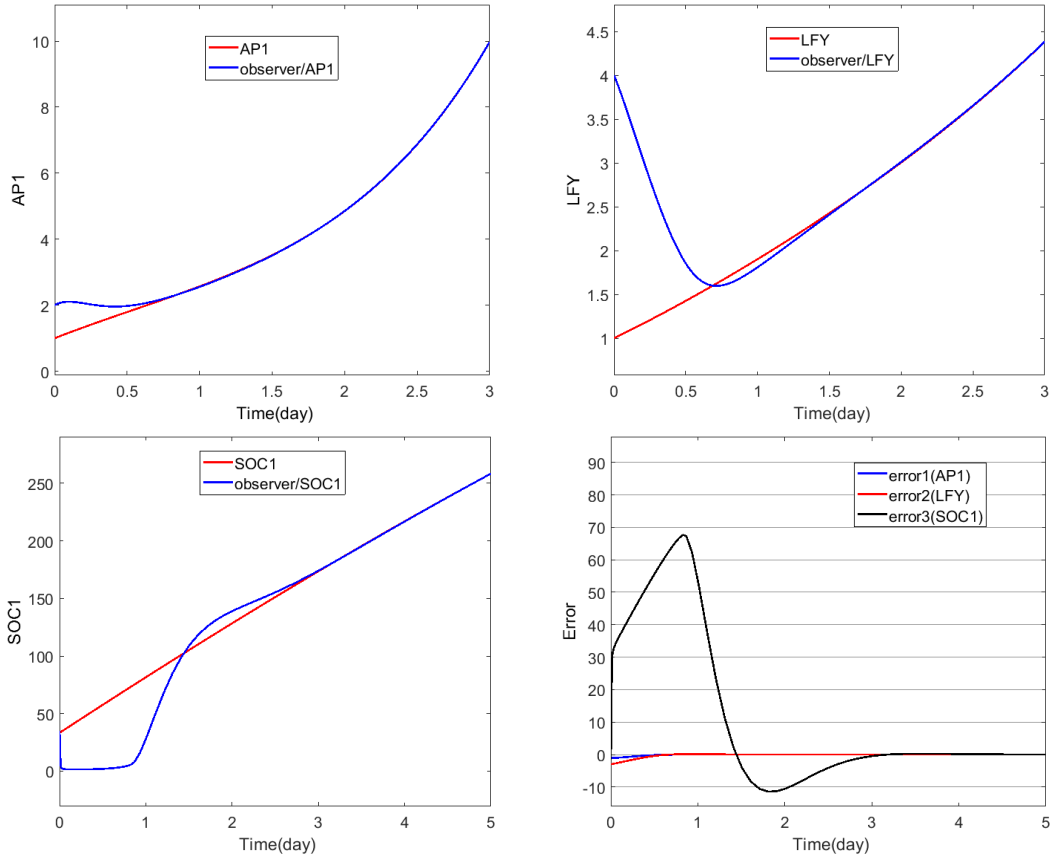

FIGURE 6.7: Observer design of $AP1$, LFY and $SOC1$ in system (6.5) and error results while gain matrix is defined as $K_\theta = \Omega^{-1}(\hat{x},u)\Delta_\theta^{-1}K$ with $\theta = 3$. The magnitute of all concentrations and errors are in nM.

Simulations in Figure 6.7, obtained by using Matlab Simulink, shows that the state-dependent high gain observer design can capture the desired behaviour faster than the previous observer design (constant high gain observer), especially for $SOC1$ variable which is almost 20 times faster.

6.3 Control design of the Arabidopsis flowering GRN

The behaviour of biological systems can be controlled by changing *inputs*, which are the certain physical quantities of systems and measuring the *outputs*, which are the physical variables of systems and represent the behaviour of systems. It is necessary that an input has direct effect on an output. In other words, an output of a system must be described with a function of the state where the input must be incorporated in this function [Kalman, 1959]. In our dynamical model $AP1$ is the output of the system which is controlled by input FT.

The behaviour of flowering process can be represented with differential equations models as given in system (3.1), (4.1) and (4.2), and exact time period of the flowering can be controlled with a state feedback control design. As mentioned before, the flowering process of Arabidopsis thaliana starts with initial (sub-threshold) value of $AP1$ and ends while $AP1$ reaches its non-trivial stable steady state value.

The main aim of this section is to obtain a desired $AP1$ values depending on time by regulating it to a reference value $AP1_{ref}$ while the other variables are bounded. To obtain a desired solution for $AP1$, it is needed to design the controller FT, which is the input factor of the system, such that the output goes to its steady state value while time goes to infinity, that is,

$$y = x_1(t) \to \tilde{x}_1 \text{ when } \lim_{t\to\infty} |x_1(t) - \tilde{x}_1| = 0 \text{ while } x_2 \text{ and } x_3 \text{ are bounded.}$$

It is clear that $\tilde{x}_1$, which refers to the reference point, $AP1_{ref}$, in the network, also represents the steady state value of x_1, characterized as $\bar{x}_1$ before. In accordance with this

purpose, state feedback controllers are designed for the simplified models of Arabidopsis Flowering GRN, given in system (6.5), which was constructed by transforming Hill functions in system (4.1) into exponential ones as

$$\begin{aligned}
\dot{x}_1 = \quad g^1(x_1, x_2, u) \quad &= -d_1 x_1 - g_1(x_2) + \varphi_1(u) + R_1, \\
\dot{x}_2 = \quad g^2(x_1, x_2, x_3, u) \quad &= -d_2 x_2 - g_2(x_1) - g_3(x_3) + R_2, \\
\dot{x}_3 = \quad g^3(x, u) \quad &= -d_3 x_3 - g_4(x_2) U_2(u) - g_5(x_3) + \varphi_2(u) + R_3,
\end{aligned} \tag{6.18}$$

where the input, constant and exponential g functions are defined as

$$\varphi_1(u) = \frac{U_1(u)}{\rho_1} = \frac{\beta_3 u}{\rho_1 d_1 (K_3 + u)}, \ \varphi_2(u) = \frac{\alpha_1 U_2(u)}{\rho_3},$$
$$R_1 = (\gamma_1 + \gamma_3)/\rho_1, \ R_2 = (\nu_1 + \nu_3 + \nu_5)/\rho_2, \ R_3 = (\alpha_3 + \alpha_5)/\rho_3,$$
$$g_1(x_2) = (\gamma_1 e^{-\gamma_2 \rho_2^3 x_2^3} + \gamma_3 e^{-\gamma_4 \rho_2 x_2})/\rho_1, \ g_2(x_1) = (\nu_1 e^{-\nu_2 \rho_1 x_1})/\rho_2,$$
$$g_3(x_3) = (\nu_3 e^{-\nu_4 \rho_3 x_3} + \nu_5 e^{-\nu_6 \rho_3 x_3})/\rho_2, \ g_4(x_2) = (\alpha_1 e^{-\alpha_2 \rho_2 x_2})/\rho_3,$$
$$g_5(x_3) = (\alpha_3 e^{-\alpha_4 \rho_3 x_3} + \alpha_5 e^{-\alpha_6 \rho_3 x_3})/\rho_3.$$

Here, U_1, U_2 input functions and the other constant variables are the same as in previous sections.

If we consider the first equation of system (6.5) at the steady state, the input function that can be written depends on $AP1_{ref}(\tilde{x}_1)$ as

$$\dot{\tilde{x}}_1 \quad = \quad -d_1 \tilde{x}_1 - g_1(x_2) + \varphi_1(u) + R_1 = 0, \tag{6.19}$$

and it can be represented as a function of x_2 by the following calculation results.

$$\varphi_1(u) = \frac{U_1(u)}{\rho_1} = \frac{\beta_3 u}{\rho_1 d_1 (K_3 + u)} = g_1(x_2) + d_1 \tilde{x}_1 - R_1.$$

which gives,

$$\tilde{u}(x_2) = \frac{d_1 \rho_1 K_3 [g_1(x_2) + d_1 \tilde{x}_1 - R_1]}{\beta_3 - d_1 \rho_1 [g_1(x_2) + d_1 \tilde{x}_1 - R_1]}.$$

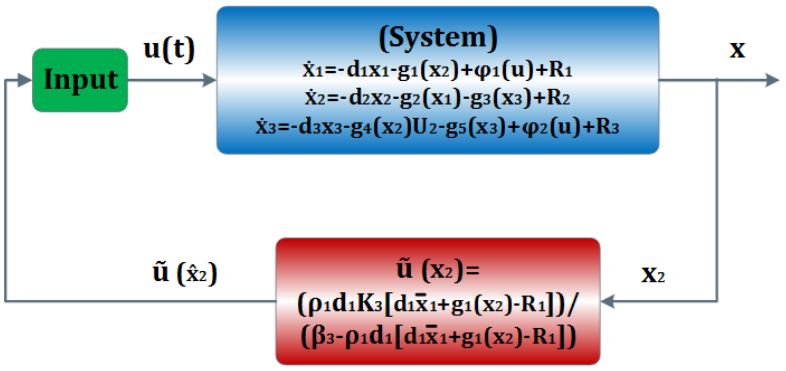

FIGURE 6.8: State feedback control design for system (6.5) where x, u, $\bar{x}$ and $\tilde{u}$ represent the state, input, reference value of output and controlled input variables, respectively.

It is necessary to be ensure that $\varphi_1(u)$ should be less than $d_1\tilde{x}_1$ due to x_2 and x_3 remaining bounded, otherwise the controller will move to infinity.

By replacing $\tilde{u}$ into system (6.18), we find

$$\begin{aligned} \dot{x}_1 &= -d_1 x_1 - g_1(x_2) + \varphi_1(\tilde{u}(x_2)) + R_1, \\ \dot{x}_2 &= -d_2 x_2 - g_2(x_1) - g_3(x_3) + R_2, \\ \dot{x}_3 &= -d_3 x_3 - g_4(x_2) U_2(\tilde{u}(x_2)) - g_5(x_3) + \varphi_2(\tilde{u}(x_2)) + R_3, \end{aligned} \tag{6.20}$$

where

$$\varphi_1(\tilde{u}(x_2)) = \frac{U_1(\tilde{u}(x_2))}{\rho_1}, \text{ and } \varphi_2(\tilde{u}(x_2)) = \frac{\alpha_1 U_2(\tilde{u}(x_2))}{\rho_3},$$

with

$$U_1(\tilde{u}(x_2)) = \frac{\beta_3 \tilde{u}(x_2)}{d_1(K_3 + \tilde{u}(x_2))} \text{ and } U_2(\tilde{u}(x_2)) = \frac{\alpha_1}{\rho_3} \frac{d_1 K_3 U_1(\tilde{u}(x_2))}{[\beta_3 K_{10} + d_1(K_3 - K_{10}) U_1(\tilde{u}(x_2))]}.$$

This system and the effect of control action $\tilde{u}$ on the input u can be simulated by using Matlab Simulink as in Figure 6.9. The control action can obtain the necessary input variable around 3 days even if it is initially unknown.

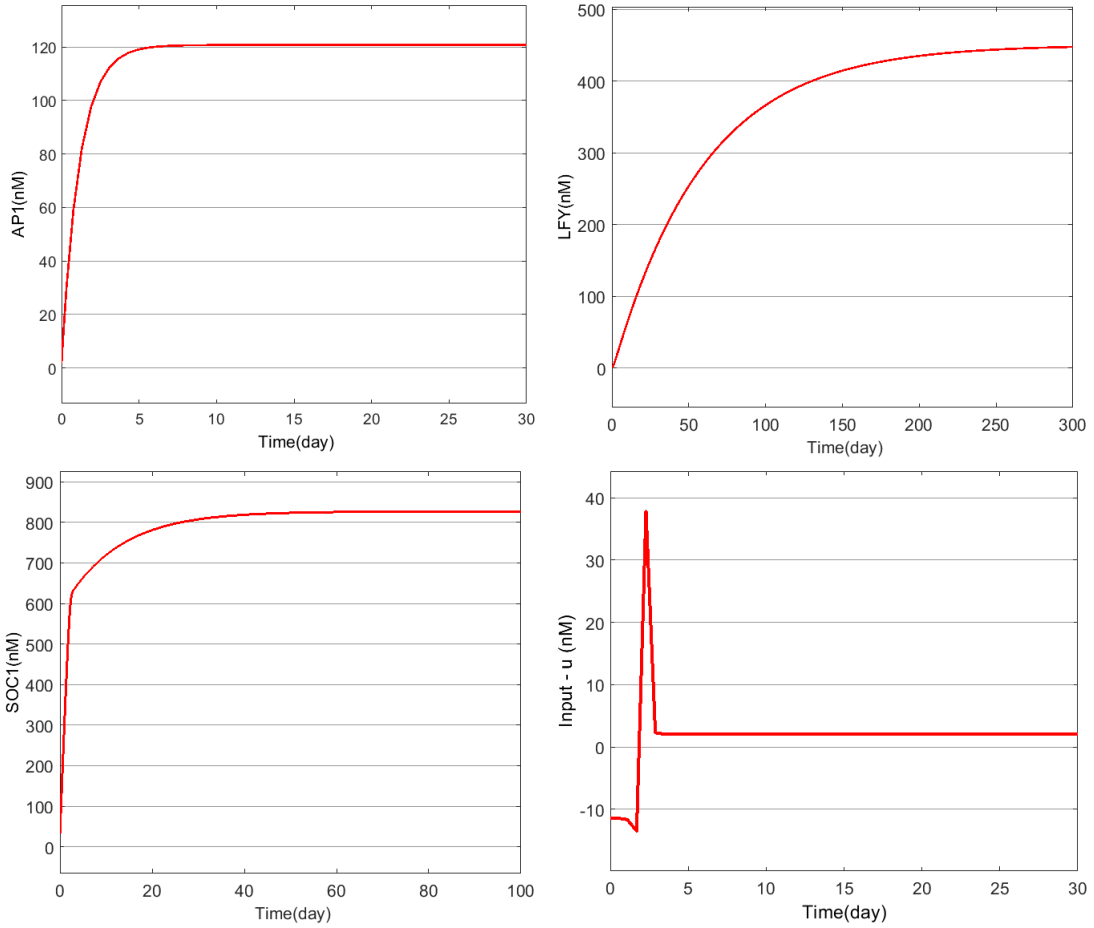

FIGURE 6.9: Simulation results of state feedback control design in system (6.5) for $AP1$, LFY, $SOC1$ and the effect of control action on the input (u) FT, respectively.

A representative diagram of the high gain observer-based state feedback control design for system (6.20) with gain matrix $K_\theta = \Omega^{-1}(\hat{x}, u)\Delta_\theta^{-1}K$ is shown in Figure 6.10.

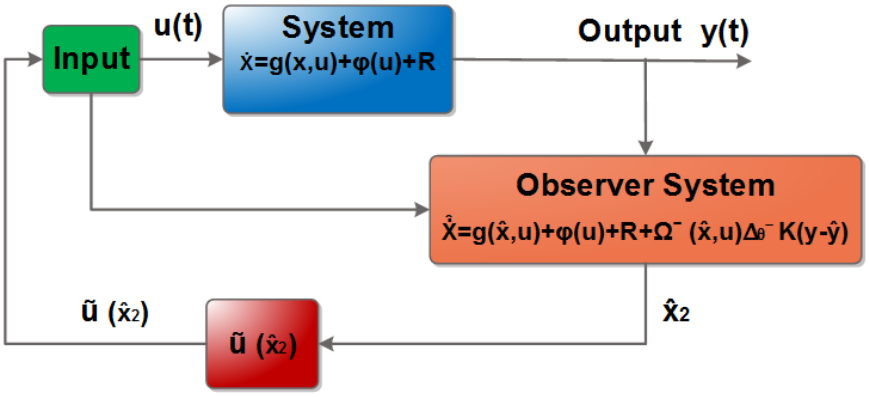

FIGURE 6.10: High gain observer-based state feedback control design of the system (6.20) where the input u represents FT.

The simulation results of this system while $\theta = 3$, are obtained with Matlab Simulink as in following Figure 6.11.

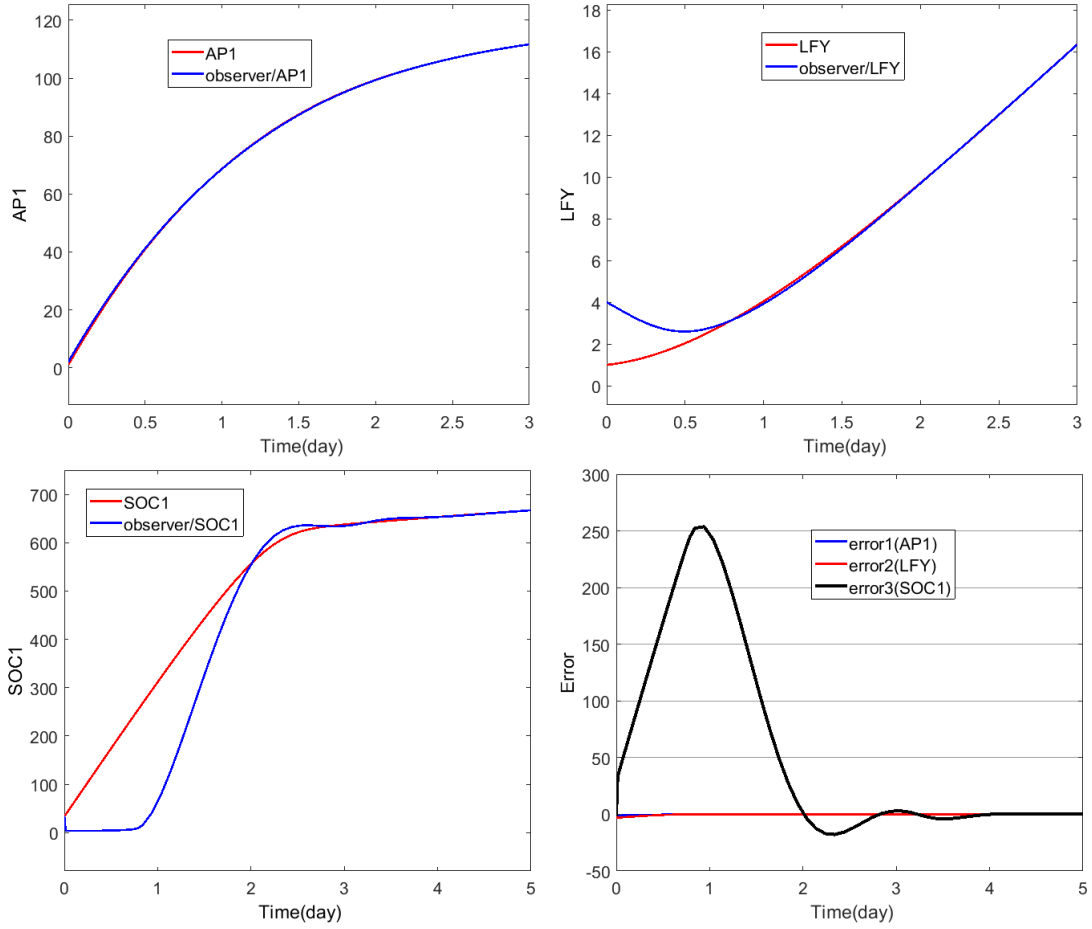

FIGURE 6.11: Simulation results of observer-based state feedback control design of the system (6.20).

6.4 Conclusion

In conclusion, the observer model of the simplified system was designed with constant and state-dependent high gain observers to estimate the unmeasured variables $SOC1$ and LFY by using the measured input, FT, and output, $AP1$, variables. To obtain an observable system where the functions are globally Lipschitz, the Hill functions in the simplified system was translated to exponential ones with Pade approximants. This is because, simplified systems with Hill functions are locally Lipschitz, not globally. The results of constant and state-dependent high gain observers were compared with both Hill and exponential functions. The constant gain observer, which is obtained independent from the state variables, shows that it can capture the simplified model, but this comes in a long time for $SOC1$ variable around 60 days while $AP1$ and LFY can be captured in a day. On the other hand, high gain observer, which depends on the state variable, can estimate the simplified model shorter than the constant gain. For example, $SOC1$ variable is estimated 20 times faster than constant gain, which is around 3 days. The comparison of the results can be seen in Figures 6.6 and 6.7.

In the second part of this chapter, a state feedback controller was designed for the simplified system (6.5) to regulate the output, $AP1$, variable with a specific (steady state) reference value $AP1_{ref}$ by controlling the input, FT, variable. Moreover, simulation results of observer-based state feedback control design of this system was performed.

Chapter 7

Conclusions, results and future works

7.1 Introduction

This thesis focused on analysing the behaviour of *Arabidopsis Thaliana* flowering GRN by considering steady states and their stability in mathematical models consisting of a large deterministic delay differential equations system and its simplified deterministic and stochastic versions. One of the deterministic simplified model was redesigned with an observer to estimate non-measured variables in the system. The behaviour of the system was then modified by controlling the input variable which ensures a target output value is obtained and that flowering conditions for Arabidopsis are met.

This chapter summaries the methods applied in the thesis as well as the presented results and gives possible future works.

7.2 Conclusions and summary of results

The thesis started by introducing the importance of system biology and gene regulatory networks. Initially, the background of gene regulatory networks and the necessary mathematical techniques, used to obtain the results, were introduced. Then, a review of the mathematical models and some of the important methods used to understand the behaviour of a gene regulatory network were given in Chapter 2.

In Chapter 3, a general review for the flowering process of *Arabidopsis Thaliana* was provided. The complexity of the *Arabidopsis Thaliana* flowering GRN and the important genes for the flowering processes were introduced. Moreover, an existing dynamic model of Arabidopsis flowering time GRN, introduced by Valentim et al. [2015] with delay differential equations, was considered to analyse the behaviour of the network mathematically. The steady state estimation of this deterministic model was analytically studied and as a results of this study, a 17^{th} degree polynomial was obtained. The steady states were numerically calculated using the estimated parameters, obtained by [Valentim et al., 2015] with polynomial data fitting method in Matlab. The analysis has shown that the system has a unique positive stable steady state and that the time for which $AP1$ reaches the steady state is an agreement with the observed flowering time between 20 and 30 days. The linear stability analysis of the dynamical model was performed, and the Routh-Hurwitz stability criterion was used to provide local stability conditions which characterise the existence of this stable steady state. As a result, the local stability of the dynamic model at the steady state depends on its parameter and concentration values. However, it does not depend on the initial values. The threshold values of the concentrations and identification of the parameter ranges for stability cannot be obtained directly from this dynamic model.

Chapter 4 focused on the deterministic simplified versions of the full dynamic model of Arabidopsis flowering GRN. In this chapter, the simplifications of the model were proposed based on decoupling of the original GRN to motifs, and they were described with three and two differential equations. Stability analysis of these simplified models were studied to investigate the parameter ranges for necessary and sufficient stability conditions and obtain threshold values of concentrations for the flowering process. Initially,

the genes $AP1$, LFY (important floral meristem identity genes) and $SOC1$ (transcription factor), which have the most important effect for the flowering process, were introduced. By decoupling the possible concentrations in the full model, a simplified system with three differential equations, which contains the concentrations $AP1$, LFY and $SOC1$, was obtained. The importance of these concentrations for the flowering process was confirmed with numerical calculations. Unfortunately, the same complexity of the full model was seen in this simplified system. Therefore, further model simplifications were performed to obtain a system of two differential equations which contains the dynamics of key floral meristem identity genes $AP1$ and LFY. These were introduced within network motifs to understand the essential characteristics of the floral transition. The effects of the input variables on both $AP1$ and LFY and also separately on one of them were analysed. Parameter ranges of necessary and sufficient conditions for the existence of positive steady states and stability were estimated. The best matching input variables in the motifs with full models were obtained by considering the parameters given in Table 3.2 and the derived steady state values in Table 3.4, which are identical to that of the full model. The results were used for the numerical investigation of the stability and steady states solutions. Analytical and numerical solutions gave us three equilibrium points for the motif, where one of them is trivial and was not considered for stability analysis due to its lack of biological meaning in terms of concentrations. The other two of them were non-trivial steady states, found as unstable (lower threshold value) and stable (upper threshold value). The range from trivial stable to unstable solution gives us the non-flowering process of Arabidopsis. This shows that the flowering process of the plant can be seen while the sufficient environmental conditions were satisfied. In other words, flowering of this plant can be seen after the concentration values reach their sufficient levels. As a result, while the full model was introduced to analyse the flowering process of Arabidopsis, motifs were constructed to obtain the necessary initial conditions (lower threshold values) of the concentrations for triggering the process. This information cannot be obtained from the full model.

Stochastic motifs, which were extended from the deterministic ones by adding additive and multiplicative white noise terms, were developed to obtain a more realistic description of gene effects and their interactions on the behaviour of Arabidopsis flowering in

Chapter 5. The effects of stochasticity on the steady state regimes were observed. The importance of this study is that it represents the first stochastic analysis of the behaviour of Arabidopsis flowering GRN.

In the first part of Chapter 5, the additive white (constant) noise was integrated into reaction rates by taking into account the rate of each variable. The changes of behaviour in this stochastic motif were presented with a fixed constant noise of 5% on a time-varying histogram. This histogram was constituted by performing 100 times implementation around unstable steady state points. The numerical solutions were obtained using the Euler-Maruyama method. They show that the flowering behaviour of the system does not only depend on the initial values but also on the amount of noise. The noise can change the behaviour of the stability region from non-flowering to flowering through a stability switch, even if the initial values are lower than the threshold values. Successful flowering results were illustrated numerically by varying the amount of noise in the $0 - 20\%$ range. This illustrates the appropriateness of stochastic models for biological systems and demonstrates the ability and necessity of studying stochastic models for Arabidopsis flowering.

In the second part of Chapter 5, the multiplicative white (state depend) noise was integrated into each reaction rate by assuming that while the behaviour of stochastic system depends on the noise, the amplitude of the noise also depends on the state of system. The stability properties of stochastic motif (5.6), constructed with the multiplicative white noise, was investigated and compared with the deterministic one. The necessary conditions (range of noise and concentrations) of this stochastic motif were analytically determined with the help of Barbashin-Krasovski theorem. In this study, Lyapunov function method was used and stability domain of the trivial solution, which is non-flowering area of the stochastic model, was considered. Numerical simulations of this stochastic motif were presented. The relation of non-flowering domain with the concentration LFY and noise was illustrated. As a result of this chapter, it can be concluded that the stability of non-negative equilibriums depend on concentrations, noise terms and parameters of the stochastic system.

In Chapter 6, observer and control design of the simplified deterministic model with three equations was studied. In the observer design section, the simplified system with Hill functions, which are locally Lipschitz, was reconstructed with exponential functions, which are globally Lipschitz continuous, by using Pade approximants. It was shown that the simplified system with exponential functions satisfies the observable condition. Two different observers (constant and state-dependent) were designed to estimate the unmeasured variables by using measured (input and output) ones, and their results were compared. Their stability conditions were obtained by using the Lyapunov function method. It was shown that state-dependent high gain observer can capture the system behaviour faster than constant high gain observer. In control design section, a state feedback controller of the simplified system with exponential functions was designed to obtain its controlled version, which helps to regulate the output variable to obtain a desired (reference) output by controlling the input variable depending on the states of the system. The reference value of the system was considered as the steady state value of the output to obtain the numerical simulations. Moreover, simulation results of an observer-based state feedback control design was also given at the end of the chapter.

7.3 Future works

In this study, the stochastic differential equation approach was applied only on motifs. This is because, the initial values of the deterministic system were estimated from analytical calculations and the behaviour of the motifs can be switched depending on both initial and noise values. On the other hand, it was not the case in full and simplified deterministic models due to there being only one positive steady state in these systems, which only represents the flowering of Arabidopsis and independent from the environmental conditions. However, we know that these conditions, which have an effect on the initiation of the flowering (inputs), are also important for the flowering of the Arabidopsis. Therefore, the necessary conditions (threshold values) for the successful flowering should be estimated. As a result, the full and simplified models were only constructed with the initial values, which are required for flowering. Here, the stochastic switching

is not a case for these models. Therefore, we assume that it is not necessary to obtain stochastic models for the full and simplified models. On the other hand, the simplified model and its motifs are constructed with ODEs. These models can also be constructed with DDEs by using the input delay as used in full model.

Furthermore, after having a delayed motif model, this can be transformed to the stochastic delay differential equations (SDDEs) by incorporating noise terms into the deterministic systems, and the behaviour of these SDDEs can be observed and be compared with stochastic ODEs.

In this study we studied an observer and control design of the simplified deterministic model with three differential equations. The full delay differential equations model (3.1) and its ODE version can be designed with an observer and control theory method by considering the outputs as $AP1$ and LFY or only $AP1$ to estimate the other concentrations while the input is FT. Observer and control design of motifs with deterministic and stochastic differential equations are still an open area for future works. Finally, the simplified model with delay differential equations and both the deterministic and stochastic motif models with delay and without delay versions can also be designed with an observer and control theory method as shown in Table 7.1.

Models	Deterministic	Stochastic	Observer and Control design
Full ODE	Has been studied	Not necessary	Open for future work
Full DDE	Has been studied	Not necessary	Open for future work
Simplified ODE	Has been studied	Not necessary	Has been studied
Simplified DDE	Open for future work	Not necessary	Open for future work
Motif ODE	Has been studied	Has been studied	Open for future work
Motif DDE	Open for future work	Open for future work	Open for future work

TABLE 7.1: The studies, which have been studied to analyse behaviour of the Arabidopsis flowering GRN, are represented with yellow colour. The green colours represent possible future work. The red colour indicates steps which are unnecessary given the purpose of the full and simplified models.

The work in this thesis gives an opportunity to develop the idea of observing the behaviour of the *Arabidopsis Thaliana* flowering regulatory network with many different ways by modifying the given dynamical models. In the following subsections, some of

the modelling methods will be introduced for future studies, where these can be applied to observe behaviour of the Arabidopsis flowering.

7.3.1 Deterministic simplified models and motifs with delay differential equations

In this study, the simplified model (4.1) was constructed by decoupling of some concentrations, and the input variable FT was considered already in the meristem of *Arabidopsis Thaliana*, which means no time delay was considered for the input variable. In other words, we assumed that the input variable FT does not have to move from leaf to meristem. However, it can also be considered that the input variable FT comes from leaf to meristem of the plant as used in the full model (3.1). Therefore, the simplified model can be reconstructed by considering the delay inputs to design within a delay differential equations system. This system can be represented by considering the dashed arrows in Figure 4.2 as delay representation of the simplified network and can be reformulated by considering the delay input functions as

$$U_1 = \frac{\beta_3 u(t-\tau)}{d_1(K_3 + u(t-\tau))} \text{ and } U_2 = \frac{u(t-\tau)}{u(t-\tau) + K_{10}}.$$

Similarly, the motifs can also be reconstructed with delay differential equations by taking inconstant input variables into account. They are represented using delayed functions as

$$F_1 = \frac{u(t-\tau)}{K_i + u(t-\tau)} \text{ and } F_2 = \frac{\beta u(t-\tau)}{K_j + du(t-\tau)},$$

and can be seen with the dash lines in Figure 4.4. Here, K_i, K_j, β and d are constant variables.

7.3.2 Stochastic motifs with delay differential equations

It was obtained from the numerical calculations that there exists only one positive steady state in the full system (3.1), which is stable, and this shows that the flowering of *Arabidopsis Thaliana* gene regulatory network does not depend on the initial or threshold values of the concentrations. This means that the dynamical model represents only the flowering of the plant with given initial values, where they are assumed to have enough value to observe the flowering process. Similarly, the simplified version of the full model, given in (4.1), was constructed with the same assumption and initial values. However, in the reality, flowering of all plants depend on the environmental conditions. The flowering process can be observed while all the concentrations have enough values, and they can be obtained with the interaction of the input variable FT in the meristem. The flowering of *Arabidopsis Thaliana* depends on the location, light, heat and weather conditions, etc. After all environmental conditions are satisfied, it can be seen that the leaf of the Arabidopsis starts growing and the FT concentration can be observed in the leaf. After FT reaches its threshold value in the leaf, it starts to move through the meristem. This process is assumed almost a half day in the full model [Valentim et al., 2015]. When it reaches to there, the flowering process starts associated with the interaction between FT and other genes. Here, obtaining this threshold value of FT in the meristem is critically important to determine the threshold value of other genes. With in this idea, the motifs, constructed with two ordinary differential equations, were obtained. We studied a specific motif (4.2) which has the best matching input variable for the full system. This motif was analysed in both deterministic and stochastic perspective. However, this motif can also be analysed with using a delayed input variable in both perspective, as introduced introduced the previous subsection.

Appendix A

Table of simplified system parameters

Regulatory interaction	Reaction	Parameters	Value/Unit	Parameters	Value/Unit
$LFY \rightarrow AP1$	$\nu_1 - \nu_2$	V_1	99.8 nM$*$min^{-1}	S_1	9.82 nM
		V_2	42.5 nM$*$min^{-1}	S_2	20.4 nM
				S_3	94.01 nM
$FT \rightarrow AP1$	U_1	β_3	10 nM$*$min^{-1}	K_3	10.1 nM
$AP1 \rightarrow LFY$	ν_1	V_3	22 nM$*$min^{-1}	S_4	346 nM
$SOC1 \rightarrow LFY$	$\nu_4 - \nu_5$	V_4	2.4 nM$*$min^{-1}	S_5	842 nM
		V_5	79 nM$*$min^{-1}	S_6	101.011 nM
				S_7	126.375 nM
$LFY \rightarrow SOC1$	ν_6	V_6	1598.976 nM$*$min^{-1}	S_8	8.518 nM
				S_9	0.1422 nM
$FT - FD \rightarrow SOC1$	U_2			K_{10}	4.8 nM
$SOC1 \rightarrow SOC1$	$\nu_7 - \nu_8$	V_7	63.7003 nM$*$min^{-1}	S_{10}	695 nM
		V_8	51.7565 nM$*$min^{-1}	S_{11}	101.182 nM
				S_{12}	147.75 nM
$AP1$		d_1	0.86 min^{-1}		
LFY		d_2	0.017 min^{-1}		
$SOC1$		d_3	0.11 min^{-1}		

TABLE A.1: Model parameters, calculated from decoupling.

Appendix B

Global Lipschitz condition of Pade approximants

Here, we show that a function $g(x, u)$, which is consisted with Pade approximants, satisfies the global Lipschitz condition, is defined in Assumption (1).

Theorem B.1. *Let $g(x, u) = e^{x^m}$ be a Lipschitz function with a positive integer m. For any $|x|$, $|\hat{x}|$, $r \in R$ with $|x|, |\hat{x}| \leq r$, we have*

$$|g(x, u) - g(\hat{x}, u)| \leq \lambda |x - \hat{x}|,$$

where $\lambda = \dfrac{de^{r^m}}{dr}$ is the Lipschitz constant.

Proof. Remember that a Lipschitz function $g(x, u)$ with a Lipschitz constant $\lambda = \dfrac{de^{r^m}}{dr}$ can be defined as

$$|g(x, u) - g(\hat{x}, u)| \leq \lambda |x - \hat{x}| = \frac{de^{r^m}}{dr} |x - \hat{x}|.$$

If we use the identity,

$$e^x = \sum_{k=0}^{\infty} \frac{x^k}{k!},$$

for any $x \in R$ and positive integer k, we have

$$|g(x,u) - g(\hat{x},u)| = \left|e^{x^m} - e^{\hat{x}^m}\right| = \left|\sum_{k=0}^{\infty} \frac{(x^m)^k}{k!} - \sum_{k=0}^{\infty} \frac{(\hat{x}^m)^k}{k!}\right| = \left|\sum_{k=1}^{\infty} \frac{(x^m)^k - (\hat{x}^m)^k}{k!}\right|.$$

For any $x, y \in R$ and positive integer k, the identities below

$$\left|\sum_{k=1}^{\infty} x^k - y^k\right| \leq \sum_{k=1}^{\infty} \left|x^k - y^k\right| \;\; and \;\; x^k - y^k = \sum_{i=1}^{k} (x-y)x^{i-1}y^{k-i},$$

satisfies that

$$\left|\sum_{k=1}^{\infty} \frac{(x^m)^k - (\hat{x}^m)^k}{k!}\right| \leq \sum_{k=1}^{\infty} \left|\frac{(x^m)^k - (\hat{x}^m)^k}{k!}\right| =$$

$$\sum_{k=1}^{\infty} \left|\frac{1}{k!} \sum_{i=1}^{k} (x^m - \hat{x}^m)(x^m)^{i-1}(\hat{x}^m)^{k-i}\right| = \sum_{k=1}^{\infty} \left|\frac{1}{k!} \sum_{i=1}^{k} (x^m)^{i-1}(\hat{x}^m)^{k-i} \sum_{i=1}^{m} (x-\hat{x})x^{i-1}\hat{x}^{m-i}\right| \leq$$

$$|x-\hat{x}| \sum_{k=1}^{\infty} \frac{1}{k!} \sum_{i=1}^{k} \left|(x^m)^{i-1}(\hat{x}^m)^{k-i}\right| \sum_{i=1}^{m} \left|x^{i-1}\hat{x}^{m-i}\right|.$$

It is clear that while $|x|, |\hat{x}| \leq r$, we have

$$\sum_{i=1}^{m} \left|x^{i-1}\hat{x}^{m-i}\right| \leq \sum_{i=1}^{m} r^{i-1}r^{m-i} = \sum_{i=1}^{m} r^{m-1} = mr^{m-1},$$

and

$$\sum_{i=1}^{k} \left|(x^m)^{i-1}(\hat{x}^m)^{k-i}\right| \leq \sum_{i=1}^{k} (r^m)^{i-1}(r^m)^{k-i} = \sum_{i=1}^{k} (r^m)^{k-1} = k(r^m)^{k-1}.$$

Therefore,

$$|x-\hat{x}| \sum_{k=1}^{\infty} \frac{1}{k!} \sum_{i=1}^{k} \left|(x^m)^{i-1}(\hat{x}^m)^{k-i}\right| \sum_{i=1}^{m} \left|x^{i-1}\hat{x}^{m-i}\right| \leq |x-\hat{x}| \sum_{k=1}^{\infty} \frac{1}{k!} k(r^m)^{k-1} mr^{m-1} =$$

$$|x-\hat{x}|\, mr^{m-1} \sum_{k=1}^{\infty} \frac{(r^m)^{k-1}}{(k-1)!} = |x-\hat{x}|\, mr^{m-1}e^{r^m} = |x-\hat{x}| \frac{de^{r^m}}{dr},$$

which verify that

$$|g(x,u) - g(\hat{x},u)| \leq \lambda\, |x-\hat{x}| = \frac{de^{r^m}}{dr}\, |x-\hat{x}|.$$

□

Bibliography

Akutsu, T., Miyano, S., Kuhara, S., et al. (1999). Identification of genetic networks from a small number of gene expression patterns under the Boolean network model. In *Pacific Symposium on Biocomputing*, volume 4, pages 17–28. World Scientific.

Al Hokayem, P. and Gallestey, E. (2017). Lecture notes on nonlinear systems and control, Spring semester, ETH Zurich. http://control.ee.ethz.ch/~apnoco/Lectures2017/NLSC_lecture_notes_2017.pdf. Accessed: 2018-01-10.

Alina, C. and Ionela-Rodica, T. (2011). Descartes' rule of signs. *Universitatii Maritime Constanta. Analele*, 12(16):225.

Amasino, R. (2010). Seasonal and developmental timing of flowering. *The Plant Journal*, 61(6):1001–1013.

Ando, S., Sakamoto, E., and Iba, H. (2002). Evolutionary modeling and inference of gene network. *Information Sciences*, 145(3):237–259.

Aström, K. J. and Murray, R. M. (2010). *Feedback systems: an introduction for scientists and engineers*. Princeton University Press.

Barbashin, E. and Krasovskii, N. N. (1961). On stability of motion in the large. Technical report, Trw Space Technology Labs Los Angeles Calif.

Bartoszewski, Z., Jackiewicz, Z., and Kuang, Y. (2015). Numerical solution of threshold problems in epidemics and population dynamics. *Journal of Computational and Applied Mathematics*, 279:40–56.

Belbas, S. and Kim, S. (2003). Identification in models of biochemical reactions. *arXiv preprint q-bio/0311024*.

Blázquez, M., Koornneef, M., and Putterill, J. (2001). Flowering on time: genes that regulate the floral transition. *EMBO Reports*, 2(12):1078–1082.

Blázquez, M. A. and Weigel, D. (2000). Integration of floral inductive signals in Arabidopsis. *Nature*, 404(6780):889.

Bocharov, G. A. and Rihan, F. A. (2000). Numerical modelling in biosciences using delay differential equations. *Journal of Computational and Applied Mathematics*, 125(1):183–199.

Boogerd, F. C., Bruggeman, F. J., Hofmeyr, J.-H. S., and Westerhoff, H. V. (2007). Towards philosophical foundations of Systems Biology: introduction. *Systems Biology, Philosophical Foundations*, pages 3–19.

Bououden, S. (2016). High gain observer design for blood glucose in type I diabetics. In *Modelling, Identification and Control (ICMIC), 2016 8th International Conference on*, pages 643–647. IEEE.

Breitling, R. (2010). What is systems biology? *Frontiers in Physiology*, pages 1–9.

Burrage, K., Burrage, P., and Mitsui, T. (2000). Numerical solutions of stochastic differential equations–implementation and stability issues. *Journal of Computational and Applied Mathematics*, 125(1):171–182.

Busawon, K., Farza, M., and Hammouri, H. (1998a). Observer design for a special class of nonlinear systems. *International Journal of Control*, 71(3):405–418.

Busawon, K., Farza, M., and Hammouri, H. (1998b). A simple observer for a class of nonlinear systems. *Applied Mathematics Letters*, 11(3):27–31.

Busawon, K. K. and De Leon-Morales, J. (1999). An improved high gain observer for single-output uniformly observable systems. In *Control Conference (ECC), 1999 European*, pages 991–996. IEEE.

Busawon, K. K. and Leon-Morales, J. D. (2000). An observer design for uniformly observable non-linear systems. *International Journal of Control*, 73(15):1375–1381.

Cao, J., Qi, X., and Zhao, H. (2012). Modeling gene regulation networks using ordinary differential equations. In *Next Generation Microarray Bioinformatics*, pages 185–197. Springer.

Carletti, M. (2007). Mean-square stability of a stochastic model for bacteriophage infection with time delays. *Mathematical Biosciences*, 210(2):395–414.

Chaves, M., Sontag, E. D., and Albert, R. (2006). Methods of robustness analysis for Boolean models of gene control networks. *IEE Proceedings-Systems Biology*, 153(4):154–167.

Chen, B.-S. and Chang, Y.-T. (2008). A systematic molecular circuit design method for gene networks under biochemical time delays and molecular noises. *BMC Systems Biology*, 2(1):103.

Chen, K.-C., Wang, T.-Y., Tseng, H.-H., Huang, C.-Y. F., and Kao, C.-Y. (2005). A stochastic differential equation model for quantifying transcriptional regulatory network in Saccharomyces cerevisiae. *Bioinformatics*, 21(12):2883–2890.

Chen, L. and Aihara, K. (2002). Stability of genetic regulatory networks with time delay. *IEEE Transactions on Circuits and Systems I: Fundamental Theory and Applications*, 49(5):602–608.

Chen, M., Li, F., Wang, S., and Cao, Y. (2017). Stochastic modeling and simulation of reaction-diffusion system with Hill function dynamics. *BMC Systems Biology*, 11(3):21.

Chen, T., He, H. L., Church, G. M., et al. (1999). Modeling gene expression with differential equations. In *Pacific Symposium on Biocomputing*, volume 4, page 4. World Scientific.

Cosentino, C. and Bates, D. (2011). *Feedback control in systems biology*. Crc Press.

Daly, R., Edwards, K. D., O'Neill, J. S., Aitken, S., Millar, A. J., and Girolami, M. (2009). Using higher-order dynamic Bayesian networks to model periodic data from the circadian clock of Arabidopsis thaliana. In *IAPR International Conference on Pattern Recognition in Bioinformatics*, pages 67–78. Springer.

De Hoon, M., Imoto, S., Kobayashi, K., Ogasawara, N., and Miyano, S. (2002). Inferring gene regulatory networks from time-ordered gene expression data of Bacillus subtilis using differential equations. In *Pac. Symp. Biocomput*, page 17.

de Hoon, M., Imoto, S., and Miyano, S. (2002). Inferring gene regulatory networks from time-ordered gene expression data using differential equations. In *International Conference on Discovery Science*, pages 267–274. Springer.

De Jong, H. (2002). Modeling and simulation of genetic regulatory systems: a literature review. *Journal of Computational Biology*, 9(1):67–103.

De Jong, H. and Geiselmann, J. (2005). Modeling and simulation of genetic regulatory networks by ordinary differential equations. *Genomic Signal Processing and Statistics. New York: Hindawi Publishing Corporation*, pages 201–239.

Dibiasio, D., Lim, H. C., Weigand, W. A., and Tsao, G. T. (1978). Phase-plane analysis of feedback control of unstable steady states in a biological reactor. *AIChE Journal*, 24(4):686–693.

Emmert-Streib, F., Dehmer, M., and Haibe-Kains, B. (2014). Gene regulatory networks and their applications: understanding biological and medical problems in terms of networks. *Frontiers in Cell and Developmental Biology*, 2.

Engelborghs, K. and Roose, D. (1999). Numerical computation of stability and detection of Hopf bifurcations of steady state solutions of delay differential equations. *Advances in Computational Mathematics*, 10(3):271–289.

Filkov, V. (2005). Identifying gene regulatory networks from gene expression data. *Handbook of Computational Molecular Biology*, pages 27.1–27.29.

Floares, A. and Birlutiu, A. (2012). Reverse engineering networks as ordinary differential equations systems. *Computational Intelligence. NOVA Science Publishers, New York*.

Friedman, N., Linial, M., Nachman, I., and Pe'er, D. (2000). Using Bayesian networks to analyze expression data. *Journal of Computational Biology*, 7(3-4):601–620.

Gallestey, E., Al-Hokayem, P., Torrisi, M. G., and Paccagnan, M. D. (2015). Nonlinear Systems and Control. *Department of Information Technology and Electrical Engineering, Swiss Federal Institute of Technology*.

Gantmacher, F., Brenner, J., Bushaw, D., Evanusa, S., and Morse, P. M. (1960). Applications of the Theory of Matrices. *Physics Today*, 13:56.

Gauthier, J. P., Hammouri, H., and Othman, S. (1992). A simple observer for nonlinear systems applications to bioreactors. *IEEE Transactions on automatic control*, 37(6):875–880.

Gauthier, J.-P. and Kupka, I. (2001). *Deterministic observation theory and applications*. Cambridge University Press.

Gauthier, J.-P. and Kupka, I. A. (1994). Observability and observers for nonlinear systems. *SIAM Journal on Control and Optimization*, 32(4):975–994.

Gebert, J., Radde, N., and Weber, G.-W. (2007). Modeling gene regulatory networks with piecewise linear differential equations. *European Journal of Operational Research*, 181(3):1148–1165.

Greenup, A., Peacock, W. J., Dennis, E. S., and Trevaskis, B. (2009). The molecular biology of seasonal flowering-responses in Arabidopsis and the cereals. *Annals of Botany*, 103(8):1165–1172.

Haddad, W. M. and Chellaboina, V. (2011). *Nonlinear dynamical systems and control: a Lyapunov-based approach*. Princeton University Press.

Hanumappa, M., Bluemel, M., Willighagen, E., and Bohler, A. e. a. Flowering Time Pathway (Arabidopsis thaliana). https://www.wikipathways.org/index.php?

title=Pathway:WP2312&direction=next&oldid=87353. Accessed: 2018-01-10.

Haubelt, A., Bullinger, E., Sauter, T., Allgöwer, F., and Gilles, E. (2002). Systems Biology-A Glossary from two perspectives. In *3rd International Conference on Systems Biology*.

Hecker, M., Lambeck, S., Toepfer, S., Van Someren, E., and Guthke, R. (2009). Gene regulatory network inference: data integration in dynamic models—a review. *Biosystems*, 96(1):86–103.

Heinrich, R. and Rapoport, T. A. (1974). A Linear Steady-State Treatment of Enzymatic Chains. *The FEBS Journal*, 42(1):97–105.

Higgins, J. (1963). Analysis of sequential reactions. *Annals of the New York Academy of Sciences*, 108(1):305–321.

Higham, D. J. (2008). Modeling and simulating chemical reactions. *SIAM Review*, 50(2):347–368.

Iba, H. (2008). Inference of differential equation models by genetic programming. *Information Sciences*, 178(23):4453–4468.

Iglesias, P. A. and Ingalls, B. P. (2010). *Control theory and systems biology*. MIT Press.

Ignatyev, O. and Mandrekar, V. (2010). Barbashin-Krasovskii theorem for stochastic differential equations. *Proceedings of the American Mathematical Society*, 138(11):4123–4128.

Irish, V. F. (2010). The flowering of Arabidopsis flower development. *The Plant Journal*, 61(6):1014–1028.

Jaeger, K. E., Pullen, N., Lamzin, S., Morris, R. J., and Wigge, P. A. (2013). Interlocking feedback loops govern the dynamic behavior of the floral transition in Arabidopsis. *The Plant Cell*, 25(3):820–833.

Jönsson, H. (2005). "Modeling in systems biology" lecture notes. http://home.thep.lu.se/~henrik/fytn05/lectureNotesSysBiol.pdf. Accessed: 2018-01-31.

Kaderali, L. and Radde, N. (2008). Inferring gene regulatory networks from expression data. In *Computational Intelligence in Bioinformatics*, pages 33–74. Springer.

Kalman, R. (1959). On the general theory of control systems. *IRE Transactions on Automatic Control*, 4(3):110–110.

Kardailsky, I., Shukla, V. K., Ahn, J. H., Dagenais, N., Christensen, S. K., Nguyen, J. T., Chory, J., Harrison, M. J., and Weigel, D. (1999). Activation tagging of the floral inducer FT. *Science*, 286(5446):1962–1965.

Karlebach, G. and Shamir, R. (2008). Modelling and analysis of gene regulatory networks. *Nature Reviews Molecular Cell Biology*, 9(10):770–780.

Kaufmann, K., Wellmer, F., Muiño, J. M., Ferrier, T., Wuest, S. E., Kumar, V., Serrano-Mislata, A., Madueno, F., Krajewski, P., Meyerowitz, E. M., et al. (2010). Orchestration of floral initiation by APETALA1. *Science*, 328(5974):85–89.

Kepler, T. B. and Perelson, A. S. (1995). Modeling and optimization of populations subject to time-dependent mutation. *Proceedings of the National Academy of Sciences*, 92(18):8219–8223.

Khalil, H. K. (2002). Nonlinear systems, 3rd edition. *New Jewsey, Prentice Hall*.

Kim, H., Lee, J. K., and Park, T. (2007). Boolean networks using the chi-square test for inferring large-scale gene regulatory networks. *BMC Bioinformatics*, 8(1):1.

Kim, S. Y., Imoto, S., and Miyano, S. (2003). Inferring gene networks from time series microarray data using dynamic Bayesian networks. *Briefings in Bioinformatics*, 4(3):228–235.

Kitano, H. (2002). Systems biology: a brief overview. *Science*, 295(5560):1662–1664.

Klimešová, M. (2015). Stability of the stochastic differential equations. EEICT.

Koyuturk, M. (2007). Systems Biology & Bioinformatics (EECS 600). Lecture notes. http://compbio.case.edu/koyuturk/teaching/eecs600_fall2007/. Accessed: 2018-01-10.

Kragt, M. E. (2009). *A beginners guide to Bayesian network modelling for integrated catchment management*. Landscape Logic.

Krämer, U. (2015). The Natural History of Model Organisms: Planting molecular functions in an ecological context with Arabidopsis thaliana. *Elife*, 4:e06100.

Krizek, B. A. and Fletcher, J. C. (2005). Molecular mechanisms of flower development: an armchair guide. *Nature Reviews Genetics*, 6(9):688–698.

Lahrouz, A., Omari, L., Kiouach, D., and Belmaâti, A. (2011). Deterministic and stochastic stability of a mathematical model of smoking. *Statistics & Probability Letters*, 81(8):1276–1284.

Lakshmanan, M. and Senthilkumar, D. V. (2011). *Dynamics of nonlinear time-delay systems*. Springer Science & Business Media.

Lantos, B. and Márton, L. (2010). *Nonlinear control of vehicles and robots*. Springer Science & Business Media.

LaSalle, J. (1960). Some extensions of Liapunov's second method. *IRE Transactions on Circuit Theory*, 7(4):520–527.

LaSalle, J. P. (1968). Stability theory for ordinary differential equations. *Journal of Differential Equations*, 4(1):57–65.

Lee, W.-P. and Tzou, W.-S. (2009). Computational methods for discovering gene networks from expression data. *Briefings in Bioinformatics*, 10(4):408–423.

Lee, W.-P. and Yang, K.-C. (2008). A clustering-based approach for inferring recurrent neural networks as gene regulatory networks. *Neurocomputing*, 71(4):600–610.

Levy, Y. Y. and Dean, C. (1998). The transition to flowering. *The Plant Cell*, 10(12):1973–1989.

Li, P., Zhang, C., Perkins, E. J., Gong, P., and Deng, Y. (2007). Comparison of probabilistic Boolean network and dynamic Bayesian network approaches for inferring gene regulatory networks. *BMC Bioinformatics*, 8(Suppl 7):S13.

Liljegren, S. J., Gustafson-Brown, C., Pinyopich, A., Ditta, G. S., and Yanofsky, M. F. (1999). Interactions among APETALA1, LEAFY, and TERMINAL FLOWER1 specify meristem fate. *The Plant Cell*, 11(6):1007–1018.

Ling, H., Zhu, Z., and Chen, C. (2012). Dynamics of genetic regulatory networks with delays. In *Networking, Sensing and Control (ICNSC), 2012 9th IEEE International Conference on*, pages 310–315. IEEE.

Luenberger, D. G. (1964). Observing the state of a linear system. *IEEE Transactions on Military Electronics*, 8(2):74–80.

Lyapunov, A. M. (1992). The general problem of the stability of motion. *International Journal of Control*, 55(3):531–534.

Ma, T., Che, J., and Cao, C. (2016). Control of nonlinear systems using filtered high-gain observer. In *Flexible Automation (ISFA), International Symposium on*, pages 483–489. IEEE.

Mackey, M. C. and Nechaeva, I. G. (1994). Noise and stability in differential delay equations. *Journal of Dynamics and Differential Equations*, 6(3):395–426.

Mandel, M. A., Gustafson-Brown, C., Savidge, B., and Yanofsky, M. F. (1992). Molecular characterization of the Arabidopsis floral homeotic gene APETALA1. *Nature*, 360(6401):273.

Manninen, T., Intosalmi, J., Ruohonen, K., and Linne, M.-L. (2015). Numerical characterization of noisy fluctuations in two different types of stochastic differential equation models of neural signaling. *BMC Neuroscience*, 16(1):P147.

Manninen, T., Linne, M.-L., and Ruohonen, K. (2006). Developing Itô stochastic differential equation models for neuronal signal transduction pathways. *Computational Biology and Chemistry*, 30(4):280–291.

Masoudi-Nejad, A., Bidkhori, G., Ashtiani, S. H., Najafi, A., Bozorgmehr, J. H., and Wang, E. (2015). Cancer systems biology and modeling: Microscopic scale and multiscale approaches. In *Seminars in Cancer Biology*, volume 30, pages 60–69. Elsevier.

Mehrkanoon, S., Mehrkanoon, S., and Suykens, J. A. (2014). Parameter estimation of delay differential equations: an integration-free LS-SVM approach. *Communications in Nonlinear Science and Numerical Simulation*, 19(4):830–841.

Murray, J. D. (2002). *Mathematical biology Vol.1, An introduction*. Interdisciplinary Applied Mathematics. Springer, New York, 3rd ed. edition.

Nielsen, U., Pellet, J.-P., and Elisseeff, A. (2012). Explanation trees for causal Bayesian networks. *arXiv preprint arXiv:1206.3276*.

Nielsen, U. H. (2003). On causal explanations in Bayesian networks. Master's thesis, IT University of Copenhagen.

Ó'Maoiléidigh, D. S., Graciet, E., and Wellmer, F. (2014). Gene networks controlling Arabidopsis thaliana flower development. *New Phytologist*, 201(1):16–30.

Oyarzún, D. A. and Chaves, M. (2015). Design of a bistable switch to control cellular uptake. *Journal of The Royal Society Interface*, 12(113):20150618.

Pullen, N., Jaeger, K. E., Wigge, P. A., and Morris, R. J. (2013). Simple network motifs can capture key characteristics of the floral transition in Arabidopsis. *Plant Signaling & Behavior*, 8(11):820–833.

Qun, L., Jiang, D., Ningzhong, S., Hayat, T., and Alsaedi, A. (2017). Dynamical behavior of a stochastic HBV infection model with logistic hepatocyte growth. *Acta Mathematica Scientia*, 37(4):927–940.

Ristevski, B. (2013). A survey of models for inference of gene regulatory networks. *Nonlinear Anal Model Control*, 18(4):444–465.

Ryan, P. T., Ó'Maoiléidigh, D. S., Drost, H.-G., Kwaśniewska, K., Gabel, A., Grosse, I., Graciet, E., Quint, M., and Wellmer, F. (2015). Patterns of gene expression during Arabidopsis flower development from the time of initiation to maturation. *BMC Genomics*, 16(1):488.

Saarinen, A., Linne, M.-L., and Yli-Harja, O. (2008). Stochastic differential equation model for cerebellar granule cell excitability. *PLoS Computational Biology*, 4(2):e1000004.

Saeed, S. H. (2008). *Automatic control system*. Seagull Books Pvt Ltd.

Sakamoto, E. and Iba, H. (2001). Inferring a system of differential equations for a gene regulatory network by using genetic programming. In *Evolutionary Computation, 2001. Proceedings of the 2001 Congress on*, volume 1, pages 720–726. IEEE.

Sanda, S., John, M., and Amasino, R. (1997). Analysis of flowering time in ecotypes of Arabidopsis thaliana. *Journal of Heredity*, 88(1):69–72.

Savageau, M. A. (1969a). Biochemical systems analysis: I. Some mathematical properties of the rate law for the component enzymatic reactions. *Journal of Theoretical Biology*, 25(3):365–369.

Savageau, M. A. (1969b). Biochemical systems analysis: II. The steady-state solutions for an n-pool system using a power-law approximation. *Journal of Theoretical Biology*, 25(3):370–379.

Schlitt, T. and Brazma, A. (2007). Current approaches to gene regulatory network modelling. *BMC Bioinformatics*, 8(6):1.

Shiriaev, A., Johansson, R., Robertsson, A., and Freidovich, L. (2008). Separation principle for a class of nonlinear feedback systems augmented with observers. *IFAC Proceedings Volumes*, 41(2):6196–6201.

Shmulevich, I. and Aitchison, J. D. (2009). Deterministic and stochastic models of genetic regulatory networks. *Methods in Enzymology*, 467:335–356.

Simon, R., Igeño, M. I., and Coupland, G. (1996). Identity genes in Arabidopsis. *Nature*, 384:7.

Socha, L. (2007). *Linearization methods for stochastic dynamic systems*, volume 730. Springer Science & Business Media.

Staveley, B. E. (2016). "Plant Development in Molecular & Developmental Biology (BIOL3530)" lecture notes. http://www.mun.ca/biology/desmid/brian/BIOL3530/DEVO_07/devo_07.html. Accessed: 2018-01-31.

Tabus, I., Giurcaneanu, C. D., and Astola, J. (2004). Genetic networks inferred from time series of gene expression data. In *Control, Communications and Signal Processing, 2004. First International Symposium on*, pages 755–758. IEEE.

Tang, T., Teng, Z., and Li, Z. (2015). Threshold behavior in a class of stochastic SIRS epidemic models with nonlinear incidence. *Stochastic Analysis and Applications*, 33(6):994–1019.

Thieffry, D. and Thomas, R. (1997). Qualitative analysis of gene networks. In *Pacific Symposium on Biocomputing. Pacific Symposium on Biocomputing*, pages 77–88.

Ullah, M. and Wolkenhauer, O. (2011). *Stochastic approaches for systems biology*. Springer Science & Business Media.

Valentim, F. L., van Mourik, S., Posé, D., Kim, M. C., Schmid, M., van Ham, R. C., Busscher, M., Sanchez-Perez, G. F., Molenaar, J., Angenent, G. C., et al. (2015). A quantitative and dynamic model of the Arabidopsis flowering time gene regulatory network. *PloS One*, 10(2):e0116973.

van Mourik, S., van Dijk, A. D., de Gee, M., Immink, R. G., Kaufmann, K., Angenent, G. C., van Ham, R. C., and Molenaar, J. (2010). Continuous-time modeling of cell fate determination in Arabidopsis flowers. *BMC Systems Biology*, 4(1):1.

Wang, C. C., Chang, P.-C., Ng, K.-L., Chang, C.-M., Sheu, P. C., and Tsai, J. J. (2014). A model comparison study of the flowering time regulatory network in Arabidopsis. *BMC Systems Biology*, 8(1):15.

Wang, R.-S., Saadatpour, A., and Albert, R. (2012). Boolean modeling in systems biology: an overview of methodology and applications. *Physical Biology*, 9(5):055001.

Welch, S. M., Dong, Z., and Roe, J. L. (2004). Modelling gene networks controlling transition to flowering in Arabidopsis. In *Tony Fischer (editor-in-chief). New directions for a diverse planet: Proceedings of the 4th International Crop Science Congress, Brisbane, Australia. See: www. cropscience. org. au*.

Wellmer, F. and Riechmann, J. L. (2010). Gene networks controlling the initiation of flower development. *Trends in Genetics*, 26(12):519–527.

Wu, F.-X., Zhang, W.-J., and Kusalik, A. J. (2004). Modeling gene expression from microarray expression data with state-space equations. In *Pacific Symposium on Biocomputing*, volume 9, pages 581–592.

Wu, H., Lu, T., Xue, H., and Liang, H. (2014). Sparse additive ordinary differential equations for dynamic gene regulatory network modeling. *Journal of the American Statistical Association*, 109(506):700–716.

Yant, L., Mathieu, J., and Schmid, M. (2009). Just say no: floral repressors help arabidopsis bide the time. *Current Opinion in Plant Biology*, 12(5):580–586.

Yeap, W.-C., Namasivayam, P., and Ho, C.-L. (2014). Hnrnp-like proteins as post-transcriptional regulators. *Plant Science*, 227:90–100.

Zak, D. E., Pearson, R. K., Vadigepalli, R., Gonye, G. E., Schwaber, J. S., and Doyle Iii, F. J. (2003). Continuous-time identification of gene expression models. *OMICS A Journal of Integrative Biology*, 7(4):373–386.

Zhang, Y., Pu, Y., Zhang, H., Su, Y., Zhang, L., and Zhou, J. (2013). Using gene expression programming to infer gene regulatory networks from time-series data. *Computational Biology and Chemistry*, 47:198–206.